JOURNAL OF ENVIRONMENTAL GEOGRAPHY
Journal of Environmental Geography 9 (1–2), 1–6.
DOI: 10.1515/jengeo-2016-0001
ISSN: 2060-467X

HYDROLOGICAL AND MORPHOLOGICAL CHANGES OF THE LOWER DANUBE NEAR MOHÁCS, HUNGARY

Judit Nagy, Tímea Kiss*

Department of Physical Geography and Geoinformatics, University of Szeged, H-6722, Egyetem u. 2-6, Hungary
*Corresponding author, e-mail: kisstimi@gmail.com

Research article, received 10 January 2016, accepted 10 April 2016

Abstract

Various direct human impacts changed the hydro-morphology of the Danube during the last centuries. The aims of the present study are (1) to analyze the water regime of the Danube River using the data of Mohács gauging station (1900-2013), and (2) to study the channel development (1952-2014) in connection with water regime changes and human impacts at a section near Bogyiszló (upstream of Mohács). According to the results the height of low water stages decreased by approx. 136 cm (1.2 cm/year), and new, high record flood stages were measured too. The discharge values appertaining to the same low water stages doubled, thus nowadays almost twice as much water flows through the cross-section of the channel at a given stage as at the beginning of the studied period. As the duration of low stages increased, the sandbar development intensified, thus the channel became narrower (by 48% at some places) and deeper thalweg evolved. Therefore, a smaller cross-section for flood-waves evolved, affecting the height of flood. These changes affect shipping, as due to riverbed incision and decrease of low water stages, the lowest shipping water level has to be set repeatedly at lower stages. Besides water extraction from the channel will have difficulties, thus irrigation and industrial cooling water supply will be limited in the future.

Keywords: Danube, hydrological water regime, low water stages, riverbed incision, bar development

INTRODUCTION

Direct human impacts on rivers, such as cut-offs of meanders, building of revetments and groynes, constructions of dams, water retention or in-channel gravel mining could cause significant alterations in river hydrology (Blanka, 2010; Kiss and Andrási, 2011; Cheng et al., 2012) and morphology too (Bonacci and Oskoruš, 2008; Williams and Wolman, 1984; Kiss and Blanka, 2012; Kiss and Andrási, 2015).

For the society the most important changes are the frequency increase of floods and the decreasing level and increasing durability of low water stages. As a result of lower water stages, the water extraction (for drinking, irrigation or industrial cooling) will be more and more difficult, and the shallow riverbed deteriorates shipping and the incision might cause damages for floodplain ecosystems (Kiss and Andrási, 2015). In the Carpathian Basin several rivers are affected by similar hydrological changes. For example on the Dráva River the level of low stages decreased by 118 cm in connection with dam constructions during the last century, resulting in channel pattern changes (Kiss and Andrási, 2011; Kiss and Balogh, 2015). On the Maros River water stages decreased by 50 cm in the past 20-30 years (Sipos, 2006), whilst on the Hernád by 60 cm in the last 50 years (Blanka, 2010), both resulting in channel narrowing.

The Danube is one of the most important commercial waterways in Central Europe. However, shipping requires significant regulation works, such as construction of revetments and groynes, which alter natural processes in river morphology. The changing hydrology (characteristically decreasing stages) is also the result of cut-offs of meanders in the 19th c., and gravel mining started in the 1970's (VITUKI, 2007). One of their consequences is that meander development terminates (Somogyi, 2001) and the low water stages start to decrease gradually, while the frequency of record-high floods increases (VITUKI, 2007). Besides several dams trap sediment and affect the hydrology (IDCPR, 2014). The second largest Danubian dam located at Bős–Gabcikovo (its hydropower plant operates since 1992) is responsible for higher durability of low stages and incision by ca. 1.5 m on the downstream sections of the river (Rákóczi, 2000; VITUKI, 2007). Due to the incision, the lowest navigable water level had to be set at lower and lower water stages, thus it was decreased by 0.9 m between 1970 and 2004. As a result, on the Hungarian–Croatian section riffles and fords inhibit shipping during low-stage periods.

Nowadays, a current topic in the Hungarian news is the planned expansion of the Paks Nuclear Power Plant, which needs increased cooling water supply, which could only be provided by damming the river downstream of Paks [1]. No preliminary impact study has been made on the possible consequences on river morphology, water regime or sediment-transport yet, nor is the present channel processes known in detail.

The aim of the present research is to reveal the long-term changes in hydrology of the Danube, and in connection with them to analyze the morphological changes of the riverbed, focusing on the development of mid-channel bars and islands

STUDY AREA

On the Danube regulation works started at the end of 19th century. Their main objective was to shorten flood-waves and increase their velocity, therefore several meanders were cut-off downstream of Budapest. One of the sharpest and thus most dangerous bend located near Bogyiszló, which played an important role in ice damming, for example during the devastating icy flood in 1838. Between Dunaföldvár and the Hungarian–Croatian border altogether 32 meanders were cut off, and the channel was almost straightened. The final step of regulation works was the construction of groynes to support shipping (Ihrig, 1973). In the 1970's in-channel gravel mining started causing intensive incision and low stages decrease, thus shipping became more difficult. The incision made the water withdrawal complicated, especially for the Paks Nuclear Power Plant, therefore the rate of dredging was reduced. However, the increasing duration of low water stages is still a problem, in connection with the Bős–Gabcikovo Dam (VITUKI, 2007).

In the present study the water stages measured at Mohács gauging station (1446.9 fkm) were analyzed and the morphological changes of a downstream section of the Danube near Bogyiszló (1493–1502 fkm) (Fig. 1). In this section the river has 4-5 cm/km gradient, and the channel width varies between 450 m and 600 m. The transported sediment is very fine-grained, especially made up of fine silt and sand (VITUKI, 2007). The studied nearly straight section was formed when the meander at Bogyiszló was cut off in 1856 to avoid the development of ice-jams (Ihrig, 1973). Along the studied section the channel development is mainly affected by groynes built since 1935 (Ihrig, 1973), though the main period of groynes construction was in the beginning of the 1950's.

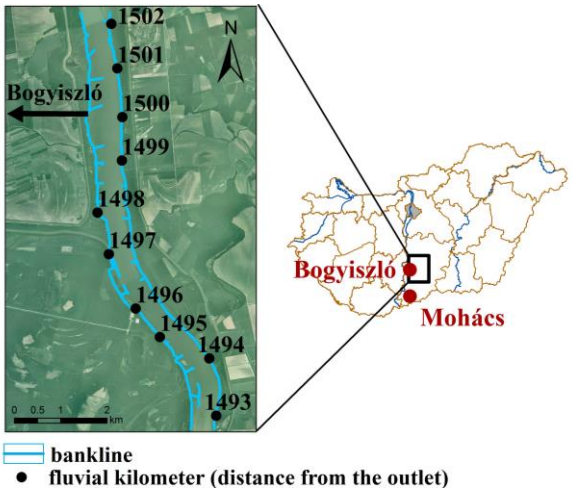

Fig. 1 Hydrological data are from Mohács gauging station, whilst the studied channel section of the Danube is located north of Mohács. (source: Google Earth)

METHODS

Daily water stages (1890–2013) and discharge values (1900–2013) measured at Mohács gauging station were analyzed (data source: ADUVIZIG). This huge dataset has been divided into ten-year periods (1900-1909, 1910-1919 etc.) to facilitate analysis. In each period we calculated the duration of different stages, the number of days when low stages (≤315 cm, occurred with a frequency of 90% in the first decade) were present, and we analyzed the water stage – discharge relationship.

We analyzed the development of the river channel near Bogyiszló using maps and aerial photographs representing the period between 1952 and 2014. The maps and aerial photos were geo-referenced, and we digitized the banklines, and bars with and without woody vegetation using ArcGIS.

RESULTS

Hydrological changes of the Danube River at Mohács

The stage duration curves of the decades show obvious decrease of water stages lower than 700 cm (Fig. 2). In the first decade (1900-1909), for instance water stages were above 315 cm during 90 % of the period, though in the last ten years (2000-2009) they were above 179 cm in accordingly, referring to a decrease of 136 cm at 90 % frequency stages.

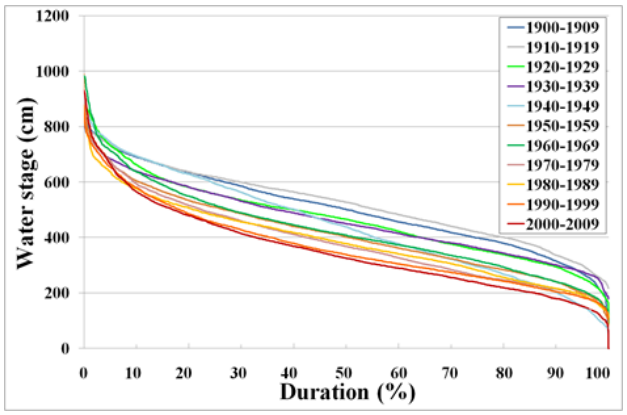

Fig. 2 Changes in the duration of water stages

Obvious change in the duration of flood stages cannot be proved, however their extremity (scattering) decreased, thus record-high flood stages (>900 cm) became more frequent since the mid-20th century (Fig. 3). Between 1900 and 1946 annual highest stages were more or less similar characterized by some fluctuations. In this period characteristically the annual flood stages were between 700 cm and 850 cm, and flood level exceeded 900 cm only once (in 1938). However, in the second half of the 20th c. and especially in the 21st c. quite high flood stages occurred, when flood stages exceeded 900 cm more often (in 1954, 1956, 1965, 1975, 2002, 2006, 2010 and 2013). This does not obviously mean that the height of flood stages continuously rises, just their frequency increases.

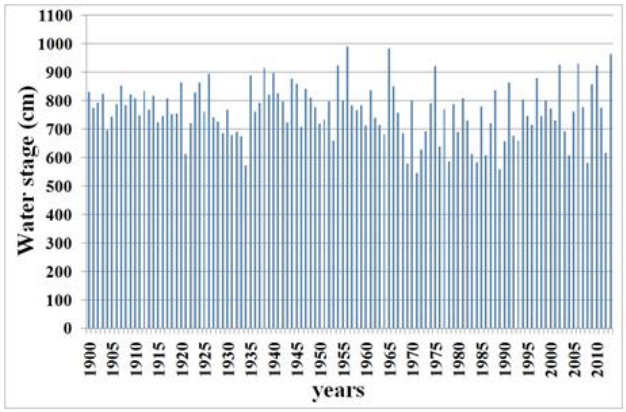

Fig. 3 Changes in the annual flood stages (1900–2013) at Mohács gauging station

Annual low water stages decreased significantly during the studied period (Fig. 4). In the first half of the 20th century (1900-1945) the level of the annual lowest stages exceeded 200 cm, their average height was 245 cm. Extremely high stages occurred in 1910–1916 and 1936–1941 when most of the water stages were above 315 cm. In the second half of the studied period (1946-2013) the level of annual low water stages decreased, thus between 1946 and 2002 their average height dropped by 84 cm to 170 cm, and since 2003 their average height decreased further to 125 cm. These results show an obvious decrease of low water stages, which could be explained by (i) more extreme water regime or (ii) by incision of the riverbed.

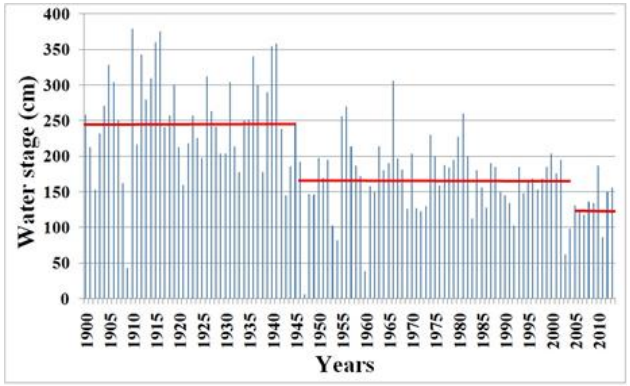

Fig.4 Level of the annual lowest water stages (1900–2013) at Mohács. The red lines represent average values of different periods

The extremity of water regime could be proved by changes in the number of days when low water stages (≤315 cm) occurred. The duration of low stages within the decades increased considerably (Fig. 5). In the first decades of the 20th century low stages occurred in 7-15 % of the decades, however from 1990 until 2013 it increased to 43-47 %, thus the duration of low stages increased by five times (by 20 day/year). This process is in connection with the operation of Bős–Gabcikovo Hydroelectric Power Plant, which started to function in 1992, or it could also be connected to the incision of the riverbed due to groynes built in the river.

Riverbed incision could be indicated by the changes of water stage – discharge (H–Q) relationship: discharge appertaining to a given water level increases in the case of incision, while it decreases in the case of aggradation. However, if the height of flood stages increase while discharges stay stable or decrease, it means that flood channel becomes narrower (Vágás, 2004). The H–Q point-clouds gradually shift upwards (Fig. 6), i.e. discharges appertaining to given water stages increase considerably. It obviously refers to the incision of the riverbed. Discharges appertaining to low water stages are gradually increasing, for example, discharges belonging to 250-300 cm water stages increased from 900-950 m^3/s to 1700 m^3/s in the last almost 110 years. This obviously proves the incision of the riverbed, as the channel transports almost twice as much water at the same water stage.

In the case of higher water stages, there is no significant increase or decrease in the relationship between water stages and discharges. However, the frequency of record-high flood stages shows an increasing trend. The increasing water stages at same discharges can be caused by the narrower flood channel.

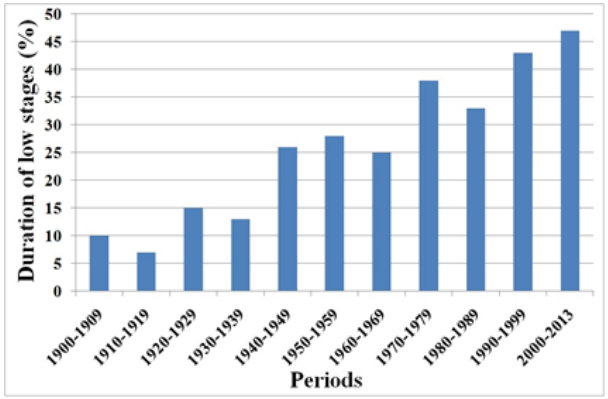

Fig. 5 Duration of low water stages (≤315 cm) at Mohács gauging station

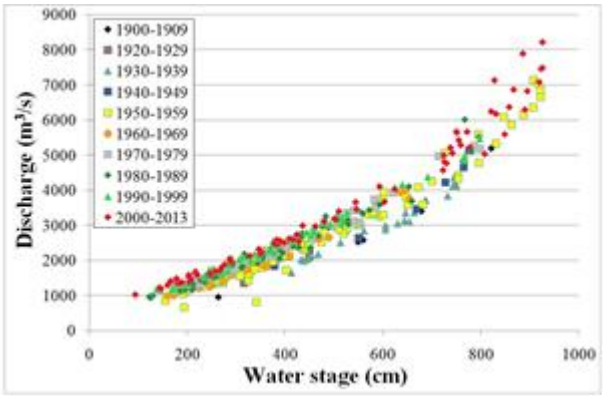

Fig. 6 Relationship between water stages and discharges measured at Mohács

Horizontal changes in the channel of the Danube near Bogyiszló

In the first analysed year (1952) there were only two bars (area: 0.046 km^2) which developed behind groynes, downstream of the mouth of a tributary (Sió River, at 1496 fkm; Fig. 7). In the following year (1953) more bars formed behind the newly built groynes. At the 1500 fkm

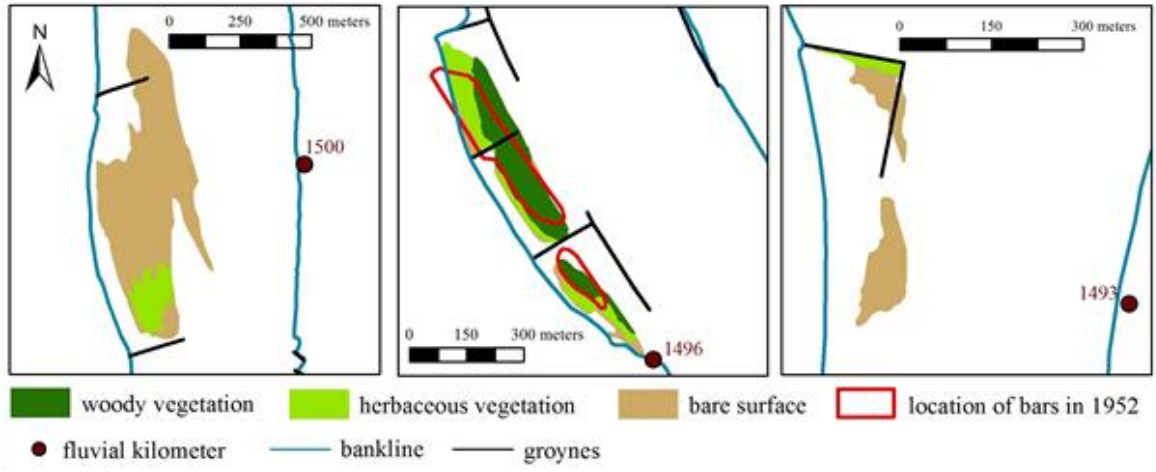

Fig.7 Location of bars (1953) in the studied section of the Danube near Bogyiszló

a large bar evolved (area: 0.22 km^2) with some herbaceous vegetation. The area of already existing bars increased (to 0.88 km^2), and by now their surface was covered by woody vegetation. In the bend, in the southernmost part of the study area (1493 fkm) new sand bars formed without vegetation.

The location and area of bars changed considerably until 2000 (Fig. 8). Along the uppermost section (1498–1502 fkm) islands developed behind each groynes, and they were already completely colonized by forests. In the bend along the southern section of the study area, the inlet of an oxbow lake became closed by a sediment plug and a small island became connected to the riverbank. Besides three more bars were formed, one of them was covered by herbaceous. In this year the total area of the bars and island was 0.4 km^2.

By 2011 the area of bars and islands doubled (0.85 km^2) and they became common along the whole studied reach. It could be explained by the increasing duration of

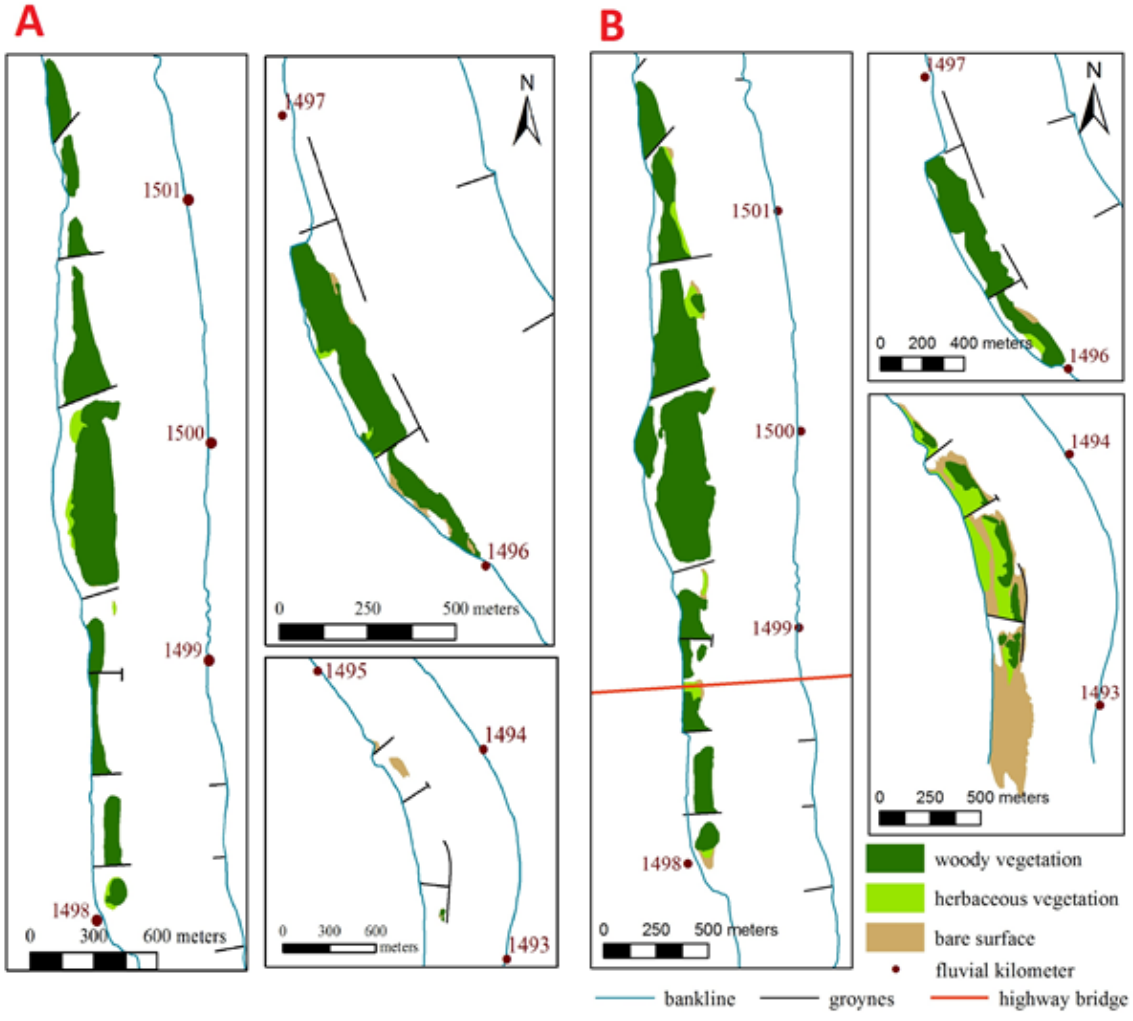

Fig.8 Location of bars and islands in the study area in 2000 (A) and in 2014 (B)

low stages, the drop of their level, and the lack of significant flood which could have eroded the material of the islands and bars. The most intensive aggradation was typical in the bend at the downstream section of the study area, as here the area of islands and bars increased from 0.13 km^2 to 0.29 km^2 within one year.

On the last aerial photo (2014) the morphology of the reach remained the same as it was in 2011 (Fig. 9). The total area of bars and island increased by 0.04 km^2 and the area of woody vegetation increased on the islands north of 1498 fkm. The number of bars decreased though their total area increased, probably because the bars coalesced and the water level decreased at the time of the shots of the aerial photographs (2011: 72 cm, 2014: 36 cm).

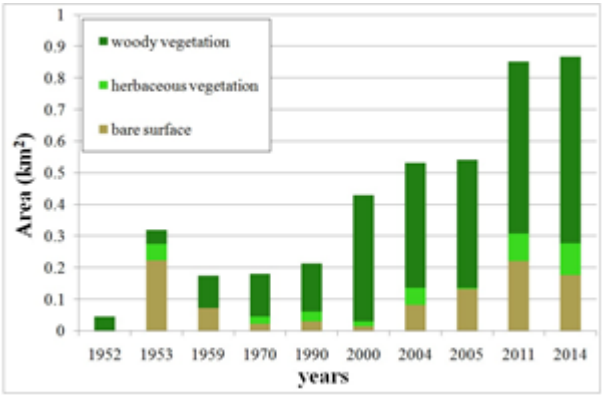

Fig. 9 Changes in total area and vegetation cover of the studied section of the Danube between 1952 and 2014

Reviewing the processes it could be stated that in the northern section of the study area (upstream of 1498 fkm) bars and islands are spatially permanent features, and they have not changed significantly since their formation. In contrary, in the southern, downstream section they are more changeable, as their material could be eroded and transported away easily during floods, and they could coalesce during low water stages. The more dynamic formation and development of these forms could be the resulted of the closeness of the thalweg.

Between 1990 and 2000 the number of bars doubled (from 4 to 10), due to the increased duration and frequency of low water stages and the descending water level. In the first decade of the 21st c. the number and size of wooded islands increased, while the area of bare and herb vegetated bar surfaces fluctuated (Fig. 9). This could only be explained by the changes in water stages, as due to descending water stages the higher surfaces of bars become watertight, thus vegetation could colonize them, while lower bars still have bare surfaces, as they are in the zone of fluctuating water level, thus they develop more dynamically as their material could be transported away by smaller flood waves.

As a result of bar formation the width of the channel decreased considerably. While in the 1950's the average channel width was 600 m, in 2014 it became 480 m. The most significant narrowing took place at 1500 fkm, where the width of the channel decreased from 780 m to 445 m.

CONCLUSIONS

At the lower section of the Hungarian Danube the height of low stages decreased by 136 cm (1.2 cm/y) during the analyzed period (1900–2013). The duration and frequency of low stages increased, and their level decreased, thus for example between 1900 and 1909 water stages exceeded 315 cm in 90 % of the decade, whilst between 2000 and 2013 they only exceeded 179 cm accordingly. On the other hand, the height of yearly highest (flood) stages became more scattered, and the frequency of record-high flood stages increased. The analysis of the relationship between water level and discharge values refers to significant changes in water regime and in river channel.

Simultaneously with the water level drop, the number of bars quadrupled in the analyzed section of the Danube between 1952 and 2000. This process became accelerated in the 1990's, when low water stages (≤315 cm) were measured almost in half (43 %) of the decade, while in the 1980's they occurred only in 33 % of the decade. As a result, sediment accumulation began behind the groynes, and woody vegetation could colonize the surface stabilizing the material of bars. The duration of low stages continued to increase (48%) in the 2000's, thus the number and area of bars continued to raise and woody vegetation could spread on their surface.

Development of bars has feedback on water stages and on the development of the river channel, as due to bars the river channel becomes narrower, which affects the height of flood stages and results in intensive riverbed incision. In the study area the average width of the channel decreased from 600 m to 480 m, though at some places it became narrower by 330 m (by 45%).

These changes affect shipping, as due to riverbed incision and decrease of low water stages, lowest shipping water levels have to be stated at lower and lower water stages. On the other hand, drop of characteristic water stages affect water management, as water extraction will face difficulties, thus irrigation and industrial cooling water supply will be limited in the future.

Acknowledgements

The research was funded by TÁMOP-4.2.1.D-15/1/KONV-2015-0002, HUSRB/1203/121/130 and NKFIH K-119193 projects.

References

Blanka, V. 2010. Kanyarulatfejlődés dinamikájának vizsgálata természeti és antropogén hatások tükrében. PhD thesis, 50–60. (in Hungarian)

Bonacci, O., Oskoruš, D. 2008. The influence of three Croatian hydroelectric power plants operation on the river Drava hydrological and sediment regime. 24th Conf. of the Danubian countries, 11p.

Geng, Q., Hui, X., Hu, G.X., Hui, Z.Y. 2012. The Change and Effect Factors of Water Level in Jingjiang River, *Int. Conf. on Modern Hydraulic Engineering* 28, 165–170.

ICPDR, 2014. Hydropower Plants in the Danube River Basin Online at: https://www.icpdr.org/main/sites/default/files/nodes/documents/map_hydropower_june_2014.pdf

Ihrig, D. 1973. A magyar vízszabályozás története, OVH, Budapest (in Hungarian)

Kiss, T., Andrási, G. 2011. A horvátországi duzzasztógátak hatása a Dráva vízjárására és a fenékhordalék szemcseösszetételének alakulására. *Hidrológiai Közlöny* 91 (5), 17–29. (in Hungarian)

Kiss, T., Blanka, V. 2012. River channel response to climate- and human-induced hydrological changes: Case study on the meandering Hernád River, Hungary. *Geomorphology 175*, 115–125. DOI: 10.1016/j.geomorph.2012.07.003

Kiss, T., Andrási, G. 2011. A horvátországi duzzasztógátak hatása a Dráva vízjárására és a fenékhordalék szemcseösszetételének alakulására. *Hidrológiai Közlöny* 91 (5), 17–23. (in Hungarian)

Kiss, T., Andrási, G. 2015. A Dráva menti ártéri élőhelyek átalakulása. In: Rakonczai, J., Blanka, V., Ladányi, Zs. (eds): Tovább egy zöldebb úton. SZTE-TFGT, Szeged, 164–173. (in Hungarian)

Kiss, T., Andrási, G. 2015. Kanyarulatfejlődés sajátosságai és antropogén hatások vizsgálata két Drávai kanyarulat példáján. *Tájökológiai Lapok* 13 (1), 73–88. (in Hungarian)

Kiss, T., Balogh, M., 2015. Characteristics of point-bar development under the influence of a dam: case study on the Dráva River at Sigetec, Croatia. *Journal of Environmental Geography* 8 (1–2), 23–30. DOI: 10.1515/jengeo-2015-0003

Kiss, T., Sipos, Gy., Fiala, K. 2011. Az Alföld töltések közé szorított folyói. In: Rakonczai, J (ed): Környezeti változások és az Alföld. A Nagyalföld Alapítvány Kötetei 7, Békéscsaba, 211–222. (in Hungarian)

Rákóczi, L. 2000. A Duna-meder sorsa Szap és Szob között. *Vízügyi Közlemények* 82 (2), 262–284. (in Hungarian)

Sipos, Gy. 2006. A meder dinamikájának vizsgálata a Maros magyarországi szakaszán. SZTE-TFGT, PhD thesis, 21–54. (in Hungarian)

Somogyi, S. 2001. Természeti és társadalmi hatások a Duna mai vízrendszerében. *Földrajzi Értesítő* 50 (1-4), 299–309. (in Hungarian)

VITUKI, 2007. A Duna hajózhatóságának javítása tárgyú projektet megalapozó tanulmány. Budapest, 29–97. (in Hungarian)

Williams, G.P., Wolman, M.G. 1984. Downstream effects of dams on alluvial rivers. USGS Prof. Paper 1286

Internet references:

[1] http://nepszava.hu/cikk/1015462-lmp-a-duna-duzzasztasaval-jarhat-paks-bovitese

JOURNAL OF ENVIRONMENTAL GEOGRAPHY
Journal of Environmental Geography 9 (1–2), 7–13.
DOI: 10.1515/jengeo-2016-0002
ISSN: 2060-467X

ANALYSIS OF URBAN SPRAWL DYNAMICS USING GEOSPATIAL TECHNOLOGY IN RANCHI CITY, JHARKHAND, INDIA

Firoz Ahmad[1], Laxmi Goparaju[2]*

[1]Department of Remote Sensing, Birla Institute of Technology, Ranchi Ormanjhi road, Mesra, Ranchi 835215, Jharkhand, India
[2]Vindhyan Ecology and Natural History Foundation, 36/30 Station Road, Dhauru Pur, Mirzapur 231001, Uttar Pradesh, India
*Corresponding author, e-mail: goparajulaxmi@yahoo.com

Research article, received 1 March 2016, accepted 11 May 2016

Abstract

The availability of remote sensing satellite data at various spatial, temporal and spectral resolutions provides enormous opportunity to map the urban sprawl. When coupled with Geographic Information System (GIS) it is possible to evaluate, analyse and integrate large data. We need to understand and quantify the urban sprawl on spatial and temporal scales which forms a basis for better planning and sustainable management of cities and towns. The city of Ranchi has witnessed unprecedented urban growth after assuming the status of a capital of Jharkhand state, India in 2000. The increasing population has put pressure on the natural resources of the city. The urban growth has been in a haphazard manner at the cost of agricultural lands, forest land and open green spaces such as park, garden and recreational forestry.

The present study analysed the urban sprawl in Ranchi city, using Landsat data from 1976, 2002 and 2015. The study revealed that the annual urban growth rate was 1.76 ha/yr over the period from 1976 to 2002 whereas the annual growth rate was 2 ha/yr over the period from 2002 to 2015. The northern side of the city has witnessed more expansion in 2002 when compared with the growth in 1976. Increase in urban density was seen at the distances of 3, 4,5,6,7 and 8km between 1976 and 2015 and the rate was higher than 25%.The driving factors of the development were infrastructure, educational and business expansion. Thus, spatial analyses of urban sprawl are a prerequisite for curbing the unplanned urban growth and ensure sustainable living.

Keywords: urban sprawl, geospatial, Landsat, Ranchi, urbanization

INTRODUCTION

The ever increasing population has led to the rise in unplanned urban growth in the suburbs of the city which is usually termed as urban sprawl (Theobald, 2001; Bugliarello, 2003). Urban growth on one hand is an indicator of economic, social and political growth whereas, on the other hand it is at the cost of forests, agriculture lands, orchards and greenery of the city (Torrens and Alberti, 2000; Barnes et al., 2001). There are several definitions which define urban sprawl; Bhatt et al. (2010) had described it as an unplanned and uneven pattern of growth driven by various processes finally leading to inefficient resource utilization. There are several negative impacts associated with urban sprawl, some of them are having an impact on ecosystem and forests leading to fragmentation of habitats (Macie and Moll, 1989) increase in air/water pollution and greenhouse gases due to increase in fossil fuel consumption (Stoel, 1999) and increase in traffic congestion (Silambarasan, 2014).

Accelerated urbanization is the current scenario in India, one of the most populated nations of the world. The urban population in 1901 was 26 million, which rose to 62 million in 1951. The period between 198 and 1991 witnessed a rise to a figure of 285 million, accounting 27.8% of the total population (Jaysawal and Saha, 2014). The degree of urbanization varies in different states of India, with Goa being the most urbanized state constituting 49.77% of the urban population. Other states like Gujarat, Karnataka, Rajasthan, Madhya Pradesh, Bihar and Jharkhand are reported to have medium urbanization (Census, 2001).

It is necessary that urban sprawl is quantified and studied at local and regional scales such that proper measures are taken to ensure sustainability in urban planning. The parameter which can be used to quantify it is the built up area (Epstein, 2002). The conventional methods of mapping are time consuming and require heavy manpower, thus becoming a Herculean task. An advanced technological approach which is able to provide us accurate information over different time scales is required. In light of this, satellite remote sensing data in conjunction with Geographic Information Systems (GIS), provides an opportunity to study urban sprawl (Pande et al., 2012; Longeley, 1999). In the past four decades in India, satellite remote sensing data have been used extensively to monitor Earth's natural resources and study the changes taking place on the surface over different time periods.

Several studies have analysed urban sprawl at regional, local and temporal scales (Boori et al., 2015; Griffiths et al., 2010). The urbanization pattern of the greater Asmara area in Eritrea was studied using satellite remote

sensing data of Landsat. They analysed land use/ land cover change using a data object based image analysis and urban sprawl using Shannon entropy (Tewolde and Cabral, 2011). Urban sprawl of the Ajmer city (Rajasthan was studied at mid-scale level for 25 years (1977-2002) where they used Landsat TM,MSS,ETM+, and IRS LISS III data (Jat et al., 2008). Landsat imagery of Kansas City of United States of America (USA) was used to generate a time series of land cover data over the past three decades (Wei et al., 2006). Long term trends and patterns of urban sprawl were studied. in south India and its surrounding area, by Rahman et al. (2010) using IRS P6 data and topographic sheets in the GIS domain along with Shannon's entropy model to assess the urban sprawl. In the Udupi district of Karnataka state in India, Urban sprawl patterns were analysed using (LISS and PAN images of 2003 and LISS IV and Cartosat images of 2013), which showed that barren /waste land was also converted to settlement /built up area (Silambarasan, 2014).

Singh et al. 2014 have studied the urban expansion in Ranchi city during the period from 1996 -2007 using an IRS LISS III sensor. Similarly, Pandey et al. (2012) using Cartosat –I stereo pairs satellite images studied the urban built up area of Ranchi township for over a period of eight decades (1927-2010). The present study is an attempt to quantify urban sprawl in the Ranchi city for a period of 39 years using Landsat data of 1976, 2002 and 2015.

The city which is the 46 th largest urban cities in India and the third largest in the state after Jamshedpur and Dhanbad (Census, 2011). It is known for coal belts and forests (Jha, 2016). The population is mainly dominated by tribes whose primary source of income is derived from agriculture, cattle farming and collection of forest produce. Deforestation, which is a consequence of urbanization has left these forest dependent communities in a pitiable situation. Low agriculture produce and poor economic condition of farmers has led them to migrate to better places in the vicinity of major towns. Establishment of Industries, infrastructure development, education and health facility etc. have attracted rural population to capital city (Kumar et al., 2011).

The objectives of the present study are 1) evaluating the urban growth in Ranchi city for the years 1976, 2002 and 2015 using Landsat data and GIS. 2) Analysing and quantifying the urban sprawl of Ranchi city during the three time periods mentioned above. It is believed that the urban growth or expansion has taken place more rapidly after the creation of the capital city of Ranchi. Thus, the study aims to analyse the urban growth patterns before and after the formation of the capital city.

STUDY AREA

The study area is the city of Ranchi. It is the capital of Jharkhand state of India, which was, carved out of the Bihar state on 15th November 2000. The southernmost part of the earlier state of Bihar constitutes Jharkhand. Since then it has progressed as a capital city opening opportunities for new employment, trade and infrastructure development. The city is located between 85^0 13' to 85^0 25'E and 23^0 13' to 23^0 26' N. The latitude and longitude of city center are 23°22′N; 85°20′E. The average elevation

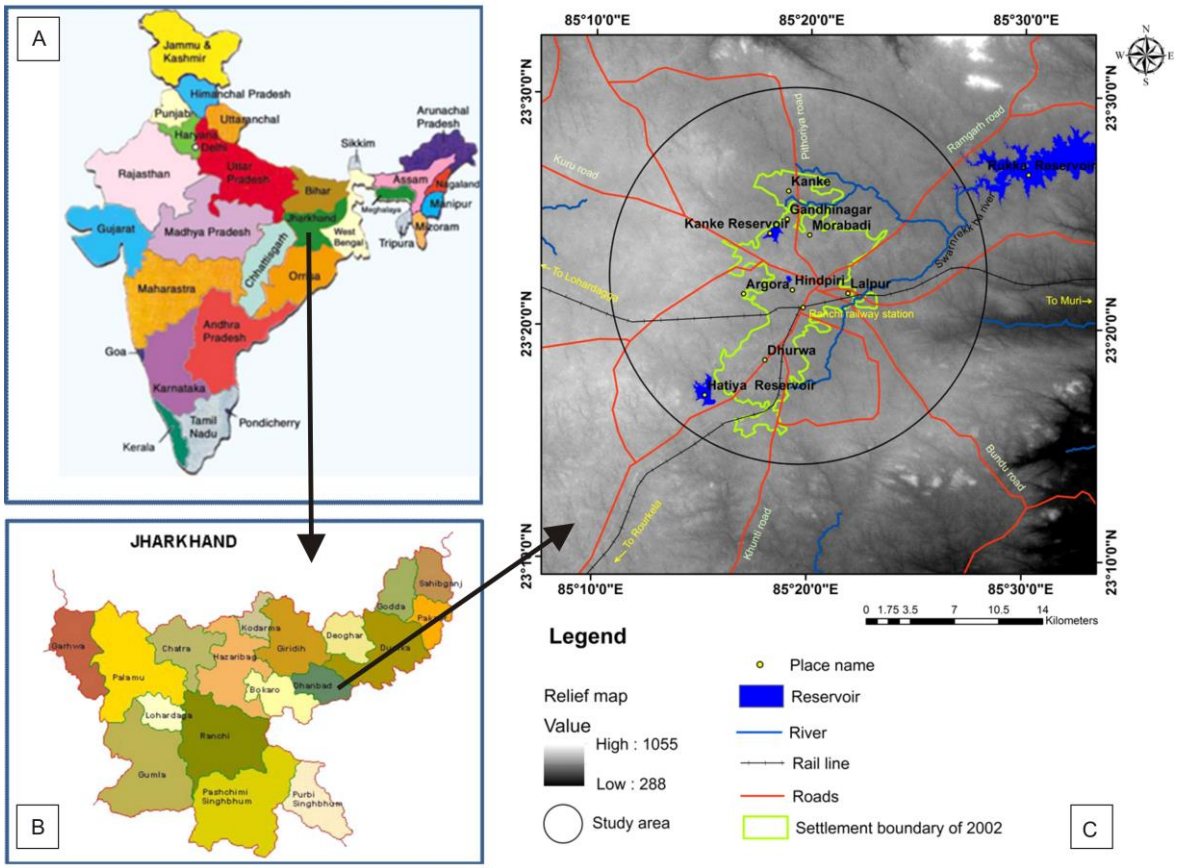

Fig. 1 The location of the study area A) map of India B) map of Jharkhand and C) relief map of the study area

of Ranchi city is 652 m from sea level. Its municipal area is 175.12 km^2. The city is adorned with numerous waterfalls and is also known as "City of waterfalls". The local river system constitutes Subarnarekha and its tributaries. The city's water supply is fulfilled by Kanke, Rukka and Hatia dams (Pandey et al., 2012).

The pleasant climate of Ranchi prevalent throughout the year is because of its location and the surrounding forests. It was once the summer capital and was given the status of the hill station. Summer temperatures range from 20 °C to 42 ^{0} C, winter temperatures from 0 °C to 25 ^{0} C degrees. The coolest months are December and January. The annual rainfall is about 1430 mm (56.34 inches). Figure 1 shows the location of the study area.

The census in India is conducted at an interval of ten years. The population of Ranchi city as per census data for the past four decades is as follows: In 1971, 255 thousands of human population; in 1981, 489 thousands; in 1991, 599 thousands; in 2001, 846 thousands and in 2011, 1073 thousands (Ranchi Master Plan 2037, 2015).

MATERIAL AND METHODS

Image acquisition and preprocessing

The satellite image used for the analysis was of Landsat 2 MSS (1976); Landsat 7 ETM + (2002) and Landsat 8 (TIRS) for the year 2015. The details of the data are given in Table 1.The satellite data selected was cloud free. All the datasets were downloaded from United States Geological Survey (USGS) website as a georeferenced data set. The images were corrected for radiometric and atmospheric distortions during the pre- processing stage. The data obtained was in a Geo TIFF format for each individual band. The various bands were layer stacked to produce a composite image which was converted into IMG format for further study and analysis. Image processing software used was ERDAS Imaging (version 9.0) and ARC GIS Spatial Analyst (version 10.1).

Table 1 Details of satellite data

Image Dates	20-12-1976	23-12-2002	9-5-2015
Spacecraft	Landsat 2	Landsat 7	Landsat 8
Sensor	MSS	ETM+	OLI_TIRS
Spatial resolution (m)	60	30 15 (PAN)	30 15 (PAN)
Radiometric resolution (bit)	8	8	16
Number of bands	4	8	11
Path / Row	151/44	140/44	140/44
Projection	UTM	UTM	UTM
Zone	45	45	45
Datum	WGS84	WGS84	WGS84
Ellipsoid	WGS84	WGS84	WGS84

Image classification

The bands utilized for analysis are Landsat MSS (4, 3, 2); Landsat 7 ETM+ (5, 4, 3) and Landsat 8 (5, 4, 3). The study area was extracted from the false colour composite (Fig. 2). The images retained their original pixel size despite the chances that there might be a difference in classification accuracies. To maximize correspondence between classified maps, a uniform methodology was applied on each dataset.

The urban area boundary was visually interpreted on false colour composite and extracted from each of the datasets of three time periods. On FCC it appears as cyan/white and of various geometric shapes such as rectangle, square, etc. In each of the extracted urban area data, Normalized Difference Vegetation Index (NDVI) was executed to delineate the vegetation classes in the urban landscape by using the density slicing method (Singh, 1989; Pilon et al., 1988). The NDVI is the best suited index to delineate vegetation from the FCC.

An unsupervised classification approach is a classification procedure based on ISODATA algorithm, in which the similar pixels are assigned into a group (Lillisand and Keifer, 2004). Thus, it was used for extracting water and urban (settlement). Finally vegetation, urban and water were integrated in one layer using the ERDAS Imagine model maker. Flowchart (Fig. 3) shows the methodology adopted for the following study.

Thus, according to Anderson (1976) we successfully delineated first level of LULC classes, namely vegetation, water and urban for each time period. The description of various classes is mentioned in the given Table 2. Accuracy assessment is a significant step in image classification for evaluating quality of classified image (Forkuoand and Frimpong, 2012). Accuracy assessment was computed for each classified dataset using a stratified random sampling method wherein 100 points were generated for each category and each point was assigned to the respective class based on ground knowledge.

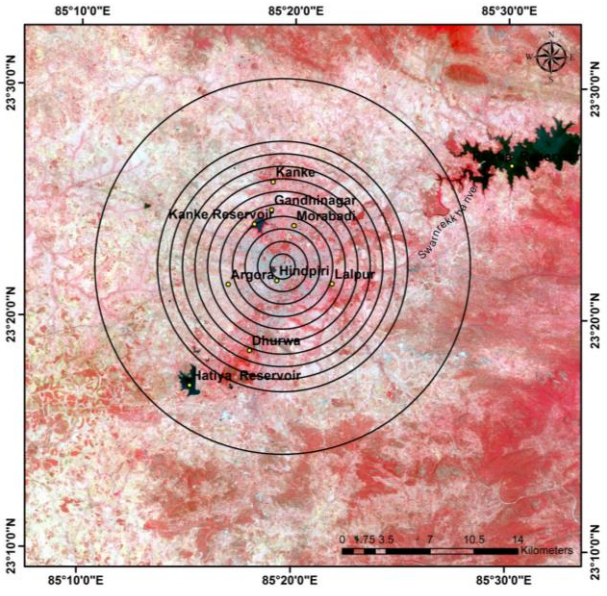

Fig. 2 The study area –false colour composite (FCC) of Landsat data (2015). The bands used are NIR-Band 5, R-Band 4, and Green-Band 3 along with multi buffer ring around the city

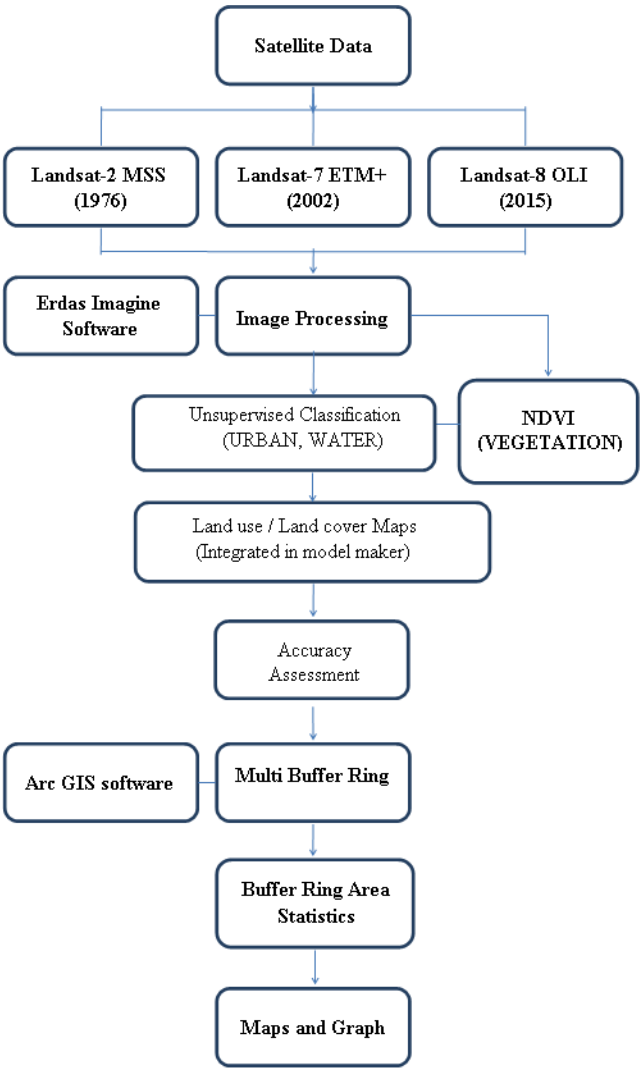

Fig. 3 Flow chart explaining the methodology

Table 2 Description of land use/land cover classes

Urban/built up	Residential, Commercial, Industrial , Transportation, Roads, Mixed urban and Open in urban
Vegetation	Agriculture, Plantation, Parks, Orchards and Forest
Water bodies	Dams or Reservoirs, Ponds, River, Lakes, Stream, Seasonal waterlog area

After classification of the images, multi buffer rings were created in Arc GIS (using the multiple ring buffer option), specifying the distance of 1 km from the city centre. Ten such rings were generated each ring of 1 km buffer. Beyond the tenth ring, one ring of 5 km buffer was generated. In ERDAS Imagine the matrix option of GIS utility was utilized to extract the area of each class in different ring. The city center point of our study is taken Firayalal Chowk (latitude and longitude 23°22′12" N; 85°19′30" E).

The matrix generated for all the time periods were analysed in MS EXCEL for urban density and urban growth rate using the following formulae (1) respectively:

$$UD = \frac{SA}{TA} \quad (1)$$

where UD means urban density of the specified ring, SA implies settlement area of the specified ring and TA means total area of the specified ring.

Urban growth rate

In order to monitor the spatial distribution of urban expansion intensity, we adapted the annual urban growth rate index (AGR). Annual urban growth rate (AGR) is used for evaluating the speed of urbanization (Maquboli et al., 2015; Boori et al., 2015). AGR (2) is defined as follows (Xiao et al. 2006):

$$AGR = \frac{UA_{n+i} - UA_i}{nTA_{n+i}} \times 100\ \% \quad (2)$$

where AGR means annual growth rate, A_{n+i} refers to the total land area of a ring, and nT is the interval of time (No. of years) between initial and final year; UA_{n+i} denotes the urban area at the final year whereas UA_i denotes the urban area at the initial year.

RESULTS AND DISCUSION

Land use/land cover maps

The final output map of land use/land cover shows three major categories that are vegetation, settlement (urban/built-up) and water (Fig. 4). The overall accuracy of the land use/ land cover of the year 1976, 2002 and 2015 were 90%, 92% and 92% respectively. The kappa accuracy, noted was 0.83, 0.87 and 0.87 respectively. The complete area statistics of land use/land cover of the year 1976, 2002 and 2015 is given in Table 3.

For all the three time periods analysed, it is seen in table 3 that there is an increasing trend in the urban area from 1976 (5034.16 ha), 2002 (10,335.24 ha) and in 2015 (14,561.39 ha) whereas the area of vegetation first decreased from 10.69% in 1976 to 9.23% in 2002 and later slightly increased to 9.71% in 2015. The area of water has first increased from 0.53% to 1.38 % from 1976 to 2002 and later on reduced to 0.81% in 2015 (Table 3). The increase in water is attributed to the fact that in 1976, the Kanke dam site was not included in urban built up area, in 2002; the Kanke dam reservoir has been included. Whereas in 2015 the decrease in water body is because of seasonal variation as the data belongs to the summer season.

Later using the Equation 2 and details from Table 3, urban growth was calculated. It was seen that 58.53% growth in built up area (settlement) over the period of 39 years from 1976 to 2015. In the first 26 years (from 1976-2002), urban growth was 45.84% at an average annual growth rate of 1.76 ha/yr. In between time period (2002 – 2015) over the period of 13 years urban growth was

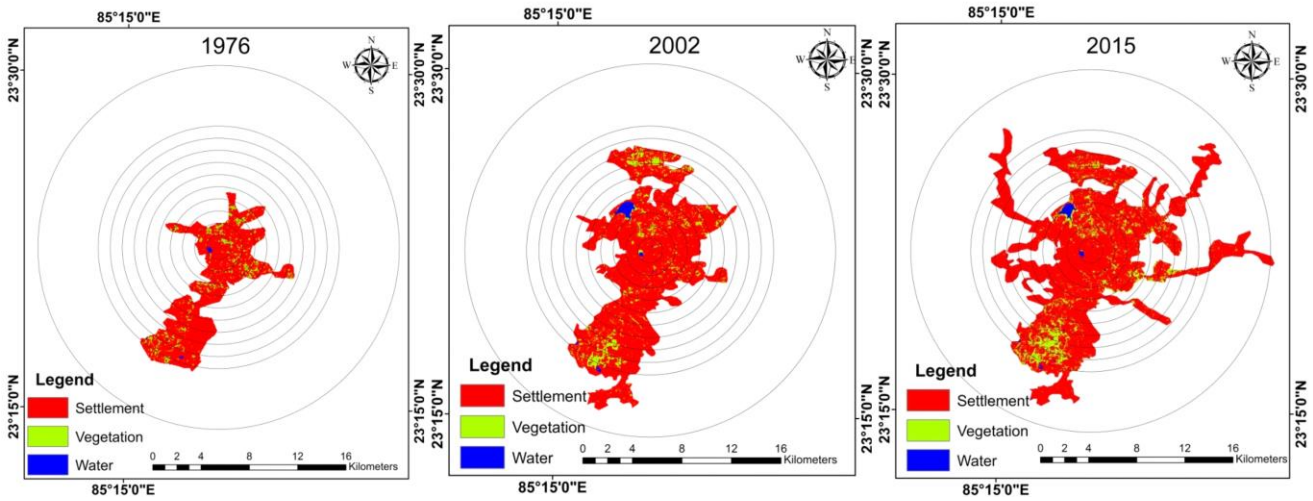

Fig.4 Multi buffer ring around the city overlaid on Land use/Land cover map in 1976, 2002 and 2015

25.96% with the average annual growth rate 2 ha/yr. Thus, the city expanse rate has increased furthermore 13.6% (0.24 ha/year.) over the period of 2002 to 2015 when compared with the period 1976 to 2002 (Fig. 5).

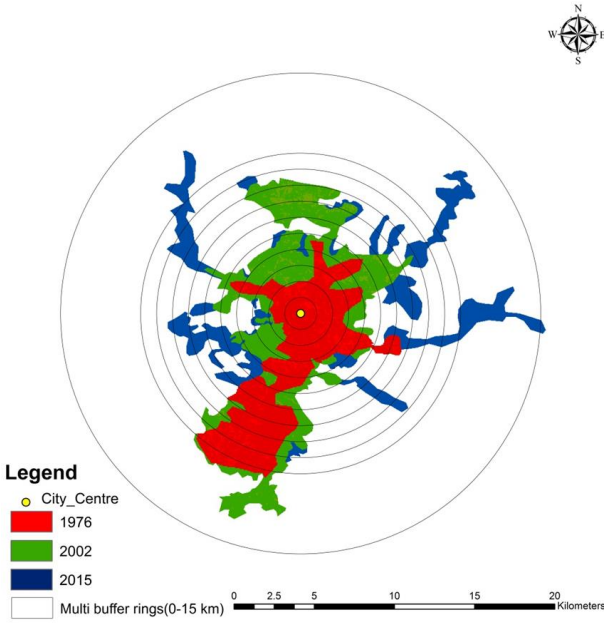

Fig.5 Urban growth of Ranchi city

Urban density patterns and urban growth rate

The city (Land use/Land cover class) density patterns around the city center were also examined to ascertain whether different zones have represented different densities. Figure 6 shows 11 (10+1) buffer ring zones from 1 to 10 km at a distance of 1km each and one 5 km buffer ring from 10 to 15 km distance. The observations show that it has been reasonably true that the first three zones represent the areas that are within the walking distance from the city center.

It is observed that in the city center, the urban density was more than 85% for the last 39 years. In 1976, urban density was reduced dramatically around 50.8% on the distance of 3 km from the city center and 15.6% on 5 km, and less than 1 % at 15 km (11th ring).

When comparing the time periods of 1976 and 2015 on the distances of 3, 4, 5, 6, 7 and 8 km, the urban density has increased very high (more than 25%).If we compare only the time periods of 1976 and 2002 at the distances at 3, 4 and5 km, the urban density has highly increased (more than 25%). From 2002 to 2015, at the distances of 7 and 8 km, urban density was increased (more than 15%) (Fig. 6).

In 1976, at the city center urban density was 86%, the share of vegetation was 8.6%, and water was 5.3% (Fig. 6). From 1 to 2 km distance from the center, the urban/built-up area reduces to (76.13%) and

Table 3 Zonal statistics of land use/land cover (1976, 2002 and 2015)

Land use/ land cover	Area in 1976 (ha)	%	Area in 2002 (ha)	%	Area in 2015 (ha)	%
Urban (settlement)	5034.16	88.77	10335.24	89.38	14561.39	89.46
Vegetation	606.24	10.69	1067.49	9.23	1581.74	9.71
Water	30.61	0.53	160.11	1.38	133.01	0.81
Total	5671.01	100	11562.84	100	16276.14	100

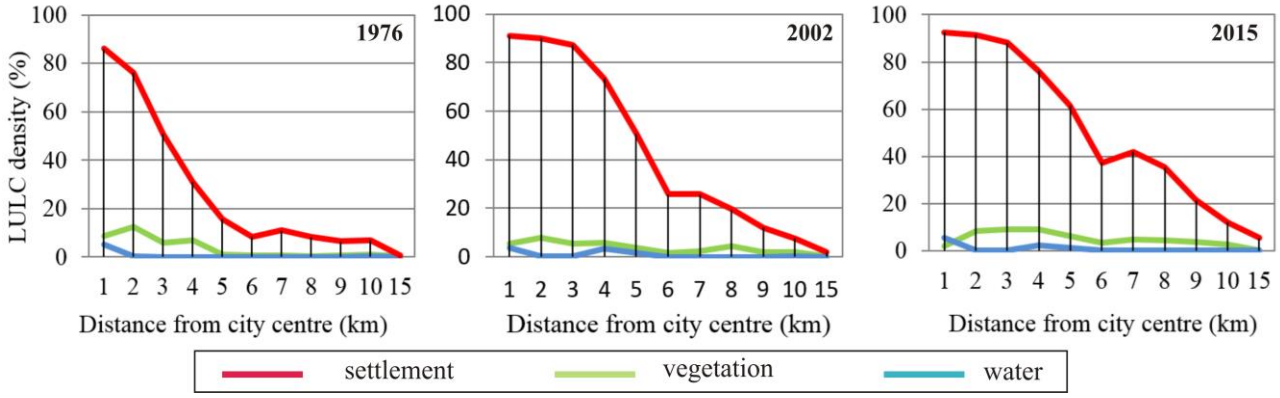

Fig.6 Land use/Land cover class density percentage from 1-15 km distance for 1976, 2002 and 2015

vegetation increases to 12.3%. From 2 to 3 km distance from the center, the urban/built-up area reduces to (50.8%) and vegetation also reduced to 5.82%. From 4- to 6 km distance, both urban and vegetation classes were showing a decreasing trend.

In 2002, the city center urban density was 91%, the share of vegetation was 5.3%, and water was 3.7% (Fig. 6). At a distance of 1-2 km from the center, the urban/built up area is more or less the same (90%) whereas vegetation has increased up to 7.7%. At a distance of 2 to 3 km from the center, the urban/built-up area very slightly reduces to (87.3%) and vegetation has reduced to 5.35 %. At a distance of 4 to 5 km from the center, the urban/built-up area sharply reduces to 50.78% and vegetation has also shown a decrease of 3.6 %. From 5 to 6 km distance from the center, the urban/built-up area sharply reduces to 25.74% and vegetation has reduced to 1.58 %. At 15 km (11th ring) the urban/built-up area was 2% and vegetation has decreased to less than1 %.

In 2015 (Fig. 6) at the city center, urban density was noted was 92.6% and vegetation was 2%, and water was 5.3%. From 1 to 3 km distance, urban/built-up areas reduce at a slow pace to 88.2 %, but the vegetation area increased to 9.1 %. From 6 to 7 km distance from the center, the urban/built-up area increased to 42 % and vegetation has increased to 4.85 %. From 7 to 8 km distance from the center, the urban/built-up area reduces to 35.37% and vegetation has reduced to 4.54 %. From 1 to 8 km distance from the center, the urban/built-up area has always been found to be greater than 35 % in 2015 whereas urban/built-up area was always found to be greater than 35%, in 2002 is up to 1 to 5km distance. Urban/built-up density and vegetation is continuously showing decreasing trend from 7 km onwards to 15th km(11th ring) reached up to 5.3 %, 0.27% respectively at 11th ring.

Description of spatial expansion

It is observed that in 2002 the northern side of the city has more urban growth as compared to the growth in 1976 as seen in Figure 4. The city has witnessed growth and development in north east, north west, west and south from the core of the city. It has been noticed that major growth is concentrated along national highways (NH-23, NH-33 and NH-75) which serve as major transportation corridors. Even though it is observed that built up development took place in Ranchi in a haphazard manner (Kumar et al., 2011). Since past 83 years as records say the township has increased more than six times (Pandey et al., 2012). Earlier the built up area was concentrated around the city center like Ranchi lake and northern parts like Kanke, later, after 1976, a sudden increase built up area in north, east and west of the city centre was seen. A whole sale vegetable market Pandra Mandi is situated at a distance of 8 Km from the city centre (along NH-75), which is a hub for villagers to sell their produce. It is equipped with modern facilities to store the farm produce. Various institutes like Indian Institute of coal management (established in 1994) in Kanke, Reliance Mega mart, Birsa Agricultural University (Faculty of Forestry established in 1980) are some of the major institutes and shopping complex in this area.

In the north of the city, along Kanke dam are new establishments in localities like Morabadi, Jawahar Nagar and Gandhinagar. New colonies such as Pundag, Nijam Nagar and Bhitha Basti have sprouted which once bore a deserted look few years ago. National Highway (NH-23) in northeast leads to Mesra which has become an educational hub with various new technical and educational Institutions. In the south of the city after Ranchi became a capital, massive expansion of Ranchi airport is seen. It is an extension of Doranda locality and with the development people have started residing there too. In the west is the Harmu Nadi, where once open fields were there, now taken over by residential and commercial establishments. Engineering and Medical colleges have come up in areas like Baryatu, Tatisilwai and Namkum, which are on the outer fringes of the Ranchi city. In 2007, Khelgaon a sports complex has also been established at Hotwar (along NH-23) during the national games.

Future growth is likely to be noticed in and around areas like Kanke, Bariayatu, Ratu, Buti, Namkum, Tatisilwai and Hatia. Thus, the increase in built up area has been at the cost of agriculture and open fields. Higher development is observed in low elevation zones due to availability of ground water (Pandey et al., 2012). As over a period of time, demand for water has increased, putting at stake the water bodies in the Ranchi urban area.

CONCLUSIONS

The above study shows that coarse resolution satellite data like Landsat can be successfully used to monitor the urban sprawl of Ranchi city. The study quantifies the urban sprawl at various distances from the city centre. Simultaneously, changes in vegetation and water were also noted. Initially the urban/built up area was concentrated in the city centre, which gradually spread both north and south directions. Mostly land used for urbanization was open spaces in the city and left over lands between adjoining buildings. Later, vegetated areas were also converted to built up area. As a result, the city has witnessed increase in traffic congestion, pollution, and loss of the green cover, erratic rainfall and unpleasant weather.

In order to achieve sustainability in urban planning, we should develop the open spaces as parks, playgrounds and nurseries. Along roadsides spaces should be spared for planting trees which provide shade and purify the polluted air. Water bodies should not be encroached for residential purposes. A buffer around them must be left before any construction work is undertaken. Water conservation practices should be encouraged by the government as well as the public to combat the water crisis in the future.

Such data are vital information for city planners and managers to curb unplanned urban growth provide proper drainage facility and ensure that the natural resources are not exploited badly. Incorporating such data in town planning and management would benefit the citizens and further ensure a sustainable livelihood.

Acknowledgements

The authors are grateful to USGS portal for the free download of Landsat data which was used in the analysis. We are also grateful to the reviewers for providing valuable suggestions.

References

Anderson, J.R., Hardy, E. E., Roach, J.T., Witmer, R.E. 1976. A land use and land cover classification system for use with remote sensor data. Geological survey professional paper No. 964 (Washington, D.C., United states government printing office).

Barnes, K.B., Morgan III, J.M., Roberge, M.C., Lowe, S. 2001. Sprawl Development: Its patterns, Consequences, and Measurement. Towson University, Towson.

Bhatta, B., Saraswati, S., Bandopadhyay, D., 2010. Urban sprawl measurement from remote sensing data. *Applied Geography* 30 (4), 731–740. DOI: 10.1016/j.apgeog.2010.02.002

Boori, M.S., Netzband, M., Choudhary, K., Vozenilek, V. 2015. Monitoring and modeling of urban sprawl through remote sensing and GIS in Kuala Lumpur, Malaysia. *Ecological Processes* 4, 15. DOI: 10.1186/s13717-015-0040-2

Bugliarello, G. 2003. "Large urban concentrations: A new phenomenon," In Reader,A., Heiken,G., Fakundiny, R., and Sutter, J,(eds). Earth Science in the City: New York: American Geophysical Union, pp.7–19.

Census of India 2001. http:// www.censusindia.net

Census of India 2011. http://www.census2011.co.in/census/district/113-ranchi.html

Epstein, J., Payne, K., Kramer, E. 2002. Techniques for mapping suburban sprawl. *Photogrammetric Enggineering and Remote Sensing* 63 (9), 913–918. DOI: 10.1111/0031-868x.00005

Forkuoand, E.K., Frimpong, A. 2012. Analysis of Forest Cover Change Detection. *International Journal of Remote Sensing Applications* 2, 82–92.

Griffiths, P., Hostert, P., Gruebner, O., Van Der Linden, S. 2010. Mapping megacity growth with multi-sensor data. *Remote Sensing of Environment* 114, 426–439. DOI: 10.1016/j.rse.2009.09.012

Jat, M.K., Garg, PK., Khare, D., 2008. Monitoring and modelling urban sprawl using remote sensing and GIS techniques. *International Journal of Applied Earth Observation* 10, 26–43. DOI: 10.1016/j.jag.2007.04.002

Jaysawal, N., Saha, S. 2014. Urbanization in India: An impact assessment. *International Journal of Applied Sociology* 4(2), 60-65.

Jha, T. 2016. How can Jharkhand fight distress migration? Down to Earth.

Kumar,A., Pandey, A.C., Hoda, N., Jayseelan, A.T. 2011. Evaluation of urban sprawl pattern in the tribal dominated cities of Jharkhand state, India. *International Journal of Remote Sensing* 32 (22), 7651–7675. DOI: 10.1080/01431161.2010.527391

Lillesand, T. M., Kiefer, R. W. 2004. (5th ed.) Remote Sensing and Image Interpretation, John Wiley, New York.

Longley, P. A., Goodchild, M. E., Maguire, David, J., Rhind, R., David W. 1999. Geographic Information Systems Vol.I and II, John Wiley and Sons, New York.

Macie, E., and Moll, G. 1989. Trees and exurban sprawl. American forests, July/August, 61–64.

Makbouli,Y., Hakdaoui,M.,Ghafir,A., Elmutaki,S. 2015. Monitoring urban evolution between 1975 and 2015 using GIS and remote sensing technics: case of Lâayoune City (Morocco) Geomatic and Environment Laboratory, Department of Geology University Hassan II/Faculty of Science Ben M'sik- Casablanca: *International Journal of Advanced Research* 3 (10), 331–342.

Pandey, A.C., Kumar, A., Jayseelan, A.T. 2012. Urban built up area assessment of Ranchi township using Cartosat 1 stereopair satellite images. *Journal of Indian Society of Remote Sensing* 41 (1), 141–155. DOI: 10.1007/s12524-012-0209-4

Pilon, P.G., Howarth, P.J., Bullock, R.A. 1988. An enhanced classification approach to change detection in semi-arid environments. *Photogrammetric Engineering and Remote Sensing* 54 (12), 1709–1716.

Rahman, A., Agarwal, S.P., Netzband, M., Fazal, S. 2010. Monitoring urban sprawl using remote sensing and GIS techniques of a fast growing urban centre, India. *Applied Earth Observations and Remote Sensing* (1), 56–64. DOI: 10.1109/jstars.2010.2084072

Ranchi Master Plan 2037, 2015. Ranchi Municipal Corporation, Urban development Department, Jharkhand.

Silambarasan, K., Vinaya, M.S., Sureshbabu, S., 2014. Urban sprawl mapping and landuse change detection in and around Udupi town: a remote sensing based approach. *International Journal of Scientific Research Engineering and Technology* 2 (12), 815–820.

Singh, A. 1989. Digital Change detection techniques using remote sensing data. *International Journal of Remote Sensing* 10 (6), 989–1003.

Singh, U.S., Tomar, V., Pandey, P.C., Rani, M., Kumar, P. 2014. Geospatial strategy for assessment of urban change dynamics using LISS III- sensor. *Bulletin of Environmental and Scientific Research* 3 (4), 10–17.

Stoel, T. 1999. Reining in Urban Sprawl. *Environment: Science and Policy for Sustainable Development* 41, 6–16. DOI: 10.1080/00139159909604624

Tewolde, M.G., Cabral, P. 2011. Urban sprawl analysis and modelling in Asmara, Eritrea. *Remote Sensing* 3, 2148–2165. DOI: 10.3390/rs3102148

Theobald, D.M. 2001. Quantifying urban and rural sprawl using the sprawl index, in Annual Conf. Assoc. American Geographers, New York.

Torrens, P.M., Alberti, M. (2000). Measuring sprawl. Working paper no. 27, Centre for Advanced Spatial Analysis, University College, London.

Wei,J., Jia,M., Twibell, R.W., Underhill.K. 2006. Characterizing urban sprawl using multistage remote sensing images and landscape metrics. *Computers Environment and Urban systems* 30 (6), 861–879. DOI: 10.1016/j.compenvurbsys.2005.09.002

Xiao, J., Shen, Y., Ge, J., Tateishi, R., Tand, C., Liang, Y., Huang, Z. 2006. Evaluation urban expansion and land use change in Shijiazhuang, China, by using GIS and remote sensing. *Landscape and Urban Planning* 75, 69–80. DOI: 10.1016/j.landurbplan.2004.12.005

JOURNAL OF ENVIRONMENTAL GEOGRAPHY
Journal of Environmental Geography 9 (1–2), 15–21.
DOI: 10.1515/jengeo-2016-0003
ISSN: 2060-467X

OPEN SOURCE WEB GIS SOLUTIONS IN DISASTER MANAGEMENT – WITH SPECIAL EMPHASIS ON INLAND EXCESS WATER MODELING

Levente Juhász[1], Ádám Podolcsák[2*], János Doleschall[2]

[1]Department of Physical Geography and Geoinformatics, University of Szeged, Egyetem u. 2-6, H-6722 Szeged, Hungary
[2]Compet-Terra Kft., Kálvin tér 2, H-6721 Szeged, Hungary
*Corresponding author, e-mail: adam.podolcsak@competterra.com

Research article, received 24 February 2016, accepted 26 May 2016

Abstract

In recent years, the increased frequency of inland excess water in the Carpathian Basin gets more and more attention. The authors developed a web based pilot application for disaster management, with special emphasis on inland excess water hazard management. Free and open source software was used to generate a model, and our work was based on Web GIS standards (OGC), which makes further development possible. The developed Web GIS application provides functions to support the data collection regarding channels and ditches, and on-line hydrological analysis based on OGC Web Processing Services (WPS). Hydrological analysis aims to visualize the areas potentially at risk, depending on different precipitation quantities and various values of influencing factors. In order to run the prototype a sample data set was gathered including reference maps, technical parameters and current condition of canals and ditches. The methodology of crowdsourcing can produce valuable Volunteered Geographic Information (VGI) that can fulfill the data requirements of disaster management applications. The prototype supports Crowdsourcing in the following aspects: free user access to the system's analysis functionality, stakeholders may digitize the position of ditches, modify the status of the existing ditch system according to current conditions and add or modify parameters relevant for the analysis. The application demonstrated the usability of stakeholder generated geographic information and web processing for disaster management. The idea of integrating user-generated data into the various tasks of a disaster management agency is promising. However, maintaining data quality and standards compliance remain important issues.

Keywords: crowdsourcing, volunteered geographic information, open source, web processing, disaster management

INTRODUCTION

The United Nations Office for Disaster Risk Reduction defines disaster management as the organization and management of resources and responsibilities for addressing all aspects of emergencies such as preparedness, response and initial recovery steps. Disaster management involves plans and institutional arrangements to engage and guide the efforts of governmental, non-governmental, voluntary and private agencies in comprehensive and coordinated ways to respond to the entire spectrum of emergency needs (UNISDR). A Common view is that disaster management is a continuous cycle of pre-disaster, response and post-disaster phases (Fig. 1).

The role of GIS remained more research-oriented than operational until the beginning of the 21th century (Zerger and Smith, 2003). In recent years, most of the technological barriers have been overcome and numerous operational applications and adaptations of GIS exist all over the world. Examples show the wide usage of mobile GIS as an effective, fast and cheap data collection method (Montoya, 2003; Chen et al., 2010). However, applications are not limited to data collection. Several examples can be found in literature that use complex modelling methods for disaster management (Alparslan et al., 2008). A prominent example was designed to mitigate the harms of earthquakes in Bolu Provance, Turkey by applying a complex suitability model. The lack of dynamics in early examples is obvious. Currently, Web GIS and the development of web based GIS applications are much more widespread. Standards provided by OGC (Open Geospatial Consortium) and readily available compliant software components make application development easier and faster.

Another important aspect of such application is the data being used. It is hard to disagree that decisions made during a disaster can both affect properties and lives, so data quality is an important factor. On the other hand, insufficient amounts of data can limit the success of every task in disaster management, so using alternative data sources should also be considered. Crowdsourcing is a method that uses voluntary contributors to do a specific task (Estellés-Arolas and González-Ladrón-de-Guevara, 2012). For disaster management, it is possible collect data from volunteer individuals. The spread of crowdsourcing is strongly related to the growth of the digital world. A great amount of people use the internet and many of them have smartphones as well. In 2012 68% of the Hungarian households had broadband internet connections (KSH, 2014). In the first quarter of 2013, data traffic was 20% larger than in the same period of 2012. This fact represents

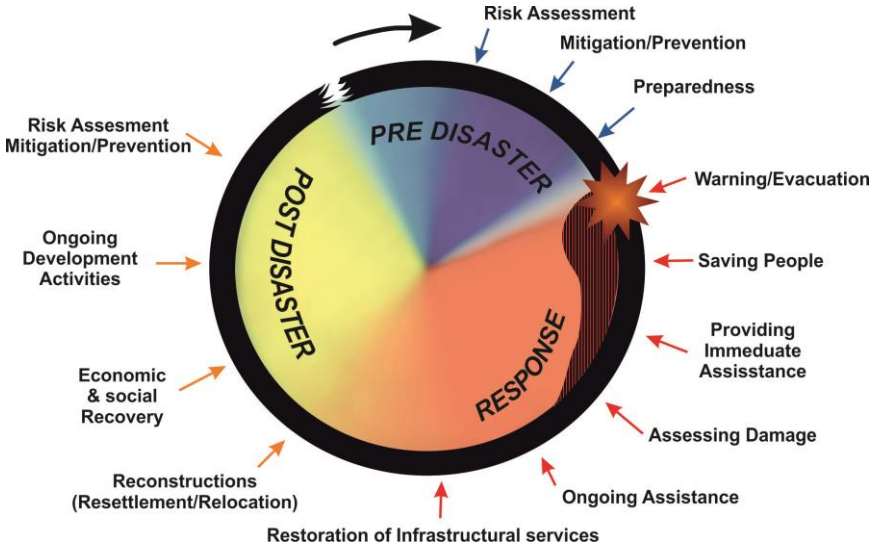

Fig. 1 Disaster management cycle (Barnier 2006)

the growing usage of smartphones in Hungary (KSH, 2014). These platforms can be the basis of a successful crowdsourcing application. However, organizing and processing crowdsourced data can be challenging. The main task is to ensure that the data produced by the "crowd" adheres to predefined standards.

This kind of data is often referred as Volunteered Geographic Information (VGI) in literature (Goodchild, 2007). All research agrees that it is highly heterogeneous and can be massive in volume. Another aspect is the lack of traditional Quality Assurance (QA) techniques in most VGI platforms (Goodchild and Li, 2012). Terminology used in scholarly literature is not standardized yet but a number of researchers suggested different classifications of VGI (Craglia et al., 2012). Geographic information is essential for emergency managers in all phases of emergency management. Data quality is a major factor since ineffective decisions caused by incorrect or imprecise data can both affect lives and properties. The possible benefits of using VGI during crises can make it a significant source of information by providing relevant data almost real-time (Goodchild and Glennon, 2010; Li and Goodchild, 2010). Previous studies have shown the importance of VGI during a crisis event. Geo-social media is ideal for emergency communications. Moreover, it can be considered as an information source for emergency managers (Vieweg et al., 2010; Lantonero and Shklovksi, 2010) since there are more than six billion human potential "sensors" in the world. Those citizen sensors can collect and share relevant crisis-related information through various platforms (Goodchild, 2007). It is important to show that a significant portion of users who share relevant information also include some kind of location information in their messages (Vieweg et al., 2010; MacEachren et al., 2011). This information therefore can be easily placed in the geographic space.

Recently, a new cooperation has been started in Hungary. The Directorate for Disaster Management and the University of Szeged teamed up to survey all the fire hydrants within Csongrád County. The Directorate asked university students to collect information of each fire hydrant, survey its position and take a picture of the surroundings. Officials of the directorate trained students what information is needed and how to collect them. The University provided the GIS equipment and the methodology. Since then, the data collected during the survey (including photos and databases) is being used by the Fire Department of the Directorate to make their operative work more effective. Operators in the center guide field teams to the appropriate fire hydrant and provide them relevant information while in the field (Huszár et al., 2013).

Properties of the rain and residual water drainage systems (spatial extent, condition, width, depth) and other anthropogenic establishments are relevant data for modelling inland excess water (Rakonczai et al., 2011; Szatmári and van Leeuwen, 2013; Leeuwen et al., 2013). As Vivacqua and Borges (2011) mentioned, knowledge of past events plays an important role in emergency situations. In the case of inland excess water, this knowledge can be gathered from local individuals.

In addition, Free and Open Source Software are now common in GIS and geography as well. All kinds of GIS software can be found depending on the needs, although their categorization is not easy (Steiniger and Hunter, 2013). Steiniger and Weibel (2009) have identified seven major types of them:

- Desktop GIS
- Spatial Database Management Systems
- Web Map Servers
- Server GIS
- Web GIS clients
- Mobile GIS
- Libraries and Extensions

Earlier, most open source and free software were developed by research institutes, universities or government agencies. In recent years, most of these projects are being developed by a new industry that develops and supports open source software. Private companies have also joined the market.

In opinion of Siki (2009), the main benefits of using free and open source software are not the low price but the direct interaction between the developers and users. They

all belong to the same community resulting in shorter development periods. Using open source and free software is also financially beneficial since instead of spending money on commercial licenses, resources can be reallocated to actual development tasks.

A web-based application named VINGIS can be mentioned in Hungarian literature that uses PostgreSQL, php and MapServer as open source components (Katona and Molnár, 2005). International examples cover the wide range of disaster and emergency management such as Ushahidi (non-profit software company that develops free and open source software (LGPL) for information collection, visualization, and interactive mapping), that support resource organization and management.

Considering the above, the main goal is to develop a web Platform, which supports the crowdsourcing based local management of environmental hazards. With the platform the defenses against surface water hazards at local level can be made easier and more effective; hazards (excess or lack of surface water) may cause less damage to the local economy. The further aim for developing the web platform is to use only free and open source technologies. This would be able to reduce the financial cost of development of disaster management application drastically while making them easier to distribute and increase the user base.

METHODOLOGICAL APPROACH

Framework of Modelling

When developing a web based GIS application, the first step is usually to set up a web server that can handle incoming requests and generate corresponding responses. Common Open Source web servers are Apache, nginx and the Cherokee HTTP Server (Apache http Server project; nginx http server; Cherokee http server project). Another main component of the server side is a map server that can provide geospatial data for our application. Functionalities of map servers usually rely on OGC's (Open Geospatial Consortium) standards. The Web Map Service (WMS) provides georeferenced map images generated from spatial data (OGC, 2014). WMS is mostly used to visualize maps, but basic spatial queries can be also defined to filter data. The Web Feature Service (WFS) can add more functionality to an application since it was designed to transfer the actual geospatial features over the network. Unlike WMS, this service does not provide a simple image for clients that can be easily shown, so clients must render data to be shown on screen. Furthermore, WFS is bidirectional. Edits and modification of the database is possible via so-called transactions. This aspect of the WFS is a way to integrate crowdsourcing to an application, where users can add and modify data to a predefined dataset. This way, VGI can be generated through the application and integrated directly into the spatial database. Tasks can involve data collection (on screen digitizing) or attribute editing. The most well-known Open Source map servers are GeoServer and MapServer (GeoServer; MapServer). On the client side, different mapping frameworks can be used. OpenLayers, Leaflet and Geomajas are most common. They allow users to navigate in an interactive map, but they are also capable of editing geospatial data. A simplified scheme of a web application is shown in Fig. 2, where the server side components are marked in green. Clients can connect to a webserver, which runs on a host machine. Other software components, like a map server can be installed on the server machine.

Applications with architecture of Fig. 2 are not too sophisticated. They provide the simplest functionality possible. However, complex GIS analysis or modelling tasks requires application to use complex GIS functionality. OGC's Web Processing Service (WPS) standard can enlighten the application with all the GIS analysis functions and methods needed by running a backend software on the server machine and providing results to the client. Some map servers (such as GeoServer) have a built-in WPS implementation with a few simple algorithms. There are also standalone WPS implementations independent from map servers. An open source solution is developed by 52 North's (52NORTH) geoprocessing community. This WPS implementation can work with different backends (such as GRASS GIS or the Sextante library). Sextante and GRASS GIS are commonly used full GIS packages with large collections of spatial analysis algorithms. WPS allows the Web GIS application to use the whole functionality of such packages from a web browser. Based on these protocols, a prototype application for disaster management has been developed, with one of the stages already in operation (Podolcsák and Juhász, 2013).

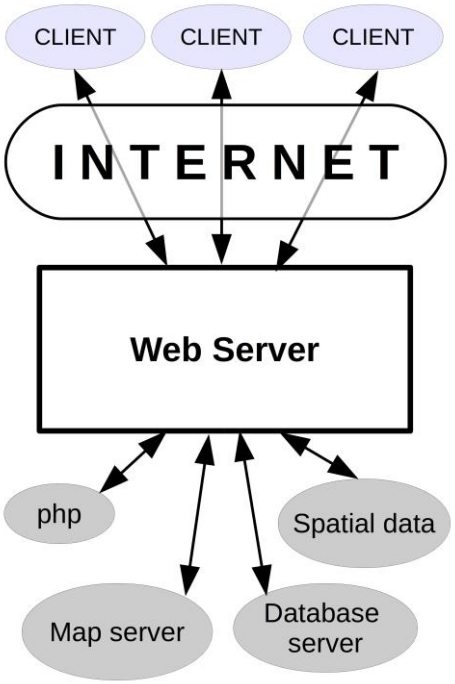

Fig. 2 Generalized architecture of a Web GIS application

The Prototype Application

As for modelling inland excess water coverage, a Web GIS application can offer support in the mitigation phase of disaster management (Fig. 1). It is of interest whether it is possible to fulfill the data requirements of such application by crowdsourced data. In theory, an engaged and well-trained community can provide relevant information in compliance with the predefined quality and technical

standards. Inappropriate operation of rain diversion systems (including ditches, dams, drainage channels) highly influences the formation of inland excess water (Szatmári et al., 2011).

Local farmers know the current conditions of such systems around their land. Relevant parameters can be the width, depth of the channels, or even their existence. It is very unlikely that the individuals who work on their fields every day have no such information. On the other hand, this data is difficult to obtain from other sources, therefore it is beneficial to gather this information from them. It is a mutual benefit, because they are also affected by inland excess water formation since it can cause either profit or loss. Proactive actions, like modelling water coverage for different rain events, based on the condition of rain drainage systems can result in more effective agricultural activities as well. The prototype application enables users to add and edit ditches in agricultural lands. Furthermore, it shows the likely water cover for various fictional scenarios. These scenarios are different from each other based on rain intensity and soil humidity. The outputs from the modelling also use the current geodata of the ditch system previously provided by users, therefore it is dynamic. Users can then visually interpret the changes in water cover and the influence of the ditch system. Each individual then may or may not decide whether further actions are needed near their lands (Podolcsák and Juhász, 2013). The application is a technical demonstration, where the authors wanted to prove that it is possible to develop an Open Source, community based Web GIS application to support disaster management. Algorithms used to calculate the possible water cover may not be accurate, but this was not an objective of the research. It is also important to note that possible users of the application most likely have very limited GIS expertise, if any. In this manner, data input methods and the visual outputs have to be as easy to understand and use as possible. In addition, since non-professional users are more likely to generate inaccurate data, data quality will be a major factor. This aspect needs to be further addressed. It is likely that applying Quality Assurance techniques are necessary, such as filtering and automatic correction will improve the overall accuracy of this application.

WPS Processes

The framework was developed using solely Free and Open Source Software components. The client side is based on the OpenLayers library including some custom solutions. Server side components are the Apache web server, a MySQL relational database, GeoServer, Apache Tomcat servlet engine, a WPS implementation and GRASS GIS as the geospatial modelling engine in the background. Using the 52North WPS implementation enables our application to use almost the entire functionality of GRASS GIS. This method is able to handle any type of GIS tasks in a web environment. In other words, traditional and highly complex GIS functionality can be achieved "directly" in a web browser (Podolcsák and Juhász, 2013). Figure 3 shows the multitier architecture of our prototype application.

Users access the application via the user interface allowing them to draw new ditches and modify attributes of the drainage network. Users can view the predicted extent of water cover while browsing the User Interface. Data modifications are sent as WFS requests towards GeoServer, whereas running simulations are

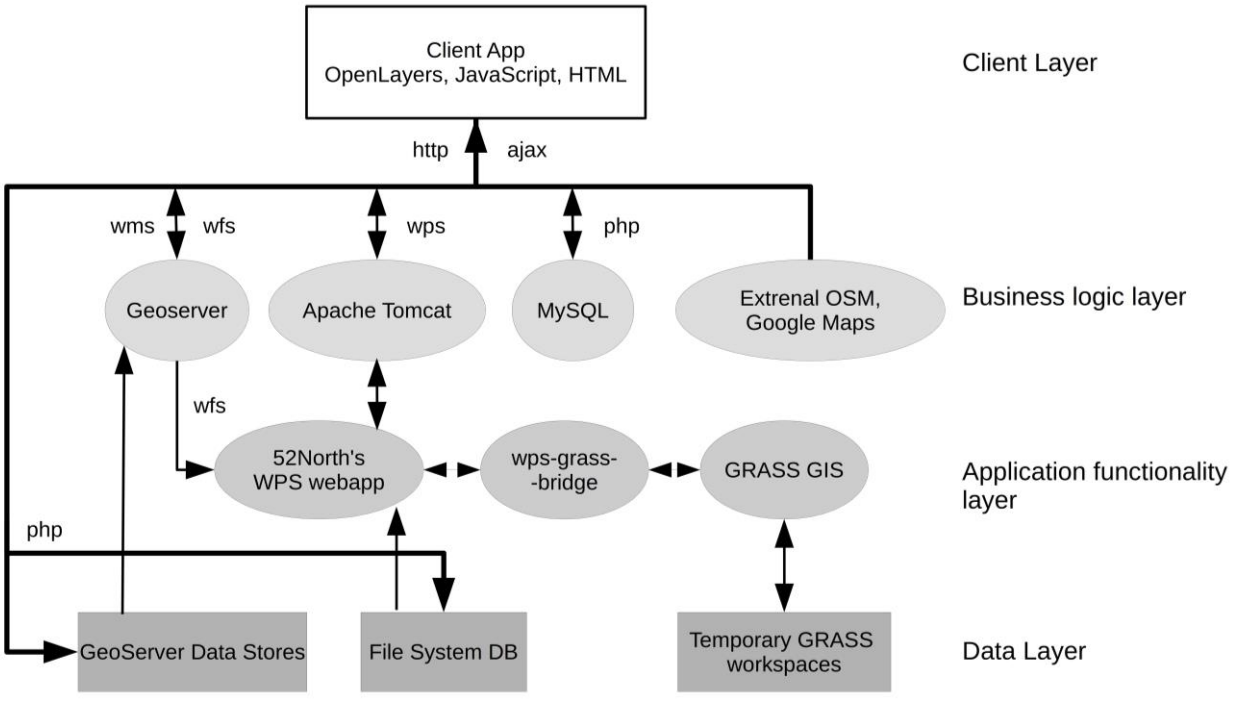

Fig.3 Multi-tier architecture of the prototype

sent as WPS requests towards GRASS GIS. These requests are defined according to the WFS and WPS specifications and they run asynchronously via AJAX (Asynchronous JavaScript and XML). Using the AJAX technique ensures the continuous operation of the application, since users do not have to wait for a process to finish, they are still able to use the application. Geospatial tasks (modelling inland excess water cover) are transferred over the network as WPS processes. A flowchart of a request-response pairs can be seen on Fig. 4**.** The model was built using the following data layers: DTM (Digital Terrain Model), runoff conditions, participation rate, infiltration rate and surplus surface water. The surface water flow direction and the area of surface water patches were determined based on the derivates of DTM. For the modelling a layer of soil types and another layer of surface cover types were also used. Based on these the infiltration rate (in mm/h) was calculated. The surplus of water values were calculated using soil types, surface covers and precipitation rate.

Although factors that have influence on the formation of inland excess waters do not change within such short time (Pálfai, 2004), it can be suspected that ditches choked with weed or artificial barriers prevent residual water from flowing away. This means that near real time analyses can also be useful. Possible users of this application can be anyone affected by inland excess water, like local farmers, local government or hydrological professionals (Podolcsák and Juhász, 2013).

MODELLING THE RESULTS

The system supports two main business processes: the creation and update of the data model and the management of the environment (mitigation of risks and utilization of surface water). In the back-end (System Administration), the developers or experts process the data, the modelling and manage the users. Firstly, the GIS model will be set up, which will make an Initial Analysis based on input data, using GRASS GIS modules (v.to.rast, r.grow, r.slope.aspect, r.buff, r.sim.water, r.math (r.mapcalc)).

The Initial Analysis will help to optimize the model for quick update to perform the Pre-processing of analysis. The Pre-processing of analysis step is linked to the Analysis/Planning part of the Front End (End Users' Functionality) process, to visualize existing probabilities of hazards. The local community members, farmers can view the other relevant maps in the platform. After visualization, the End Users can plan or analyze intervention against the hazard. Additionally, in the User Community Management the End Users can harmonize and discuss the Plan/analysis intervention phase together in order to make actions to mitigate risk in the Intervention phase.

If the users decide on mitigation actions the pre–processing of analysis can be performed again and the existing risk can be visualized in Analysis/Planning phase with the new parameters. In the Back-end system administration section, a feedback system, ensures the integration of new parameters in to the model.

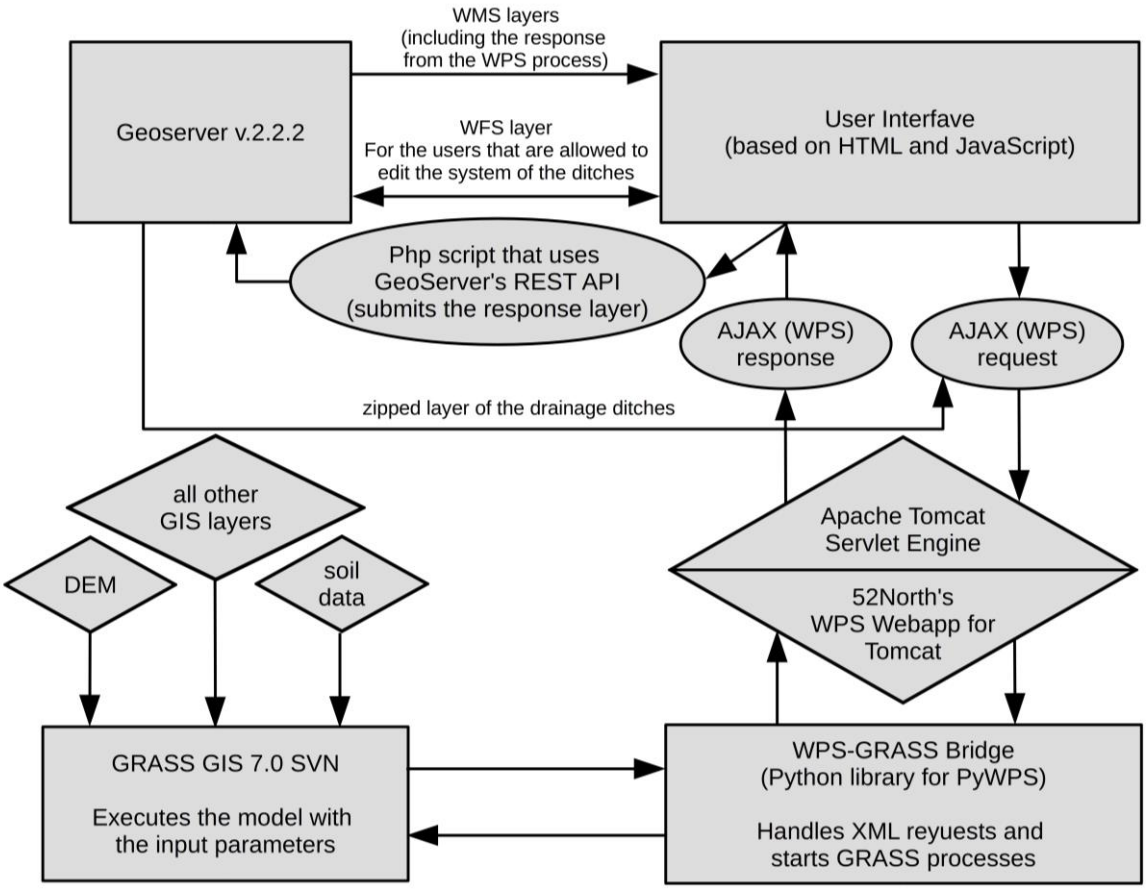

Fig. 4 Flowchart of WPS processes

Model outputs highly depend on the quality of input data. The accuracy of the input Digital Terrain Model (DTM) is crucial to determine surface flow directions. Currently, the application uses a DTM derived from elevation information in the 1:10,000 scale Hungarian topographic maps. Since the application tries to model local differences in water coverage, a more detailed terrain model would be beneficial, such as DTMs from Aerial Laser/LIDAR Scanning (ALS) or stereo photogrammetry (Szatmári et al., 2013).

Crowdsourced data is also present in the application since the properties of the ditch system can be edited by the community. They can also add or remove and modify sections. This data is used to make changes to the original DTM. This DTM modification based on the width, length and slope of the ditches will allow residual waters to "flow away". Furthermore, these ditches will lower the amount of residual waters along them.

Figures 5 and 6 show the possible water coverage in the application. Fig. 5 represents a scenario where ditches (dotted lines) have no influence on the formation of inland excess waters. Three major water patches can be identified on the picture visually regardless to the position of the ditches. This can be a real scenario in case of buried ditches when ditches are blocked by vegetation or other artificial barriers. It can also be seen that patterns and position of residual water align to the system of the point bar, and infill the lower parts. Fig. 6 illustrates a scenario where ditches along roads have influence on the formation of residual waters. It is quite visible that the extent of water cover decreased due to the influence of ditches in this area.

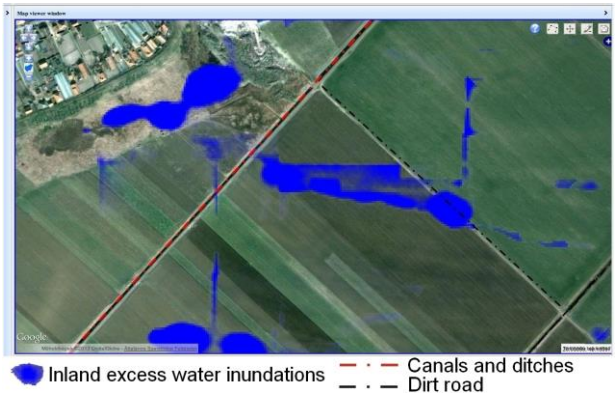

Fig. 5 Inland excess water cover seen on the application without the effect of the ditches

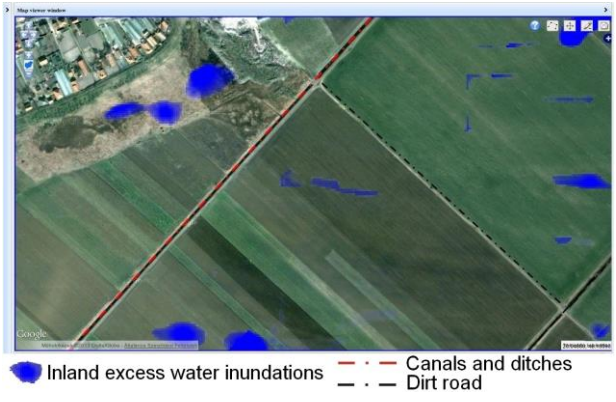

Fig. 6 Inland excess water cover seen on the application with the effect of the ditches

Users can now decide whether it is worth widening or digging ditches along their agricultural lands based on the visual results of the modelling with the new or modified ditch network. In this way, the application helps proactive decisions to be made to prevent inland excess waters. As we previously mentioned, using a more detailed DTM would be beneficial to get more accurate results. Furthermore, a vector based network analysis would be more ideal for modelling water flow in ditches.

DISCUSSION AND CONCLUSIONS

Disaster Management can describe the tasks and utilities of an organization that deals with disasters and emergency situations. Information is crucial for making effective decisions, because disasters can affect both lives and properties. Although disaster managers mostly rely on traditionally sourced, high quality data, this is not always available. Volunteered Geographic Information or crowdsourced geodata is a new trend in our field. This kind of data is the product of the so-called Web 2.0, in which non-professional users became creators and providers of spatial information. Although this data is heterogeneous and lacks traditional Quality Assurance, it can be valuable because the shortage of data also limits effective decisions of disaster/emergency managers. Therefore creating Web Applications that integrate VGI data sources into existing ones is an interesting research topic of recent years.

Using Free and Open Source Software to develop geospatial applications is beneficial for many reasons. They are valuable for companies and application developers not just because of the low financial costs, but also the shorter development cycles, as well as the often helpful and fast developing user community, that can help solve problems. Open Source software is widely used in many areas. Numerous GIS solutions exist that can compete with commercial products.

The use of Web Processing Service solutions is an interesting and promising direction for our field. It allows web applications to use complex GIS functionality over the internet. It allows Web GIS applications to move from an interactive map towards a fully functioning spatial processing framework in a web browser.

The authors have developed a prototype application, which proves that a Web GIS application can be developed to integrate the ideas of crowdsourcing and GIS, therefore can possibly create valuable VGI. The application is useful for disaster management since it can model possible extent of inland excess waters.

The application was developed using Free and Open Source software solutions. It contains an easy-to-understand user interface with interactive maps and the possibility of editing features. Users can add new features or modify existing ones. Data generated this way can be considered as VGI or crowdsourced geographic data and it is used in the modelling process. Furthermore, it uses the WPS standard to execute a complex GIS analyses. Previously this kind of functionality was unknown for Web GIS applications.

The application is a technological demonstration of integrating available software components. It clearly shows that Free and Open Source Software is capable to provide full GIS functionality and to generate valuable geographic information over the internet. Quality Assurance of the generated data and refinement of the used algorithms to create a more correct model is a challenging task for the future. It can be expected that the number of such application will arise in the near future since the technology does not limit the possibilities. Standards and software components are freely and easily available.

Considering the numerous expansion option of prototype it should be remembered that the underlying principles can be applied in the other section too, like in e.g. agriculture, environmental protection, rural development.

References

Alparslan E., Ince, F., Erkan, B., Aydöner, C., Özen, H., Dönertaş, A., Ergintav, S., Yağsan, F.S., Zateroğulları, A.,. Eroğlu, I., Değer, M., Elalmış, H., Özkan, M. 2008. A GIS model for settlement suitability regarding disaster mitigation, A case study in Bolu Turkey. *Engineering Geology* 96 (3–4), 126–140. DOI: 10.1016/j.enggeo.2007.10.006

Chen, A.Y., Peña-Mora, F., Ouzang, Y. 2011. A collaborative GIS framework to support equipment distribution for civil engineering disaster response operations. *Automation in Construct*ion 20 (5), 637–648. DOI: 10.1016/j.autcon.2010.12.007

Craglia, M., Ostermann, F., Spinsanti, L. 2012. Digital Earth from vision to practice: making sense of citizen-generated content. International. *Journal of Digital Earth* 5 (5), 398–416. DOI: 10.1080/17538947.2012.712273

Estellés Arolas, E., González Ladrón-de-Guevara, F. 2012. Towards an integrated crowdsourcing definition. *Journal of Information Science* 38 (2), 189–200. DOI: 10.1177/0165551512437638

Goodchild, M.F. 2007. Citizens as voluntary sensors: spatial data infrastructure in the world of web 2.0 (Editorial). *International Journal of Spatial Data Infrastructures Research* 2, 24–32.

Goodchild, M.F., Glennon, J. A. 2010. Crowdsourcing geographic information for disaster response: a research frontier. *International Journal of Digital Earth* 3 (3), 231–241. DOI: 10.1080/17538941003759255

Goodchild, M.F., Li, L. 2012. Assuring the Quality of Volunteered Geographic. *Information Spatial Statistics* 1, 110–120. DOI: 10.1016/j.spasta.2012.03.002

Huszár, T., Kitka, G., Mezősi, G., Szatmári, J., van Leeuwen, B., Tobak, Z.,Kovács, F., Győri, A., Okner, A., Tóth, J., Szűcs, B., Zsom, G., Juhász, L. 2013. Tűzcsapkataszter-felmérés Csongrád megyében. Katasztrófavédelem 55 (10), 5–6. (in Hungarian)

Katona, Z., Molnár, A. 2005. Magyarország térinformatikai szőlőültetvény-nyilvántartó rendszerének -VINGIS- kialakítása. Geodézia és Kartográfia 57 (10), 24–27 (in Hungarian)

Lantonero, M., Shklovski, I. 2010. "Respectfully Yours in Safety and Service": Emergency Management & Social Media Evangelism. Proceedings of the 7th International ISCRAM Conference. Seattle. USA, May 2010

van Leeuwen, B., Henits, L., Mészáros, M., Tobak, Z., Szatmári, J., Pavić, D., Savić, S., Dolinaj, D. 2013. Classification Methods for Inland Excess Water Modeling, *Journal of Environmental Geography* 6 (1–2), 1–8. DOI: 10.2478/v10326-012-0001-5

Li, L., Goodchild, M.F. 2010. The Role of Social Networks in Emergency Management: A Research Agenda. *International Journal of Information Systems for Crisis Response and Management* 2 (4), 49–59. DOI: 10.4018/jiscrm.2010100104

MacEachren, A. M., Robinson, A. C., Jaiswal, A., Pezanowski, S., Savelyev, A., Blanford, J., Mitra, P. 2011. Geo-Twitter Analytics: Applications in Crisis Management. 25th International Cartographic Conference. Paris, France. July 2011

Montoya, L. 2003. Geo-data acquisition through mobile GIS and digital video: an urban disaster management perspective. *Environmental Modeling and Software* 27, 869–876. DOI: 10.1016/s1364-8152(03)00105-1

Pálfai, I. 2004. Belvizek és aszályok Magyarországon. Hidrológiai Tanulmányok. VITUKI. Budapest, 492 p

Podolcsák, Á., Juhász, L. 2013. Crowd sourcing in disaster management at local level; incl. a demo of a prototype application supporting proactive defense against inland waters. Workshop for building V4 network researching spatial and social aspects of Disaster Management. May 22-23. Budapest

Rakonczai, J., Farsang, A., Mezősi, G., Gál, N. 2011. A belvízképződés elméleti háttere. Földrajzi Közlemények 135 (4), 339–349. (in Hungarian)

Siki, Z. 2009. Produktív környezetben használt, nyílt forráskódú komplex térinformatikai megoldások. CASCADOSS műhelymunka tanácskozás és GRASS tanfolyam. Szeged (in Hungarian)

Steiniger, S., Hunter, A. J. S. 2013. The 2012 free and open source GIS software map – A guide to facilitate research, development, and adoption. Computers, Environment and Urban Systems 39 May 2013, 136–150.

Steiniger, S., Weibel, R. 2009. GIS software – a description in 1000 words. [http://ftp.jaist.ac.jp/pub/sourceforge/j/project/ju/jump-piot/w_other_freegis_documents/articles/gissoftware_steiniger2008.pdf]

Szatmári, J., Szijj, N., Mucsi, L., Tobak, Z., Van Leeuwen, B., Lévai, Cs., Dolleschall, J. 2011. A belvízelöntések térképezését és a belvízképződés modellezését megalapozó térbeli adatgyűjtés. In: Lóki, J. (ed). Az elmélet és gyakorlat találkozása a térinformatikában II, Debrecen, 27–35. (in Hungarian)

Szatmári, J. van Leeuwen, B. (ed.) 2013. Measurement, monitoring, management and risk assessment of inland excess water in southeast Hungary and north Serbia (Using remotely sensed data and spatial data Infrastructure) University of Szeged, Department of Physical Geography and Geoinformatics, Szeged, 154p.

Vieweg, S., Hughes A. L., Starbird, K., Palen L. 2010. Microblogging During Two Natural Hazards Events: What Twitter May Contribute to Situational Awareness. Proceedings of the ACM conference on Computer Human Interaction (CHI) 2010

Vivacqua, A.S., Borges, M.R.S. 2011. Using group storytelling to recall information in emergency response. CollaborateCom'11, In: Georgakopoulos D., Joshi, J. (eds.) Proceedings of the 7th International Conference on Collaborative Computing: Networking, Applications and Worksharing, 512–515. DOI: 10.4108/icst.collaboratecom.2011.247126

Zerger, A., Smith, D. I. 2003. Impediments to using GIS for real time disaster decision support. *Urban Systems* 27 (2), 123–141. DOI: 10.1016/s0198-9715(01)00021-7

Internet references

Apache http Server project - https://httpd.apache.org/. (last visited: May 2016)

Barnier, M. 2006. For a European civil protection force: Europe aid. Report. European Commission, Brussels, http://ec.europa.eu/archives/commission_2004-2009/president/pdf/rapport_barnier_en.pdf

Cherokee http server project - http://cherokee-project.com/, (last visited: May 2016)

GeoServer - http://geoserver.org/ (last visited: may. 2016)

KSH – Központi Statisztikai Hivatal/Hungarian Central Statistical Office 2014. Proportion of households with broadband internet connection. http://www.ksh.hu/docs/hun/eurostat_tablak/tabl/tin00089.html (last visited: February 2016)

MapServer – http://mapserver.org/ (last visited: may. 2016)

Nginx http server - https://www.nginx.com. (last visited: May 2016)

OGC – Open Geospatial Consortium 2014. OGC® Standards and supporting documents http://www.opengeospatial.org/standards (last visited: February 2016)

UNISDR – UNITED NATIONS Office for Disaster Risk Reduction. 2014, http://www.unisdr.org/we/inform/terminology (last visited: February 2016)

USHAHIDI - https://www.ushahidi.com (last visited: February 2016)

52NORTH - http://52north.org/communities/geoprocessing/wps/ (last visited: February 2016)

JOURNAL OF ENVIRONMENTAL GEOGRAPHY
Journal of Environmental Geography 9 (1–2), 23–30.
DOI: 10.1515/jengeo-2016-0004
ISSN: 2060-467X

SATELLITE BASED ANALYSIS OF SURFACE URBAN HEAT ISLAND INTENSITY

Orsolya Gémes, Zalán Tobak*, Boudewijn van Leeuwen

Department of Physical Geography and Geoinformatics, University of Szeged, H-6722, Egyetem u. 2-6, Hungary
*Corresponding author, e-mail: tobak@geo.u-szeged.hu

Research article, received 1 May 2016, accepted 1 June 2016

Abstract

The most obvious characteristics of urban climate are higher air and surface temperatures compared to rural areas and large spatial variation of meteorological parameters within the city. This research examines the long term and seasonal development of urban surface temperature using satellite data during a period of 30 years and within a year. The medium resolution Landsat data were (pre)processed using open source tools. Besides the analysis of the long term and seasonal changes in land surface temperature within a city, also its relationship with changes in the vegetation cover was investigated. Different urban districts and local climate zones showed varying strength of correlation. The temperature difference between urban surfaces and surroundings is defined as surface urban heat island (SUHI). Its development shows remarkable seasonal and spatial anomalies. The satellite images can be applied to visualize and analyze the SUHI, although they were not collected at midday and early afternoon, when the phenomenon is normally at its maximum. The applied methodology is based on free data and software and requires minimal user interaction. Using the results new urban developments (new built up and green areas) can be planned, that help mitigate the negative effects of urban climate.

Keywords: urban LST, urban heat island, Landsat

INTRODUCTION

Although, fifty three percent of the world's population lives in cities, according to the estimations only 3% of the continents is urban area (World Bank, 2014). This relatively small area is intensively used and continuously affects its inhabitants by providing them a dynamically changing residential environment.

The climate of the horizontally and vertically diverse urban surface is influenced by several factors on macro and meso (e.g. climate, elevation, relief), as well as local level. Local modifying factors, not active in non urban areas are (1) the generally higher specific heat and low albedo of anthropogenic surfaces, (2) modified water regime resulting in lower air humidity, (3) the special surface geometry modifying the flow conditions, (4) the periodical heat surplus (due to heating, traffic or industry) and (5) the increased atmospheric aerosol concentration (Unger, 1996). On meso level the impact of urban surfaces can be detected up to 9-11km (urban boundary layer – UBL), and local micro-level processes have effects up to the average roof-top level (urban canopy layer – UCL) (Oke, 1976).

The total energy balance of urban areas is similar to the rural areas, however, there are differences in the ratio of shortwave and longwave radiation. Due to the high aerosol concentration the incoming direct, diffuse and atmospherically reflected shortwave radiation is low, and the shortwave radiation reflected from the surface is also low due to the low albedo. The warmer surfaces result in higher longwave radiation, furthermore air pollution increases the reflected and diffuse longwave radiation (Unger, 2010a).

Urban heat islands (UHI) are typical microclimatic phenomena in urban areas. The air temperature of urban areas is significantly higher at night compared to the rural areas (Landsberg, 1981). The phenomenon has a horizontal as well as a vertical character. According to the typical UHI thermal profile a steep temperature gradient occurs at the rural/urban boundaries (cliff), and thereafter the temperature increases along steady horizontal gradient (plateau) and the highest temperature is at the urban centre (peak). Vertically the positive temperature anomaly can be detected reach up to 200-300 meters (Unger, 2010a). In general, a 0.5-1°C positive anomaly can be identified in urban areas compared to rural areas depending on the density and extent of built-up areas. Local urban climate is a phenomenon formed by several complex processes (Probáld, 1974).

Several publications appeared that use aerial and satellite remote sensing data to study the changing urban environment due to the dynamically increasing population. Considering the current study a significant advancement was the assessment of Roth et al. (1989), who used infrared (NIR) band of NOAA AVHRR satellite to monitor surface temperature. According to their experiences the pattern of heat release had a stronger correlation with the land cover during the day compared to the night. It is contradictory to the results calculated from measured air tem-

perature values at 2-3m height above the surface. Nichol (2005) compared ASTER night-time thermal infrared data with Landsat 7 (ETM+) daytime data to study the relationship between surface temperature and urban morphology during a daily temperature cycle. The research found the meso scale processes more important in the UBL at night, while during the day they were significant rather in the UCL. Purnhauser (2001) investigated the urban climate of Szeged in different seasons and used the sky view factor (SVF) defined by Oke (1988). It was found that in open, green areas the longwave radiation is significant; in narrow streets with high buildings an 'urban canyon effect' was observed, because the longwave radiation was trapped decreasing the loss of radiation to the atmosphere. Soósné (2009) assessed the urban climate of Hungarian and Central European cities using surface temperature, land cover and vegetation indices data from the MODIS sensor, and ASTER surface temperature data. She evaluated the spatial pattern of UHI in all 4 seasons and in 4 periods during a day (dawn – morning – afternoon – evening). Gábor and Jombach (2009) used Landsat TM data to investigate the relationship between 14 different land use class and the surface temperature. The spatial pattern and intensity of UHI in Szeged were assessed and evaluated by Unger et al. (2010b) using measured air temperature field measurements and surface temperature datasets acquired by an airborne remote sensing system.

STUDY AREA

Urban climate is highly dependent on population density. In Hungary 70% of the population lives in urban areas (in 346 towns and cities in total) (KSH, 2015). Szeged is the third most populous city in Hungary (with 163000 inhabitants). The number of inhabitants was increasing until the 1990s, and afterwards a decreasing tendency has been observed. The reasons behind the changes are the countrywide characteristic natural decrease of the population, furthermore, the migration of the people to the neighbouring villages. A migration surplus can be observed in Szeged since 2007 (KSH, 2015).

The macroclimate of an area also influences the urban climate. Hungary, and therefore Szeged being located on the South Hungarian Great Plain (Fig. 1), belong to the temperate zone; Cf type of Köppen's climate zones (warm continental climate and with significant precipitation in all seasons). Péczely (1979) categorised Szeged into the warm-dry climate zone based on its water and heat balance. The annual mean temperature, the mean summer temperature and the mean annual precipitation are 10.6°C, 20,3°C, and 489mm, respectively. The average total hours of sunshine at Szeged is 250-280 in summer months and 50-80 in winter months (OMSZ, 2016).

The city structure is characterised by avenues and boulevards built during the reconstructions after the great flood in 1879. The river Tisza devides the city in two parts: Southeast from the river, the area is mostly characterised by larger urban green areas and, family

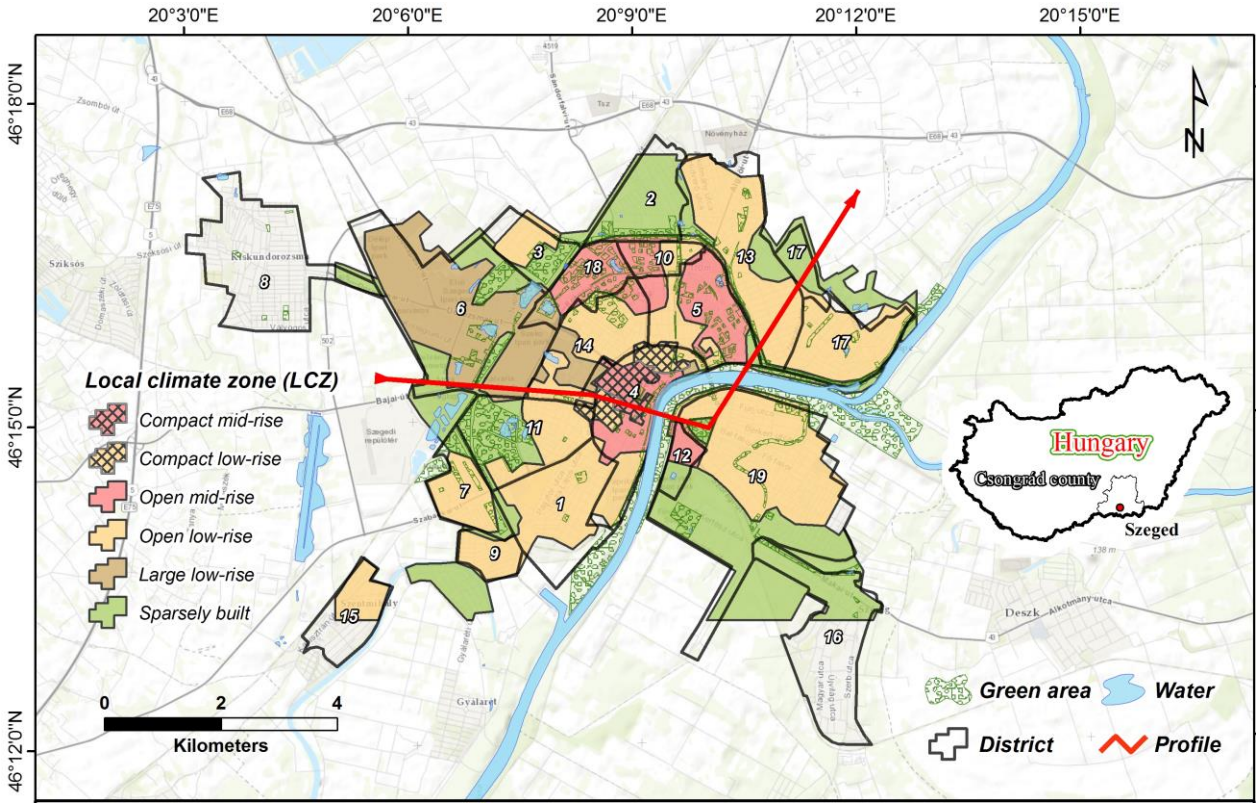

Fig. 1 Study area (1 Alsóváros, 2 Baktó, 3 Béke-telep, 4 Belváros, 5 Felsovaros,6 Iparváros,7 Kecskes, 8 Kiskundorozsma, 9 Klebensbergtelep, 10 Makkosháza-Fodorkert, 11 Móraváros, 12 Odessza, 13 Petőfi-telep, 14 Rókus, 15 Szentmihály, 16 Szőreg, 17 Tápé, 18 Újrókus, 19 Újszeged)

houses with gardens. North of the river the city centre, housing estates and industrial areas can also be found (Fig. 1).

For the uniform description of the local climate features a Local Climate Zone (LCZ) classification was developed. The categories can be well applied on plains, where the influence of the relief on the climate is less strong than in areas with large height differences (Stewart and Oke, 2012). The categories were defined based on the land cover, resulting in 10 urban and 6 rural categories. The first 3 urban categories are characterised by mainly built-up areas, green areas are represented only by a few trees. In the case of the following 3 categories the ratio of green cover is increasing, and the rest of the categories have open green areas and low built-updensity. Lelovics et al. (2014) mapped the local climate zones in Szeged (Fig. 1) using a building database, aerial photos, topographical maps, RapidEye satellite images, an infrastructure database, SVF values, building height and roughness data, albedo values of the different surfaces, NDVI images and CLC land cover data. The following categories were identified in their work in the city of Szeged: (2) compact mid-rise, (3) compact low-rise, (5) open mid-rise, (6) open low-rise, (8) large low-rise and (9) sparsely built.

DATA AND METHODS

Landsat 4, 5 TM, Landsat 7 ETM+, and Landsat 8 OLI/TIRS data from the period between 1984 and 2016 were applied in this research (Table 1). For the long-term assessment, images from the same period in July, with a 10 year interval were evaluated describing summer conditions. I interannual changes were assessed using one image for each seasons between 2015 and 2016.

The raw (DN) pixel values were processed using the Semi Automatic Classification Plugin (SCP) of the open source QGIS software (SCP) along two parallel workflows (Fig. 2). On one hand the data of the thermal band was processed, on the other hand a supervised classification was carried out on the the visible and infrared bands. Emissivity values assigned to each class were applied during the land surface temperature (LST) calculations.

The data sets used for the analyses needed to be preprocessed to land surface temperature. Each data set was preprocessed using a data specific workflow that does not use any ancillary data. During the first step, the raw digital numbers (DN) of the TM, ETM+ and OLI sensors were converted to at-satellite or top-of-atmosphere (ToA) spectral radiances (L_λ in $Wm^{-2}sr^{-1}\mu m^{-1}$) using:

$$L_\lambda = M_L * Q_{cal} + A_L \quad (1)$$

where M_L and A_L are respectively the band-specific multiplicative rescaling factor and the additive rescaling factor, which are both available from the metadata. Q_{cal} is the quantized and calibrated standard product pixel values (DN). In the next step, the ToA radiances of the visible to SWIR bands were converted to unitless ToA reflectances ρ_p by:

$$\rho_p = \pi * L_\lambda * d^2 * (ESUN_\lambda * cos(\theta s))^{-1} \quad (2)$$

where d is the Earth-Sun distance in astronomical units at the acquisition time, $ESUN_\lambda$ is the band specific mean solar exo-atmospheric irradiances, and θs is the solar zenith angle in degrees, which is equal to $\theta s = 90° - \theta e$ where θe is the sun elevation as given in the metadata. To derive the surface reflectance, it was required to apply some sort of atmospheric correction. In this research, no detailed data was available about the state of the atmosphere at the time of the data acquisition, therefore the Dark Object Subtraction (DOS) method (Moran et al., 1992) was applied to the data sets assuming that within an image some pixels are in complete shadow and their radiances received at the satellite are due to atmospheric scattering (Chavez, 1996). The surface reflectance is then:

$$\rho_s = [\pi * (L_\lambda - L_p) * d^2] * (ESUN_\lambda * cos(\theta s))^{-1} \quad (3)$$

where L_p is the path radiance (Sobrino et al., 2004):

$$L_p = M_L * DN_{min} + A_L - 0.01 * ESUN_\lambda * cos(\theta s) * (\pi * d^2)^{-1} \quad (4)$$

The surface reflectance values were used to classify the data with the spectral angle mapping algorithm (Kruse et al., 1993) into 4 land cover classes (water, vegetation, bare soil, built up) and to calculate NDVI values. The thermal bands were converted to at-satellite brightness temperature by:

Table 1 Satellite images (A: long-term / B: seasonal assessment) and meteorological data (OMSZ, OGIMET) used in the assessment

Sensor	Acquisition date/time	Pixel size (VNIR/TIR) [m]	Daily mean temperature [°C]	Daily maximum temperature [°C]	VIS (km)
Landsat 4 TM	31-Jul-1984 [A]	30/120	22.8	30.3	n.a.
Landsat 5 TM	27-Jul-1994 [A]		25.0	34.0	n.a.
Landsat 7 ETM+	22-Jul-2004 [A]	30/60	26.4	34.6	28
Landsat 8 OLI/TIRS	18-May-2015 [B]	30/100	16.9	24.1	50
	21-Jul-2015 [A,B]		25.3	32.4	70
	23-Sep-2015 [B]		17.5	23.1	15
	22-Feb-2016 [B]		7.0	10.7	50

$$T_{b\lambda} = K_2 * \left(\ln\left(\frac{K_1}{L_\lambda} + 1 \right) \right)^{-1} \quad (5)$$

not possible to apply the split window algorithm on Landsat 8 data (USGS Landsat 8, 2016), empirical emissivity values *e* (Weng et al., 2004; Mallick et al., 2012) for the earlier derived land cover classes were used with the following formula to convert the brightness temperatures to surface temperature:

$$T_{s\lambda} = T_{b\lambda} / [\, 1 + (\lambda * T_{b\lambda} / p)\, ln(e)\,] \quad (6)$$

where λ is the wavelength of emitted radiance, and

$$p = h * c / s\ (1.438 * 10\text{^-}2\ m\ K) \quad (7)$$

with *h* is Planck's constant, *s* is Boltzmann constant, and *c* is the velocity of light.

The surface urban heat island (SUHI) intensity can be defined as the difference between the temperature of urban and rural areas at ground level. Szeged meteorological station and its 750 m wide buffer zone was used as reference region in this study. This area was also used as reference for previous air temperature measurements of an urban climate research by Unger (2010a). It accurately represents the main land cover types around the city (arable land, meadow-pasture, and forest).

The spatial pattern of the SUHI intensity was analysed for the whole city and along a profile. The initial point of this line was the centre point of the reference area, the Szeged meteorological station (Fig. 1). During the allocation of the profile it was important to cross Iparváros (an industrial area), areas of different built-up ratio and vegetation cover

In this research the following main questions were addressed:

1) How the pattern of LST changed during the investigated 30 years in Szeged? What is the relationship between the ratio of built-up areas/vegetation cover and the calculated LST values?

2) How the intensity of surface urban heat island (SUHI) changed compared to the reference rural zone in the investigated period?

3) What is the interannual pattern of LST in the predefined local climate zones?

4) What are the characteristic seasonal features of the spatial pattern of SUHI?

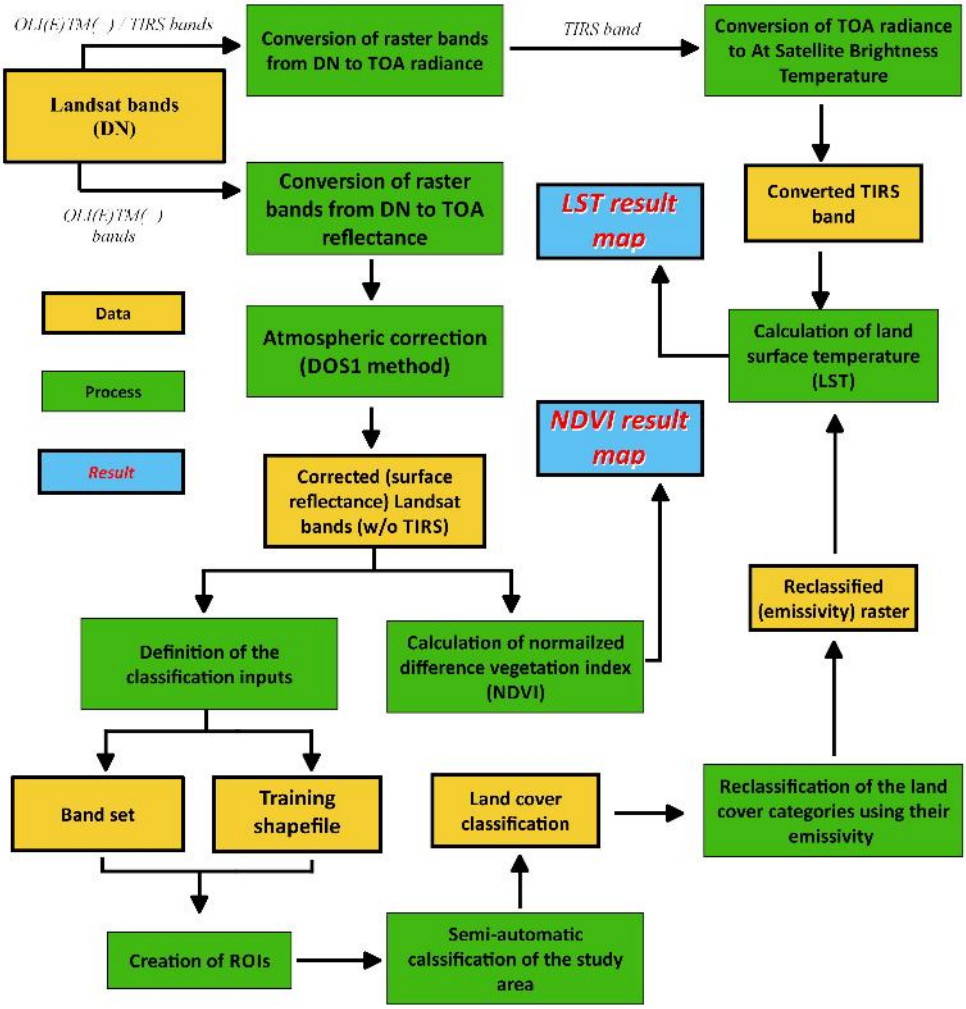

Fig. 2 Workflow of LST calculation in QGIS using Semi Automatic Classification plugin

RESULTS

Daytime surface temperature images with 30 m spatial resolution were prepared for nearly the same summer day in 1984, 1994, 2004 and 2015, and for one day in each season at same time intervals between spring 2015 and winter 2016 for the city of Szeged. For the same dates NDVI values were calculated in 30 m spatial resolution using the red and infrared bands in the data sets.

During image selection important criteria were the lack of cloud cover, since it reflects characteristic weather conditions in the given seasons and the absence of precipitation. The appropriate conditions were checked and confirmed by meteorological datasets (Table 1).

LST and NDVI between 1984 and 2015 in the investigated urban districts

The most significant changes of built up areas were observed between 1984 and 2004 (Fig. 3). In the investigated 30-years-long period the highest difference between the mean LST values was observed in the case of Petőfi-telep exceeding even 7°C. LST decrease was observed in none of the investigated districts (Table 2).

Table 2 Changes of LST and NDVI in city districts in the investigated 30 years

District		Δ LST	Δ NDVI
1	Alsóváros	5.76	0.09
2	Baktó	5.27	0.12
3	Béke-telep	6.30	0.06
4	Belváros	5.48	0.15
5	Felsovaros	5.33	0.19
6	Iparváros	6.55	0.04
7	Kecskes	4.78	0.09
8	Kiskundorozsma	5.69	0.06
9	Klebensbergtelep	6.20	0.08
10	Makkosháza-Fodorkert	5.84	0.17
11	Móraváros	5.83	0.09
12	Odessza	3.30	0.21
13	Petőfi-telep	7.08	0.04
14	Rókus	6.11	0.10
15	Szentmihály	5.38	0.06
16	Szőreg	6.10	0.03
17	Tápé	6.51	0.03
18	Újrókus	6.44	0.10
19	Újszeged	6.24	0.06

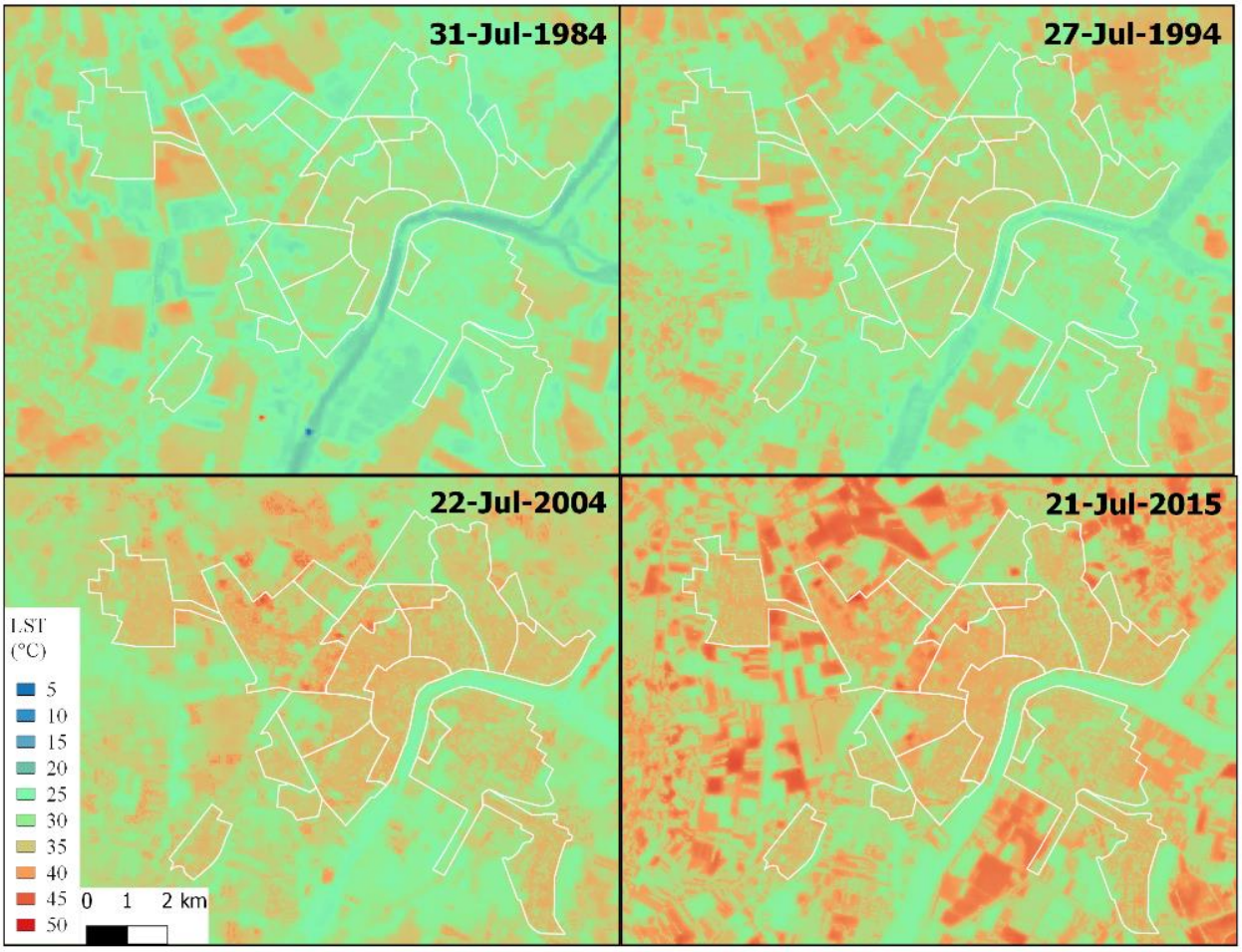

Fig. 3 Changes of LST between 1984 and 2015

The observed slight changes in NDVI values were in concordance with the significant increase of the temperature (e.g. in the case of Szőreg, Petőfi-telep, Iparváros). In those districts where a larger increase in vegetation cover occurred, only lower LST values were detected (e.g. Odessza). The most spectacular changes happened at such areas where vegetation was replaced by built-up areas (e.g. shopping malls, industrial areas). A relatively strong correlation (R=-0.69) between the vegetation indices and the changes in the surface temperature values can be identified. However, vegetation seems to be a major determining factor of LST changes, the surface material (albedo) and its geometry, furthermore the actual weather conditions also significantly impact the LST changes.

Spatial pattern of daily SUHI intensity

Based on LST values, the phenomenon of surface urban heat island was the most observable at midday and early afternoon, however urban heat islands based on the measured air temperature differences are the most pronounced at night. The applied Landsat images were captured between 9.30 and 10.30, thus they were not expected to show the highest differences (namely the maximum of SUHI intensity) compared to the rural areas. Apart from this, the temperature of the built-up urban areas significantly exceeded the mean temperature of the rural areas (Fig. 4). The highest positive intensity was observed at the industrial areas in all cases, and the rate exceeded 10°C even in this morning period. The minimum values

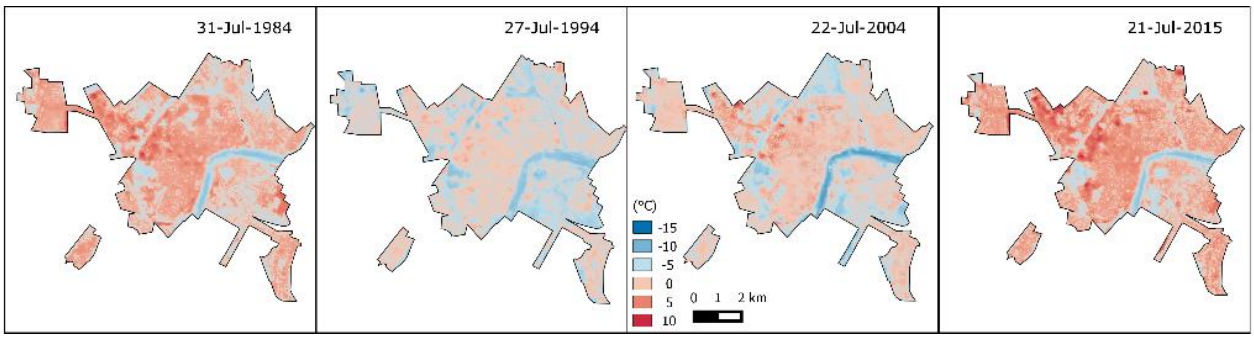

Fig. 4 UHI intensity compared to the rural areas

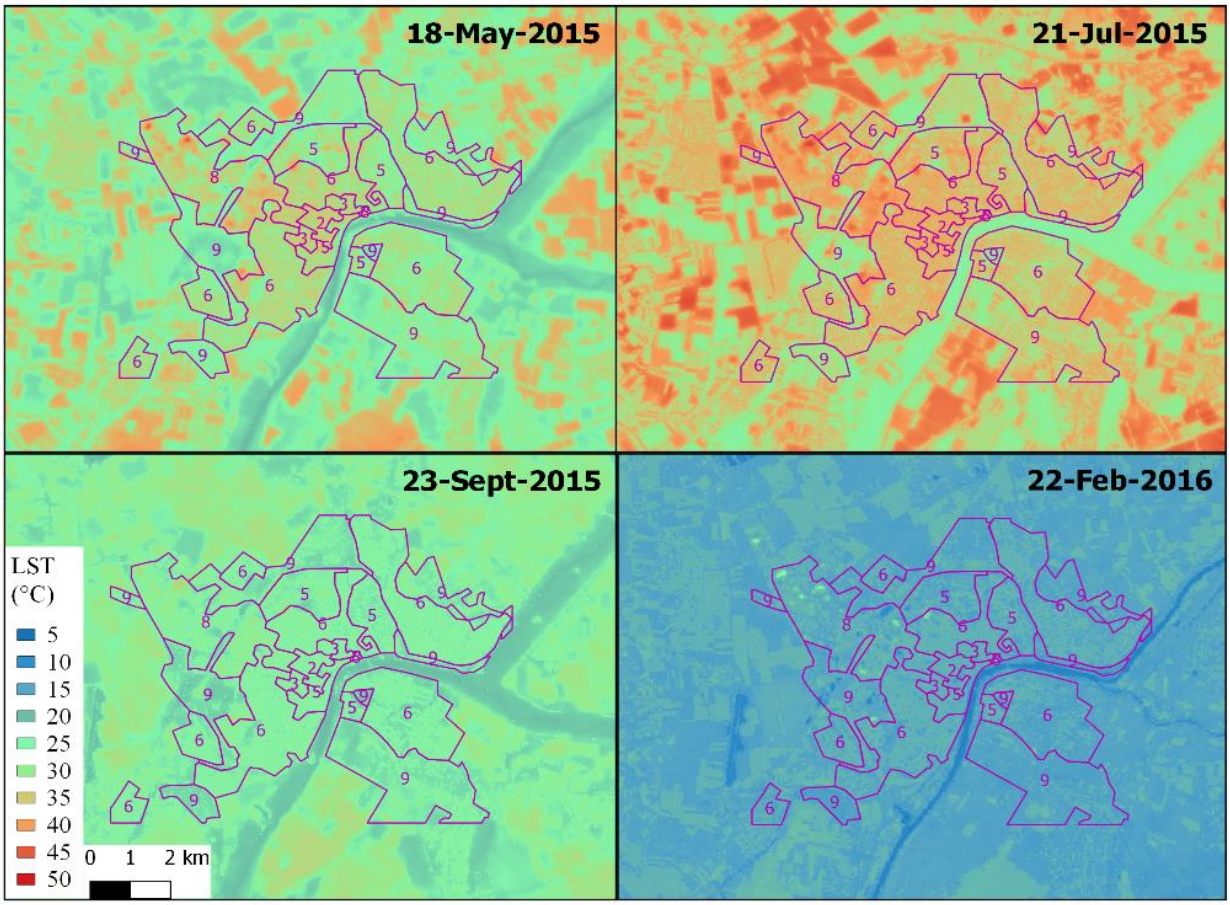

Fig. 5 Seasonal patterns of LST (2 Compact midrise, 3 Compact low-rise, 5 Open midrise, 6 Open low-rise, 8 Large low-rise, 9 Sparsely built)

were detected in the case of larger urban green areas (e.g. parks, floodplain) and the water surface of the River Tisza.

The highest mean positive SUHI intensity was detected in the densely populated city centre and Rókus districts on two out of the 4 investigated dates. The smallest mean difference was identified in a district of the outskirt area, in Baktó and once in the suburban Új-Szeged district. The least variation in temperatures was found in the city centre, while the industrial areas showed the highest standard deviation. The average difference between the surface temperature in urban and rural areas was + 1.5°C in 2015.

Seasonal changes of urban LST in the local climate zones

According to the seasonal comparison (Fig. 5) the lowest LST values were detected in the sparsely built LCZ category in spring, summer and autumn (Table 3), where the land cover has characteristically a lower ratio of built-up areas, but more gardens and sporadic tree cover. In winter the lowest LST values were detected in the open low-rise LCZ category, which consists of mostly open areas characterized by low buildings. The differences in minimum values in winter are due to the smaller influence of vegetation. The maximum temperature values occurred in the large low-rise category in all seasons, which are mostly built up areas without vegetation. These are typically the territories of large shopping malls and their parking lots.

A significant negative correlation (-0.68<R<-0.87) between the NDVI and LST values in the vegetation period was observed in the investigated districts. The lowest correlation was detected in the city centre, due to the lower vegetation cover (Table 4).

Daytime SUHI intensity along a profile in the city

The profile represents the influence of the different land cover types on surface temperature. The line intersects the River Tisza at two locations and has a 2800 m long suburban section as well. This section shows significant deviations in the different seasons (Fig. 6). The reason for this is the seasonal change of vegetation on arable lands. After the line reaches the border of the urban zone (at 2850 m), there is a significant change of the forest cover in all seasons. This decrease is followed by the increase of LST due to the industrial area. Apart from the seasonality, the absolute maximum was observed at this district (after 4000 m). The following built-up areas show a mostly steady temperature (with some exceptions). Besides the sections crossing the rivers, the absolute minimum values were characteristic for the Liget (the biggest park in Új-Szeged district) in all seasons except for winter. The winter curve was much more balanced, and the minimum was detected in the case of the forest area near the border of the urban area. The temperature of the water surfaces (at 7000 and 9000 m) was extremely low in all cases.

Table 3 Statistical parameters of seasonal LST in the different local climate zones

LCZ	LCZ name	MIN	MAX	MEAN	MIN	MAX	MEAN	MIN	MAX	MEAN	MIN	MAX	MEAN
2	Compact midrise	28.8	35.8	**33.8**	32.8	39.7	38.1	22.6	28.2	27.0	11.2	18.9	**16.9**
3	Compact low-rise	28.6	35.4	33.0	33.2	39.5	37.5	23.3	28.3	26.9	13.2	18.9	**17.1**
5	Open mid-rise	22.1	38.1	30.2	28.6	42.1	36.3	20.8	30.5	25.7	**8.0**	21.0	16.3
6	Open low-rise	23.7	41.0	31.0	28.6	43.6	36.4	21.1	31.4	26.0	9.8	24.3	16.3
8	Large low-rise	22.7	**44.0**	32.4	28.3	**47.2**	**38.2**	20.7	**34.8**	**27.0**	9.2	**28.2**	16.8
9	Sparsely built	**21.6**	41.6	**27.5**	**26.9**	44.7	**34.7**	**20.4**	32.3	**24.6**	8.6	25.4	**15.4**
	Total area	21.9	34.5	27.7	26.3	37.5	32.4	19.3	27.4	23.3	10.0	22.8	16.5
		18-May-2015			21-Jul-2015			23-Sep-2015			22-Feb-2016		

Table 4 Extremities in the relationship between average seasonal LST and NDVI values for district

District	R	LSTmean	NDVImean	R	LSTmean	NDVImean	R	LSTmean	NDVImean
Belváros	**-0.56**	32.58	0.42	**-0.59**	37.14	0.40	**-0.53**	26.72	0.39
Móraváros	**-0.88**	29.18	0.60	**-0.83**	35.09	0.55	**-0.81**	25.44	0.56
	18-May-2015			21-Jul-2015			21-Sep-2015		

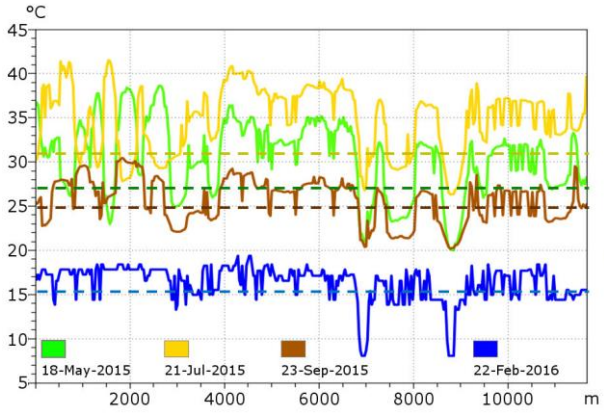

Fig. 6 Temporal patterns of LST (the dashed line represents the mean temperature of the rural areas)

The evaluation of the cross-section confirms how important the vegetation cover is in urban areas influencing the urban surface temperature. Vegetated surface can decrease the LST even by 13°C contributing to better health conditions and a positive human comfort.

CONCLUSION

The study investigated the differences of urban surface temperature compared to rural areas. The results confirmed to what rate green areas can decrease LST which has indirect impact on the air temperature. The high density of built-up areas and the huge paved surfaces are characterized by intensive warming up. In the investigated 30-years-long period the LST pattern changed only due to the new built-up areas and other urban developments. However, the absolute numbers are highly dependent on the actual weather conditions. Compared to the rural areas the SUHI intensity has significantly decreased, which is due to the increasing extent of built-up areas. The seasonal assessment confirmed the inverse correlation between vegetation and LST.

Remote sensing and GIS assessments proved to be useful tools for mapping spatial and temporal patterns of urban surface temperature. The results can be used for city planning and management in environmental and physiological aspects as well to manage the phenomenon of UHI. The advantage of the applied GIS method is the automation of the data processing, as a result of which homogenous data can be generated for large areas. The basic datasets can be downloaded for free and the temporal extent is more than 30 years. The disadvantage is the low temporal resolution, preventing the investigating of changes within one day.

References

Chavez, P.S. 1996. Image-Based Atmospheric Corrections. Revisited and Improved Photogrammetric Engineering and Remote Sensing 62, 1025–1036.

Gábor P., Jombach S. 2009. The relation between biological activity and the land surface temerature in Budapest. *Applied Ecology and Environmental Research* 7, 241–251. DOI: 10.15666/aeer/0703_241251

Kruse, F. A., Lefkoff, A.B., Boardman, J.B., Heidebrecht, K.B., Shapiro, A.T., Barloon, P.J., Goetz, A.F.H. 1993. The Spectral Image Processing System (SIPS) - Interactive Visualization and Analysis of Imaging spectrometer Data. *Remote Sensing of Environment* 44, 145–163. DOI: 10.1016/0034-4257(93)90013-n

KSH 2015. Magyarország településhálózata 2. Városok-falvak.(The Hungarian settlement system 2 – Cities and villages) Central Statistical Office, Budapest, 88 p. (In Hungarian)

Landsberg, H.E. 1981. The urban climate. The Academic Press, London, New York, 196 p.

Lelovics E., Unger J., Gál T. 2014. Designing of an urban monitoring network, based on Local Climate Zone Mapping and temperature mapping modelling. *Climate Researches* 60, 51–62. DOI: 10.3354/cr01220

Mallick, J., Singh, C.K., Shashtri, S., Rahman, A., Mukherjee, S. 2012. Land surface emissivity retrieval based on moisture index from LANDSAT TM satellite data over heterogeneous surfaces of Delhi city. *International Journal of Applied Earth Observation and Geoinformation* 19, 348–358. DOI: 10.1016/j.jag.2012.06.002

Moran, M., Jackson, R., Slater, P., Teillet, P. 1992. Evaluation of simplified procedures for retrieval of land surface reflectance factors from satellite sensor output. *Remote Sensing of Environment* 41, 169–184. DOI: 10.1016/0034-4257(92)90076-v

Nichol, J. 2005. Remote sensing of urban heat island by day and night. *Photogrametric Engineering & Remote Sensing* 71, 613–621. DOI: 10.14358/pers.71.5.613

OGIMET 2016. http://www.ogimet.com/gsynres.phtml.en

Oke, T.R. 1976. The distinction between canopy and boundary layer urban heat islands. *Atmosphere* 14, 268–277.

Oke, T.R. 1988. Street design and urban canopy layer climate. *Energy and Buildings* 11, 103–113. DOI: 10.1016/0378-7788(88)90026-6

OMSZ (Hungarian Meteorological Service) 2016. http://met.hu/eghajlat/

Péczely Gy. 1979. Éghajlattan (Climatology). Nemzeti Tankönyvkiadó, Budapest, 324 p. (In Hungarian)

Probáld F. 1974. Budapest városklímája (Urban climate of Budapest). Akadémiai Kiadó. Budapest, 126 p. (In Hungarian)

Purnhauser P. 2001. A városi hőszigetet és a városi szerkezet összefüggéseinek feltárása terepi és térinformatikai módszerekkel Szegeden. (Assessment of the relationship between urban heat island and city structure using field data and remote sensing). University of Szeged, Department of Climatology and Landscape Ecology, Szeged, 65 p. (In Hungarian)

Roth, M., Oke, T.R., Emery, W.J. 1989. Satellite-derived urban heat islands from three coastal cities and the utilization of such data in urban climatology. *International Journal of Remote Sensing* 10, 1699–1720. DOI: 10.1080/01431168908904002

Sobrino, J., Jiménez-Muñoz, J.C., Paolini, L. 2004. Land surface temperature retrieval from LANDSAT TM 5. Remote Sensing of Environment 90, 434–440. DOI: 10.1016/j.rse.2004.02.003

Soósné, D.Zs. 2009. A magyarországi és közép- európai nagyvárosokban kialakuló városi hősziget vizsgálata finom felbontású műholdképek (Analysis of urban heat islad effect in Hungarian and Central European cities using high-resolution satellite imagery). PhD Theses. ELTE Department of Meteorology, Budapest, 112 p. (In Hungarian)

Stewart, I.D., Oke, T.R. 2012. Local climate zones for urban temperature studies. *Bulletin of the American Meteorological Society* 93 (12), 1879–1900. DOI: 10.1175/bams-d-11-00019.1

Unger J. 1996. Városklimatológia – Szeged városklímája (Urban climatology – Urban climate in Szeged). Acta Climatologica et Chorologica Univ Szegediensis 31B (Urban climate special issue), 69 p. (in Hungarian)

Unger, J. 2010a. A városi hősziget-jelenség néhány aspektusa (Some aspects of urban heat island phenomenon). Doctoral Thesis, Hungarian Academy of Sciences, Szeged, 107 p.

Unger J., Gál T., Rakonczai J., Mucsi L., Szatmári J., Tobak Z., van Leeuwen B., Fiala K. 2010b. Modeling of the urban heat island pattern based on the relationship between surface and air temperatures. *Időjárás / Quarterly Journal of the Hungarian Meteorological Service* 114, 287–302.

USGS Landsat 8, https://landsat.usgs.gov/Landsat8_Using_Product.php [05.20.2016]

Weng, Q., Lu, D., Schubring, J. 2004. Estimation of land surface temperature–vegetation abundance relationship for urban heat island studies. *Remote Sensing of Environment* 89, 467–483. DOI: 10.1016/j.rse.2003.11.005

World Bank 2014. http://datacatalog.worldbank.org/

JOURNAL OF ENVIRONMENTAL GEOGRAPHY
Journal of Environmental Geography 9 (1–2), 31–38.
DOI: 10.1515/jengeo-2016-0005
ISSN: 2060-467X

ENVIRONMENTAL MONITORING SUPPORTED BY AERIAL PHOTOGRAPHY – A CASE STUDY OF THE BURNT DOWN BUGAC JUNIPER FOREST, HUNGARY

József Szatmári*, Zalán Tobak, Zsolt Novák

Department of Physical Geography and Geoinformatics, University of Szeged, H-6722, Egyetem u. 2-6, Hungary
*Corresponding author, e-mail: szatmari@geo.u-szeged.hu

Research article, received 15 April 2016, accepted 11 June 2016

Abstract

Wildfire poses a serious risk in several regions of the world threatening urban, agricultural areas and natural ecosystems as well. Nature conservation has important role to be prepared for the management of postfire environmental degradation and restoration for protected areas preserving valuable ecosystems. The improving temporal and spatial resolution of remote sensing and GIS methods significantly contributes to map the changes for accelerating management steps of restoration. In this study a severe wildfire and its impacts were assessed in case of a protected area of the Kiskunság National Park in Hungary, which was partly burnt down in 2012. The aim of this research was to efficiently and accurately assess the damages and to plan and execute the restoration works using remote sensing tools. Aerial data collection was performed one month, and one year after the fire. In 2014 the regenerated vegetation was surveyed and mapped in the field. Using the aerial photographs and the field data, the degree and extent of the fire damages, the types and the state of the vegetation and the presence and proportion of the invasive species were determined. Semi-automatic methods were used for the classification of completely, partially damaged and undamaged areas. Based on the results, the reforestation of the burnt area is suggested to prevent the overspreading of white poplar against common junipers and to clean the area from the most frequent invasive species. To monitor the regeneration of the vegetation and the spreading of the invasive species, further aerial photography and field campaigns are planned.

Keywords: wildfire, aerial photography, invasive species, supervised classification

INTRODUCTION

Wildfire poses a serious risk in several regions of the world these days. This growing risk proves that climate change has an omnipresent influence on the fundamental environmental and ecological resources. Paton and Shroder (2015) point out, that wildfire has had a significant effect on ecosystems for millennia and ecosystems have been formed through people working with the fire rather against it. A social-ecological perspective should always be considered if we want to understand and manage wildfire risk (Buergelt and Paton, 2014). Wildfires mean a hazard and a huge threat in recurring drought periods which are caused by climate change. Societies and communities exposed to facing wildfire hazards may experience more and more frequent, large-scale, devastating wildfire events (Adams, 2013). It is evident that the majority of fires are human induced; the Mediterranean region accounts for the larger proportion of human-caused fires in the world (95%) (Leone et al., 2009). In most of European countries, forest fire outbreaks result from human activities without intention to provoke damage (i.e., they start by accident, negligent actions, or risk behavior) (Tedim et al., 2015). The increase in the number of wildfire hazards in recent years has brought a combined results of the ever-larger droughts and all-pervading reporting (Mockenhaupt, 2014), which has called forth the increased number of remedial methods in dealing with fires.

Wildfires have the unique characteristic due to the complex interdependencies that exist between humans and the forest sources of wildfire hazards. Forests have always presented the crucial territory for agriculture, livelihood, hunting and forests and other natural environments have also played important roles in sustaining human well-being (Clayton and Opotow, 2003). Climate change will have an effect on the patterns of wildfire risk and their distribution (Nicholls and Lucas, 2007). Locally, wildfire consequences affect directly air quality, ecosystems and landscapes. Secondary consequences can be traced when we examine the impact of fire hazards on water and soil quality. These can cause instant damage to vegetation and fauna and have direct and indirect impacts on soils through heat release and ash deposition, and contribute to postfire environmental degradation (Vallejo and Alloza, 2015). At the beginning of this century a large-scale flooding period and forest fires started this is why the European Parliament had to adopt the "European Parliament resolution on Natural Disasters (fires, droughts, and floods) environmental aspects (2005/2192(INI))". To protect the forests throughout the EU is one of the most crucial actions of the EU Forest Action Plan, in which the member states are invited to

support forest fire prevention measures, restoration of forests after being damaged by natural disasters (Tedim et al., 2015).

There are two main periods in the year when forest fires pose a great risk in Hungary. The first group of fire incidents is connected with the beginning of agricultural work (burning of fields and stubbles) which starts after the snow has thawed and the weather is characterised by the lack of precipitation between February and April. New plantations are usually prone to more extensive damage in these wildfires, while vegetation consisting of older trees is less endangered. The second group of forest fires occurs from June to September when the dry litterfloor of deciduous and coniferous forests fuels these fires in the hot, drought-stricken summer months. These incidents are mainly characteristic of the drier areas of Bács-Kiskun and Csongrád counties on the Great Hungarian Plane [1].

The increased frequency of forest fires observed in the past few decades is most likely to be caused by the more and more extreme climate (less precipitation, higher mean temperature, winters without sufficient snow covering), which ultimately leads to the drying out of plant litter. Due to climate and vegetation circumstances, naturally induced forests fires are of no account (about 1%) in Hungary. 99 % of forest fires are human induced (negligence or arson). Most fires are induced by (adults' and infants') negligence and only a small proportion of fires are caused by arsonists [2].

In this study a severe wildfire and its impacts were assessed in case of a protected area of the Kiskunság National Park in Hungary, which was partly burnt down in 2012. The aim was to support the professionals of the national park in their work to estimate damage effectively and properly as well as to plan, organize and implement restoration measures by providing remote sensing strategies and tools, i.e. methods of collecting, processing and analysing data (Szatmári et al., 2014).

STUDY AREA

The study area, the Bugac Juniper Forest is located in the Kiskunság Sandland, in the Danube-Tisza Interfluve (Fig. 1). The No. VI protected area of the Kiskunság National Park (KNP) is situated about 7 km north to the settlement of Bugac. Crescent-shaped sand dunes are the most characteristic features of the surface, they stretch out about 4 km long, and they may even reach 12-18 m height in this region. The majority of sand and loess found here are alluvial deposits of the paleo-Danube. These deposits were shaped into sand dune lines by north-west winds in the Pleistocene and Holocene. The beginning of the Holocene marked the anchor of these aeolian forms, but later in the Boreal period the wind started to move them again (Borsy, 1989). Saline lakes were formed in the interdunal depressions (Temesi, 1986).

The predominant plant association of the area is the open perennial sand grassland. The extent of land cover is about 50%, it reaches its biggest diversity in spring and autumn, while the association usually dries out in summer. Its environmental protection value makes the open perennial sand grassland a very important one (Facsar, 1996); most of the endemic herbaceous plants of Hungary can be found in this association (e.g. Hungarian or sand fescue (*Festuca vaginata*), different feather grass species (*Stipa sp.*)). The natural multi-layer flora on the top and the southern slope of the sand dunes as well as steeper parts of the area is made up of juniper-poplars

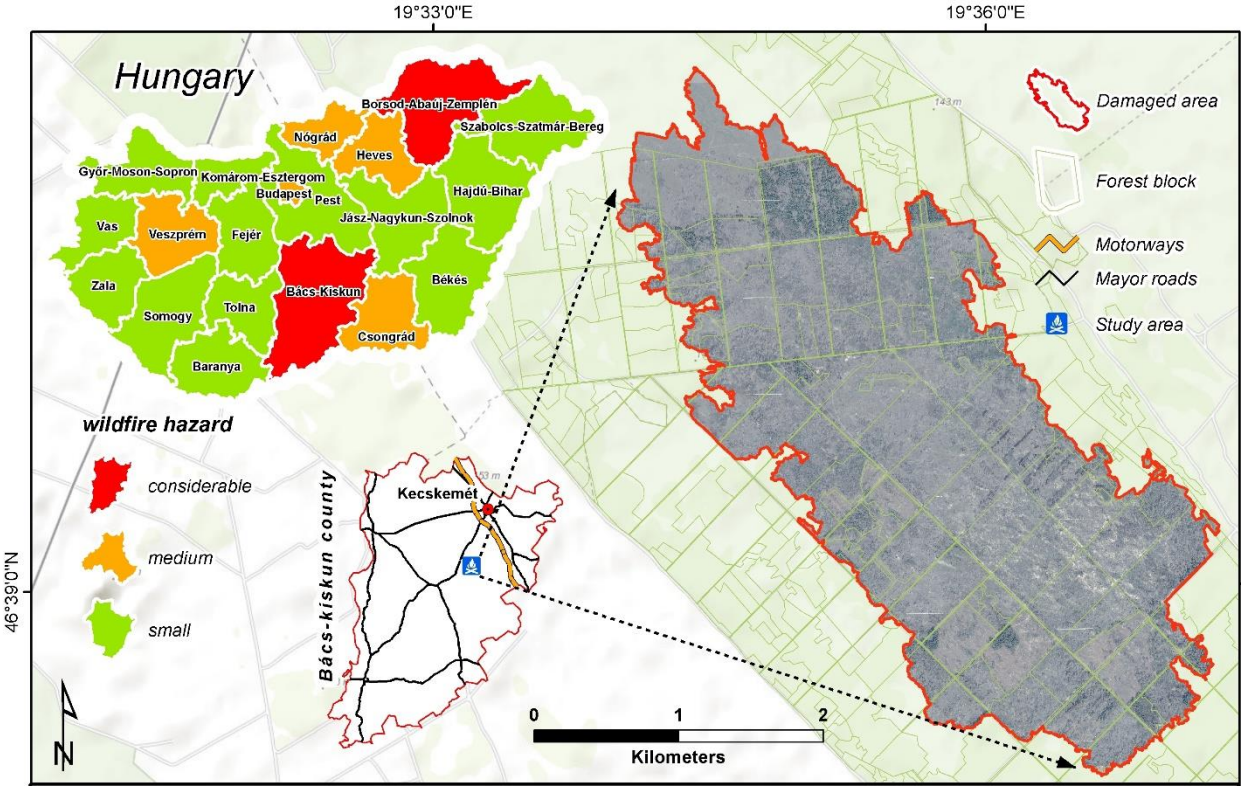

Fig. 1 Wildfire hazard of the Hungarian counties and the location of the study area in Bács-Kiskun county, characterized by a considerable wildfire hazard

(*Festucetum vaginatae juniperetosum*). The canopy layer consists of white poplars (*Populus alba*) mainly, and sometimes grey poplars (*Populus canescens*), the understorey layer consists of common junipers (*Juniperus communis*) as well as small groups of common hawthorns (*Crataegus monogyna*) and blackthorns (*Prunus spinosa*). There are several rare orchid species to be found in the forest floor such as the Red Helleborine (*Cephalonthera rubra*), the Royal (*Epipactis etrorubens)* and the Bugac Helleborine (*Epipactis bugacensis*) (Borhidi, 2003). English oaks (*Quercus robur*) also mix into the closed canopy layer of the associations in the valleys and on the sand dune slopes. Surface fires, when surface litter and other dead vegetal parts and smaller shrub burn have been common in this type of forest vegetation. They can develop in whole fire season. Forest litter, needles, dead twigs and branches get totally dry in arid periods without rainfall and start easily burning as a consequence of negligently lighted fire [2].

On 29 April 2012, a fire broke out in the study area, and it was finally extinguished on 5 May 2012. The south-southeast winds took its smoke as far as the outskirts of the capital as is shown on satellite images (Fig. 2). Wildfire suppression was made difficult by embers in tree hollows that kept on smouldering for days, unfortunate soil conditions, and sudden gusts of the wind. It was a high-alert wildfire that flamed up numerous times until the afternoon of 1 May 2012, and more than a fifth of the protected area had burnt to the ground. Both flora and fauna suffered considerable loss, for example, many protected reptiles and bird hatchlings fell victim to the fire.

The Hungarian state contributed to the restoration of the damaged vegetation by mobilising new work force who helped the employees of the national park clean up debris, plant saplings, and eradicate invasive plant species that started to spread aggressively in the burnt area.

METHODS

Aerial photography

Remote sensing data were collected by equipping a Cessna 172 with a high resolution aerial photography system (Tobak et al., 2008a). Out of the numerous advantages of the system, its cost efficiency (Novák, 2015), and its operativity can be highlighted (Tobak et al., 2008b). The fact that the system is easy to operate becomes particularly important in projects that investigate quickly changing phenomena (Bakó, 2010). The central unit of the aerial photography system is a Trimble Aerial Camera which is a 39-megapixel model with a PhaseOne P45+ back wall, interchangeable 47 mm RGB and CIR (color-infrared) imagery lenses, and various controllers. The camera system is supported by adequate power supply, GPS tools to provide correct navigation, and a portable computer. The Aero TopoL software of the system supports both the planning and navigational phases (Tobak, 2013).

In order to estimate damage as soon as possible, the study area was surveyed one month after the forest fire (7 June 2012), while monitoring its regeneration and the spread of invasive species happened one year later (1 July 2013). The same monitoring system and procedure were applied on both occasions. A precise flight route was planned before the aerial survey itself, which enabled us

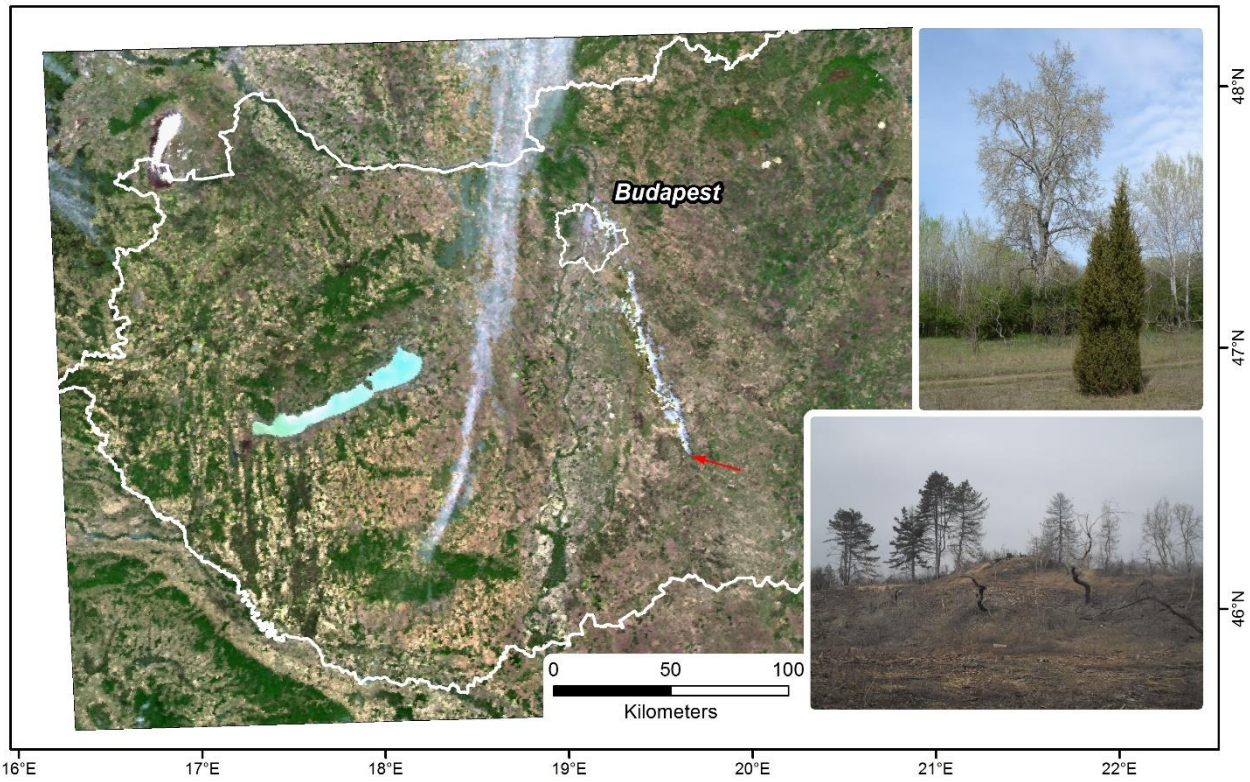

Fig. 2 Spread of the smoke of the 2012 Bugac forest fire as depicted on a satellite image [3], *Common juniper* with an old white poplar (*Populus alba*) in the background and a part of the burnt area

to prepare the geometric file of the flight rows and image centres based on the data of the study area borders given by the KNP. It is the basic requirement of navigation- and position-based aerial photography. The images were collected with a 60-70% overlap in the along track direction, and 20-30% in the cross track direction. These overlaps allowed the continuous cover of the study area as well as its spatial analysis (e,g. altimetry). A further important parameter of aerial photography is GSD (ground sample distance) which, in our case, was 20 cm (2012 survey) and 10 cm (2013 survey) respectively. 58 images were taken in 4 flight rows from altitudes of 1,400 m and 700 m in 2012, and 179 images were taken in 7 flight rows from the same altitudes in 2013 (Fig. 3).

Data acquisition was followed by raw data – navigational and image – processing. The co-ordinates of the actual flight route and the aerial photo processing centre can be obtained in ASCII format, which can be integrated into a geographical information system directly after being converted to the proper format. It means that we had 3 co-ordinates and one camera rotation angle (kappa) value, out of the 3 possible ones (omega-phi-kappa), per image at our disposal as initial exterior orientation parameters. This information is the input data for the aerial triangulation of the aerial photographs. The unit of the camera rotation angle was degree and the centre co-ordinates were recorded in the EOV (Unified National Map Projection) system in metres.

Creation of orthophotos

By using small format aerial photography system, photographs can be taken at any time at any frequency, which provides precise orthophotos for further image classifications and analyses. The so-called block of aligned photos was prepared from individual photographic images. The auto detection of common points in the overlapping image parts and the initial parameters of the exterior orientation are used in this process. After aligning the images the software automatically starts detecting common points in the overlapping parts of the block, and creates a sparse 3D point cloud. In order to filter our gross geometric errors, a mesh is generated based on the sparse cloud.

In order to match the model and the actual geographic space accurately, on site ground reference points are also needed. Professionals of the KNP placed 162 foil stripes in the study area so that they could be identified in the images too. The co-ordinates of these stripes were fixed with RTK GNSS, and during data procession they served as GCPs (Ground Control Points) in the exterior orientation of the model. A homogeneous distribution of 8-9 GCPs in the multi-overlapping image parts were enough in the total block of aligned photos. As a result, an orthomosaic (an orthophoto from rectified photos, with the same geometric resolution as the original aerial photos) is produced on the basis of the oriented aerial photo block of the whole study area.

Analysis of aerial photos

The orthorectified RGB and CIR images can be used in a wide range of studies. The common characteristic of these studies is that they require high spatial and temporal resolution and visible as well as near infrared spectral information. The detailed analysis of the processed data was done in the total of the study area. The applied methods can be categorised into manual, semi-automatic, and automatic methods based on the extent of the necessary intervention of the analysing process. In order to optimise

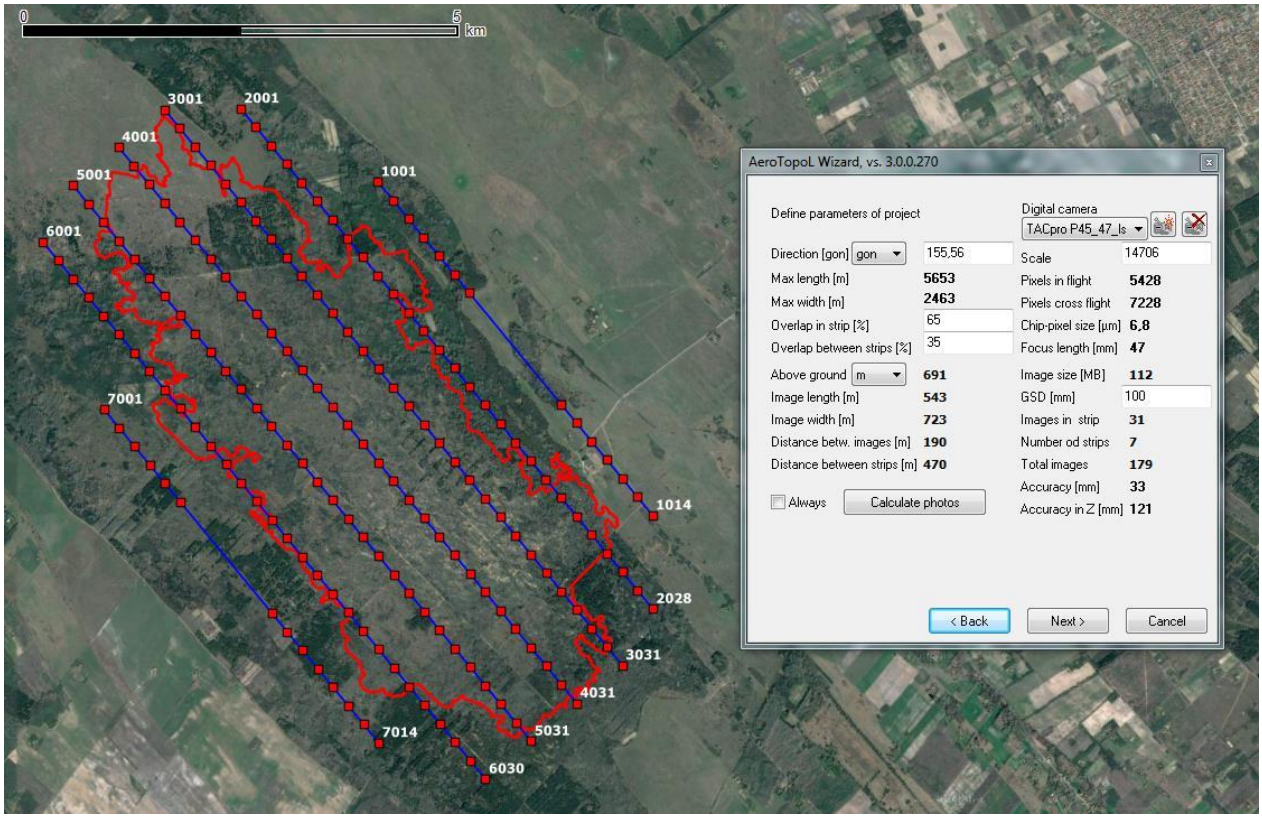

Fig. 3 Flight plan and its parameters of the 2013 aerial survey campaign

the ratio of temporal and personal resources of the analysis to the expected quality and availability of the results, semi-automatic methods were employed primarily.

Manual analysis was employed to the visual separation and bordering of the parcels damaged to a varying extent. At this step it was important for the analyst of the data to be profoundly familiar with the study area, which was established by the on site fieldwork with the professionals of the KNP and a thorough GPS survey.

Remote sensing data were stored in raster format, and different image classification algorithms were run on them. We also tested the *ISODATA* technique, which automatically allocates the image elements to classes. In this case, identifying (labelling) classes happens afterwards. From the supervised classification methods, which demand bigger user intervention, the Maximum Likelihood algorithm was applied. In this classification method, classes were created on the basis of previously identified training sites with already known vegetable type and damage extent.

On site field survey

On site data collection took place on 9 April 2014, the state of the study area and the vegetation was surveyed. Each parcel was categorised during the on site field survey, then the descriptive data of the surveyed objects were captured systematically in geographic information system. The type of the vegetation, the name of the most densely occurring invasive species, the extent of the species' spread were all categorised from 1 to 5. Special data belonging to certain polygons were also captured, these data included information such as the newly planted poplars, the aging vegetation

Invasive species and their land cover rate in the study area

Invasive plants (or adversed introduced plants) are usually plant species which are not native to a specific location. Invasive plant species usually do not have any special requirements, tolerate a wide range of environmental conditions, and have no natural controls therefore their pest-resistance is high. By adapting fast, they drive local native or indigenous species to (near) extinction. They have a tendency to spread aggressively and, as a result, they may seriously disrupt the native ecological system (Sipos, 2004).

The invasive species in the study area are as follows: tree of heaven or ailanthus (*Ailanthus altissima*), false acacia or black locust (*Robinia pseudoacacia*), common milkweed or silkweed (*Asclepias syriaca*), wild black cherry (*Prunus serotina*), non-native Canadian (also known as American) poplar (*Populus x canadensis hybrids, Populus x euramericana syn.*), and black pine (*Pinus nigra*). During the on site field survey 5 categories of invasive plant species were created on the basis of their density:

1. no presence in the parcel
2. 0-10% density in the parcel
3. 10-25% density in the parcel
4. 25-50% density in the parcel
5. over 50% density in the parcel

Surveying the vegetation of the study area

The following types of vegetation were identified in the parcels of the study area when surveying vegetation and its general state: white poplars, junipers, white poplar-junipers, Scots and black pines, false acacias, and open grasslands in some places. On the basis of the damage caused by the forest fire, intact and burnt parcels were identified.

RESULTS

Extent of damage based on remote sensing data

Interpreting the pre-processed – orthorectified – aerial photographs meant manual delineating of parcels in the simplest case. In accordance with the expectations of the KNP, this method was employed when surveying the damage to the non-native (introduced and purposefully planted) pine trees. On the basis of the forest maps 24% (202 ha) of the study area (a total of 835 ha) was classified as intact, 38 % (318 ha) as partly, and 38% (318 ha) as totally damaged (burnt) (Fig. 5A, [4]).

The results of the supervised (Maximum Likelihood) and the automatic (ISODATA) methods of the (semi-)automatic workflow are shown in a sample area of 11 ha, which represents the analysed categories of the whole study area. The supervised classification of the previously fixed training sites allocated 50% of the sample area as damaged (burnt), 30% as partly damaged, and 12% as intact. The rest of the study area, ca. 8%, was allocated as shadowed or open sandland (Fig. 5B).

The results of the ISODATA clustering run with 9 initial classes showed a more heterogeneous picture, at the same time, the border lines of the most damaged area was clearly seen here too. This method allocated 30% of the pixels to the damaged (burnt) class, 28% to the partly damaged, and 14% to the intact classes. The proportion of the shadow areas was bigger (21%) (Fig. 5C).

Types of vegetation

The study area (1748 ha) was covered by white poplars (622 ha, 34.8%), white poplar-junipers (488 ha, 27.3%), Scots pines (307 ha, 17.1%), open grasslands (185 ha, 10.3%), junipers (115 ha, 6.4%), and false acacias (68 ha, 3.8%) two years after the wildfire (Fig. 6). Scots pines are found in the periphery, which may indicate that this type of vegetation may have a certain protecting role.

On the basis of on site field data, more than half of the study area was damaged in the wildfire. Juniper and Scots pine associations were damaged the most extensively (Fig. 7). There were no visible traces of wildfire damage in the open grassland associations, they had regenerated from seeds found in the soil.

The burnt white poplar associations were sprouting which indicated their strong regeneration ability. The size of the sprouts were between 1-1.5 m. There were many aging stands in the forest which indicated the bad health state of the vegetation. The dead, burnt tree trunks left in the study area after the suppression of the wildfire were all decaying.

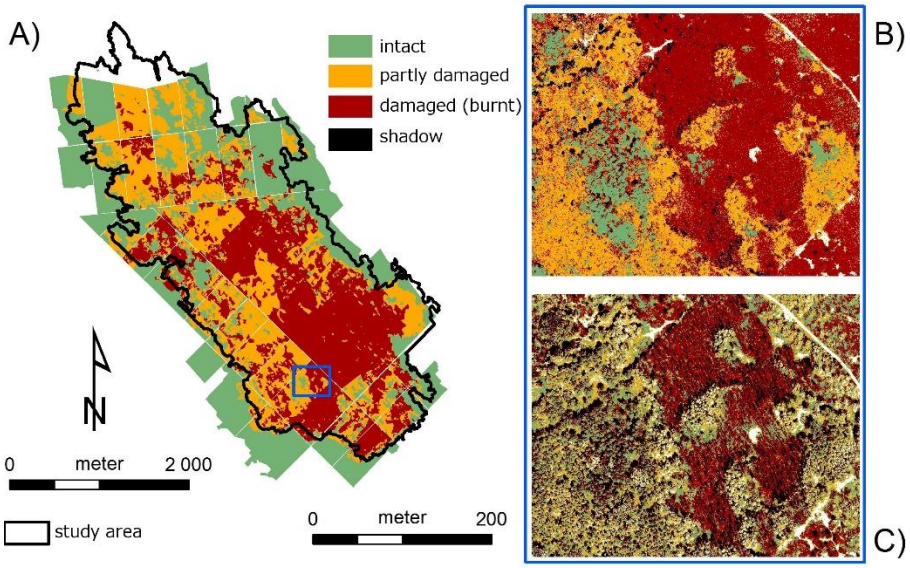

Fig. 5 Manual bordering of the damaged sites of varying damage extent (A) and their classification (B: supervised classification, C: ISODATA clustering) on the basis of aerial photos

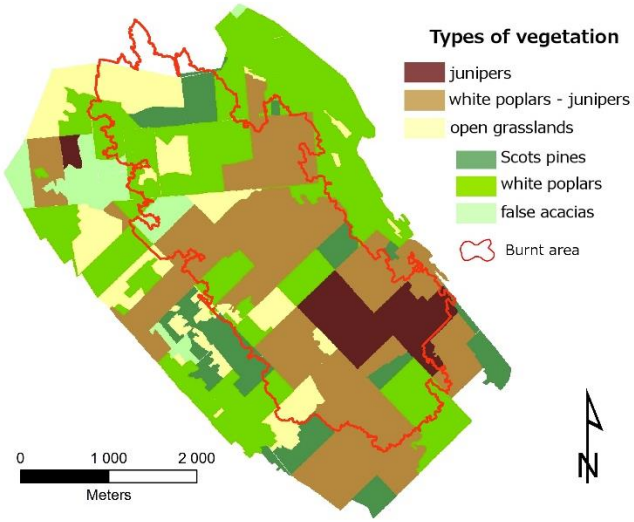

Fig. 6 Location of different types of vegetation in the study area

Invasive species and the extent of their appearance

The rehabilitation of the study area in the Bugac Juniper Forest started in 2012. In the beginning, the dead and burnt wood pieces and logs were not removed from the study area, this process has been in progress since then. However, the transport of these tree remnants is not advantageous as disturbing the area makes it easier for invasive species to appear and spread. At the same time, processing and transporting the remnants is necessary to stop the appearance and rapid swarming of pests that endanger both the remaining and the newly growing vegetation.

The spreading of the invasive plant species in the study area is rapid. The distribution of these species in the forest is as follows: 46% false acacia, 3% Canadian poplar, 8% ailanthus, 2% black pine, 0.04% wild black cherry, and 18% common milkweed (Fig. 8). The most aggressively spreading invasive species is common milkweed. False acacia shows the greatest extent of spreading, this species strongly degrades the conservation value of this more strictly protected area. There were no signs of invasive species in the juniper associations, although it was damaged the most in the wildfire. Figure 9 also shows that the invasive plant species appear in the periphery of the forest and in the open grassland associations.

Fig. 7 An aerial photograph showing the damage to juniper associations

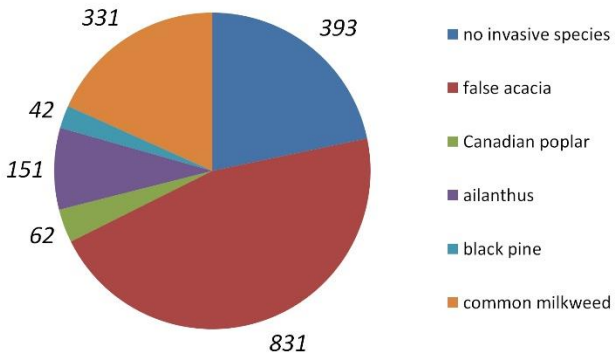

Fig. 8 The appearance of invasive species (ha)

DISCUSSION AND CONCLUSIONS

The extent of damage, the type and state of vegetation, and the extent of the invasive species' appearance were all categorised by processing and analysing aerial photos and on site field survey. Databases were designed for further expansion, too, so that other types of data can be recorded and studied here in the future. The analysis of remote sensing data was aided by semi-automatic classification methods.

Our analyses and geoinformatic database help professionals regenerate the forest and stop the spreading of invasive plant species. In order to successfully regenerate vegetation, it is necessary to plant new stands. New planting of pine forests may be important because they may serve as a protecting belt around the inner area of the forest, and they may as well be buffer zones where the appearance of invasive species is not considerable. Sprouts of white poplar associations in the Bugac Juniper Forest must be controlled so that they will neither spread too much nor suppress junipers' spreading.

It is also important to cut out invasive plant species continuously, and more parcels have to be cleared of the sprouts of false acacia and ailanthus. Stopping common milkweed from spreading in open grasslands is another significant task, which is made more difficult by the fact that common milkweed spreads very aggressively in the area. Their eradication is also made difficult by their mode of spreading: common milkweed reproduces both by seeds and rhizomes, and forms a colony or a long, thick line quickly crowding over other plants.

Further aerial photography and on site field survey are planned to follow the regeneration of the area and monitor the undesirable spread of invasive plant species. With our work we would like to contribute to the regeneration of one of the most visited sites of the Kiskunság National Park introduced in our study.

Acknowledgements

We wish to express our thanks and gratitude to Róbert Aleksza, Zoltán Filotás and Gergely Folberth fromthe Kiskunság National Park, and Csaba Lestyán from the Hungarian Forest Management Bács-Kiskun County Government Offices for their assistance in our work.

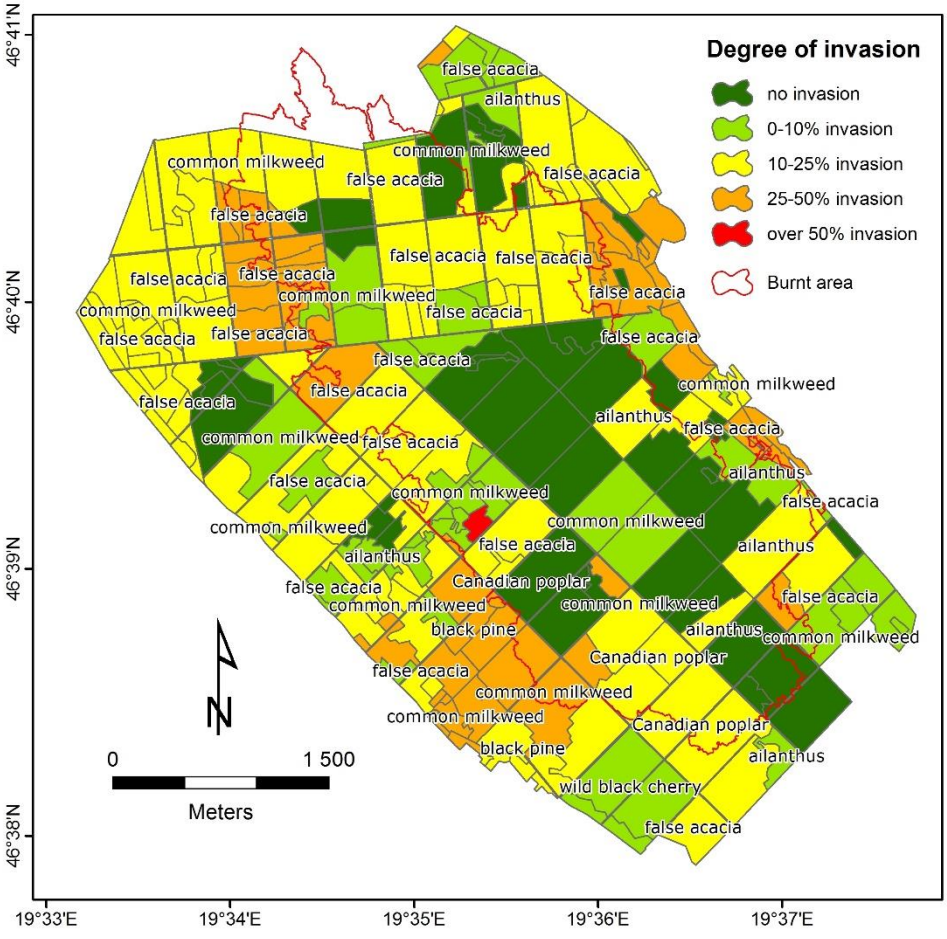

Fig. 9 Invasive species and degree of invasion

References

Adams, M.A. 2013. Mega-fires, tipping points and ecosystem services: managing forests and woodlands in an uncertain future. *Forest Ecology and Management* 294, 250 – 261. DOI: 10.1016/j.foreco.2012.11.039

Bakó, G. 2010. Igen nagyfelbontású légifelvétel-mozaikok készítése kis- és középformátumú digitális fényképezőgépekkel. (High resolution aerial photogrammetry with small- and middle format digital cameras). *Geodézia És Kartográfia* 62 (6), 21 – 29. (in Hungarian)

Borhidi, A. 2003. Magyarország növénytársulásai (Plant associations of Hungary) Akadémia Kiadó, Budapest, 466 – 467. (in Hungarian)

Borsy, Z. 1989. Az Alföld hordalékkúpjainak negyedidőszaki felszínfejlődése (Evolution of the alluvial fan of the Hungarian Great Plain in the Quaternary). *Földrajzi Értesítő* 210 – 220. (in Hungarian)

Buergelt, P.T., Paton, D. 2014. An ecological risk management and capacity building model. *Hum. Ecol.* 42, 591– 603. DOI: 10.1007/s10745-014-9676-2

Clayton, S.D., Opotow, S. 2003. Identity and the Natural Environment: The Psychological Significance of Nature. MIT Press, Cambridge, 347 p.

Facsar, G. 1996. Évelő nyílt homokpusztai gyepek. (Open sand steppes) In: Fekete G., Molnár Zs., Horváth F. (eds.) A Magyarországi élőhelyek leírása és határozókönyve a nemzeti élőhely-osztályozási rendszer. Vácrátót, 71-72, p. 114 (in Hungarian)

Leone, V., Lovreglio, R., Martı´n, M.P., Martı´nez, J., Vilar, L., 2009. Human factors of fire occurrence in the Mediterranean. In: Chuvieco, E. (Ed.), Earth Observation of Wildland Fires in Mediterranean Ecosystems. Springer-Verlag, Berlin Heidelberg, 149–170.

Mockenhaupt, B. 2014. Fire on the mountain. *The Atlantic* 72– 86.

Nicholls, N., Lucas, C. 2007. Interannual variations of area burnt in Tasmanian bushfires: relationships with climate and predictability. *Int. J. Wildland Fire* 16(5), 540– 546. DOI: 10.1071/wf06125

Novák, Zs. 2015. Az ortofotó-térképek, a légi fotogrammetriai felmérések bekerülési költsége 2015. évben. (Prices of orthophotos and aerial photogrammetry assessments in 2015) *Remote Sens.* 5(3), 433– 437. (in Hungarian)

Paton, D., Shroder, J. F. (eds) 2015. Wildfire Hazards, Risks, and Disasters. Elsevier, 283 p.

Sipos, F. 2004. Kiskunsági Nemzeti Park Igazgatóság.(Kiskunság National Park Directorate) In: Mihály B., Botta-Dukát Z. (eds.): Özönnövények. Biológiai inváziók Magyarországon. Természet-BÚVÁR Alapítvány Kiadó. Budapest. 399– 403. (in Hungarian)

Szatmári, J. Kovács, F., van Leeuwen, B. Tobak, Z. Mezősi, G. Mucsi, L. Juhász, L. Huszár, T. Kitka, G. 2014. Távérzékelés a katasztrófavédelem szolgálatában.(Remote sensing in disaster management) In: Márkus B. (ed.) Térinformatika, Székesfehérvár, p. 399 (in Hungarian)

Tedim, F., Xanthopoulos, G., Leone V. 2015. Forest Fires in Europe: Facts and Challenges. In: Paton D., Shroder J. F. (eds): Wildfire Hazards, Risks, and Disasters. Elsevier, 76 – 99. DOI: 10.1016/b978-0-12-410434-1.00005-1

Temesi, I. (ed.) 1986. Bugac- Ősborókás. Tájak – Korok – Múzeumok. Budapest, 16p. (in Hungarian)

Tobak, Z. 2013. Analysis of urban surfaces using high spatial and spectral resolution aerial imagery. Phd theses, University of Szeged, 122p.

Tobak, Z., Kitka, G. Szatmári, J., van Leeuwen, B. Mucsi, L. 2008a. Kisgépes, kisformátumú (SFAP) CIR légifelvételek készítése, feldolgozása és alkalmazása környezeti vizsgálatokban. (Capturing and processing of SFAP CIR aerial photos and their application in environmental assessments) IV. Magyar Földrajzi Konferencia előadásai. 618 p. (in Hungarian)

Tobak, Z., Szatmári, J., van Leeuwen, B. 2008b. Small format aerial photography – remote sensing data acquisition for environmental analysis. *Journal of Environmental Geography* 1 (3-4), 21– 26. DOI: 10.2478/v10326-012-0001-5

Vallejo, V.R., Alloza J.A. 2015. Postfire Ecosystem Restoration. In: Paton D., Shroder J. F. (eds.): Wildfire Hazards, Risks, and Disasters. Elsevier, 229– 246. DOI: 10.1016/b978-0-12-410434-1.00012-9

Internet references:

[1] http://goo.gl/TGiWCq

[2] http://erdotuz.hu/forest-fires-in-hungary/

[3] http://goo.gl/MlNFDU

[4] http://goo.gl/b3dmPx

JOURNAL OF ENVIRONMENTAL GEOGRAPHY
Journal of Environmental Geography 9 (1–2), 39–44.
DOI: 10.1515/jengeo-2016-0006
ISSN: 2060-467X

CONSTRAINING THE AGE OF FLOODPLAIN LEVELS ALONG THE LOWER SECTION OF RIVER TISZA, HUNGARY

György Sipos*, Tímea Kiss, Orsolya Tóth

Department of Physical Geography and Geoinformatics, University of Szeged, H-6722, Egyetem u. 2-6, Hungary
*Corresponding author, e-mail: gysipos@geo.u-szeged.hu

Research article, received 22 April 2016, accepted 2 July 2016

Abstract

During the Late Pelistocene-Holocene transition the fluvial landscape of the Great Hungarian Plain changed considerably as a consequence of tectonic, climatic and geomorphological factors. Geochronology, and especially luminescence dating, is a very important tool in reconstructing these changes. The present study focuses on the Lower-Tisza region and addresses the timing of the development of different floodplain levels. In the meantime the luminescence characteristics of the investigated alluvial sediments were also assessed, with a special emphasis on the comparison of silty fine grain and sandy coarse grain results, as in the given medium and low energy environment fine grain sediments are more abundant, however, based on the literature, coarse grain samples are more reliable in terms of luminescence dating. Measurements were performed on 12 samples originating from the point bars of two large palaeo-meanders, representing different floodplain levels along the river. Results indicate the applicability of both grain size fractions for dating purposes, though fine grain subsamples overestimate in average by 1.5 ka the ages yielded by coarse grain subsamples. Consequently, fine grain samples can be used for outlining only general trends, and results need to be controlled by coarse grain measurements where possible. Based on the ages received, the upper floodplain was actively formed until 13-15 ka, when incision and the development of an intermediate floodplain level started. The meander on the intermediate flood plain level developed then very actively until 9 ka. As indicated by the received age information the intensity of meander formation could be highly affected by climatic and especially vegetation control. However, reconstruction can be refined later by further sampling and the application of the results of the present paper.

Keywords: OSL, alluvial sediments, River Tisza, palaeo-fluvial record

INTRODUCTION

The primarily alluvial environment of the Great Hungarian Plain hosts numerous generations of palaeochannels which developed in response to highly varying water and sediment discharges during the Late Pleistocene and Holocene (Gábris and Nádor, 2007; Kiss et al., 2015). In several cases these channels are located on well identifiable floodplain levels, referring to incision governed by either tectonic or climatic processes. The evolution of the fluvial network, and especially the development of the Tisza has been addressed by several earlier studies (e.g. Somogyi, 1967; Gábris, 1986; Borsy, 1989, Kiss et al., 2013), focusing on its palaeo-discharge, pattern changes or the age of certain channel generations.

A key question of fluvial development along the Lower Tisza, affected by tectonic subsidence (Nádor et al., 2007), is the morphology and separation of different floodplain levels. Kiss and Hernesz (2011) and later Kiss et al. (2012) identified two separate levels: a higher and a lower floodplain. The later has several meander cores or umlaufbergs being the remnants of the pre-incision floodplain surface. Based on optically stimulated luminescence (OSL) data, they put the start of incision earlier than 20.1±2.1 ka and the termination of it to 8-9 ka. More recently by extending the morphological analysis to the Serbian section of the river Hernesz (2015) separated a further, intermediate floodplain level as well. The dating of palaeochannels on these floodplain levels was carried out by using OSL on coarser sand sized, but also on fine grain silty sediments, however the comparability of results has only been partly assessed (Hernesz, 2015).

A major underlying principle of OSL dating is that sediment grains during transportation are exposed to sunlight, which resets the OSL signal to zero. Consequently, during laboratory measurements the time elapsed since the last exposure to light, or in other words the time of deposition can be determined. In certain sedimentary environments however resetting is not always complete, which results in partial bleaching, making measured OSL ages higher than the true age. Fluvial deposits are greatly affected by the phenomenon.

Previously, several researches addressed the role of grain size in the bleaching process (Hu et al., 2010; Vandenberghe et al., 2007; Alexanderson, 2007). Most of them concluded that coarser grains (sand) are more suitable for luminescence dating than finer grains (silt), as resetting is more adequate in their case. This is explained

by the possible coagulation of fine grains (Hu et al., 2010) and the more frequent exposure of coarser grains on bar surfaces (Rittenour, 2008).

The most common minerals used for OSL dating are quartz and feldspar. Although both minerals are applicable, the choice depends on various factors. Quartz saturates at lower doses, but on the other hand feldspars suffer from anomalous fading (Vandenberghe, 2004). In summary most of the researches emphasize that in terms of fluvial sediments with an age up till several 10 ka the most confident luminescence ages can be received if coarse grain quartz is applied (Bøtter-Jensen, 2006).

The primary aim of the present research was to investigate the development time of two floodplain levels along Lower Tisza by using OSL. Another goal was to assess the rate of morphological evolution in case of the studied palaeomeanders, which provides valuable additional information on the environment in which they were developing. Furthermore, the investigations also allowed to test the luminescence characteristics of alluvial sediments in the region and to compare ages retrieved from the fine grain and coarse grain fraction of OSL samples, since in many situations, as a consequence of the medium energy environment only silty sediments are available for dating.

STUDY AREA

Our research focused on the Lower Tisza Basin where palaeomenaders remained recognizable only in a relatively narrow N-S belt along the Tisza River (Fig. 1). The width and wavelength of these channels significantly exceed contemporary values even if compared to that of the Danube. Two major channel generations were investigated (Fig. 2): one located on the higher floodplain level (Site1), having larger but more blurred pointbars and main channel (meander wavelength=25 km, width=1000 m), and another lying on the intermediate level (Site 2), being smaller but having much intense forms (meander wavelength=9.2 km, width=500 m). The elevation difference is around 1 m between the two floodplain levels.

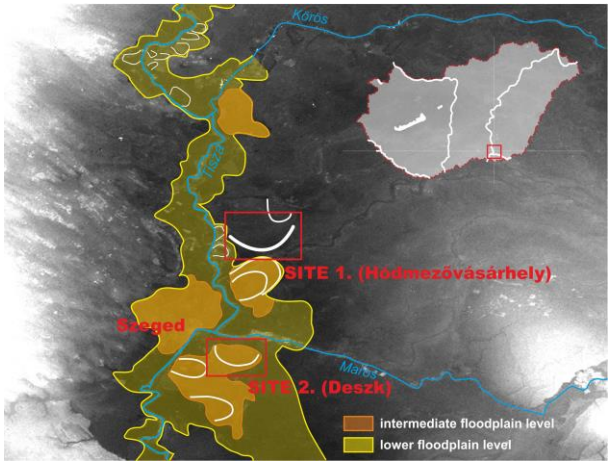

Fig. 1 Location of the studied meanders, the border of the lower and upper floodplain surfaces, and situation of intermediate floodplain levels based on Hernesz (2015)

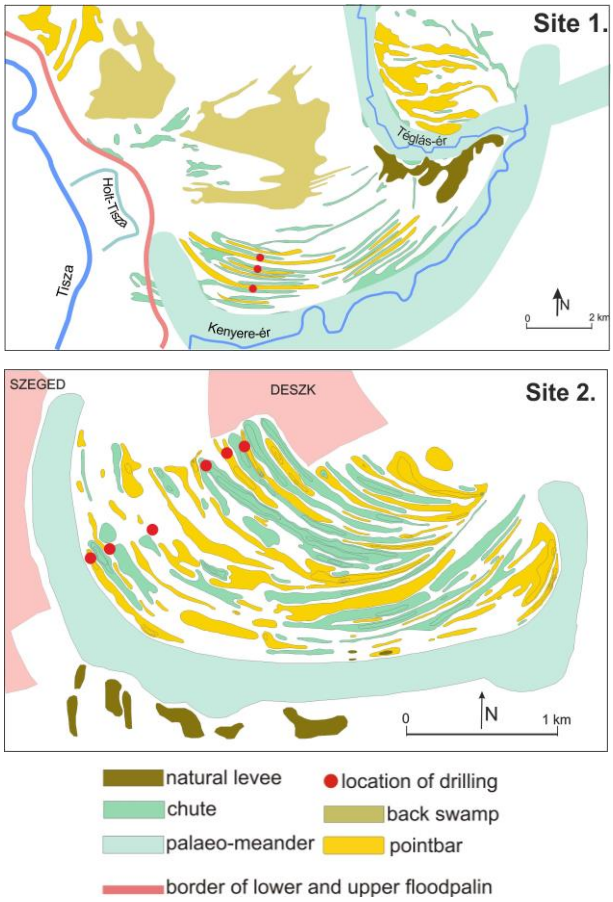

Fig. 2 Geomorphology of the study sites and the location of the drillings

METHODS

The age and development rate of meanders were determined by the means of luminescence dating (OSL). 10 drillings were made to sample pointbar and channel sediments of two megameanders (Fig. 2). Fluvial stratigraphy and sedimentological correlations were set up by laser grainsize analysis (Fritsch Analysette 22 MicroTec plus). OSL samples were taken from layers with increased sand content, using drilling and undisturbed steel cylinders.

In all 12 sediment samples were measured by OSL. Samples were mainly silty, but usually containing an adequate amount of sand for dating, therefore where it was possible the polymineral fine grain and quartz coarse grain fractions were dated simultaneously in order to assess the adequacy of different materials for dating purposes. The preparation of the samples has followed usual laboratory techniques (Aitken, 1998; Mauz et al., 2002). For coarse and fine grain dating the 90-150 µm and the 4-11 µm fractions were used, respectively. The separation of fractions was made by sieving and settling. The carbonate and organic material content was removed by repeated treatment in 10% HCl and 10% H_2O_2. In case of coarse grains, a Na-polytungstanate (LST Fastfloat) heavy liquid separation was applied for the separation of the quartz fraction. This step was followed by a 50 min etching in 40% HF, aiming at removing any remaining feldspar contaminations and the outer layer of quartz for dosimetry

reasons. Coarse grains were adhered to stainless steel discs by silicone spray (2 mm mask), fine grains (2 mg/aliquot) were settled to aluminium discs by using acetone. A number of aliquots were prepared for luminescence tests and for equivalent dose (D_e) determination.

Measurements were made using a RISOE DA-15 TL/OSL luminescence reader by applying the SAR (Wintle and Murray, 2006) and DSAR (Roberts and Wintle, 2001) protocols on the coarse grain sand and the fine grain silt fraction, respectively. In terms of fluvial samples usually the sand sized quartz fraction is investigated, assuming that it usually has more chance for complete bleaching during sediment transport. In this case comparative measurements were made to test the applicability of the fine grain component too.

Concerning the coarse grain fraction a combined preheat-cutheat test was used for determining optimal heating parameters during the SAR measurements. Preheat temperatures varied between 200 °C and 260 °C, while cutheat temperatures between 140 °C and 220 °C. In case of fine grain samples a simple preheat test was applied, with a constant cutheat at 160 °C. During the tests SAR recycling ratios (ratio of two sensitivity corrected luminescence signals generated by identical regeneration doses) and recuperation (thermal and photo transfer of electrons to OSL traps) values were monitored to determine the best thermal treatment. Subsequently, known doses were administered to 5-5 aliquots of each sample and a SAR measurement was run in order to determine the given dose/measured dose ratio (dose recovery test), which is a robust test for assessing the applicability of the SAR procedure. Known doses were set to be close to the preliminary D_e, assessed prior to any of the tests.

SAR measurements were performed on 24-48 aliquots, standard rejection criteria were used to select those aliquots performing well during the measurements (recycling ratio being within 1.00 ± 0.05, D_e error being lower than 10%, recuperation being lower than 5%). Single aliquot D_e values were analysed using the central age and the minimum age models (Galbraiht, 1999) in case of coarse grain and fine grain samples, respectively.

Environmental dose rate (D*) was determined by using high-resolution, extended range gamma spectrometry (Canberra XtRa Coaxial Ge detector), using 500 cm^3 marinelli beakers. Dry dose rates were calculated using the conversion factors of Adamiec and Aitken (1998). Wet dose rates were assessed on the basis of in situ water contents. The rate of cosmic radiation was determined on the basis of burial depth following the method of Prescott and Hutton (1994).

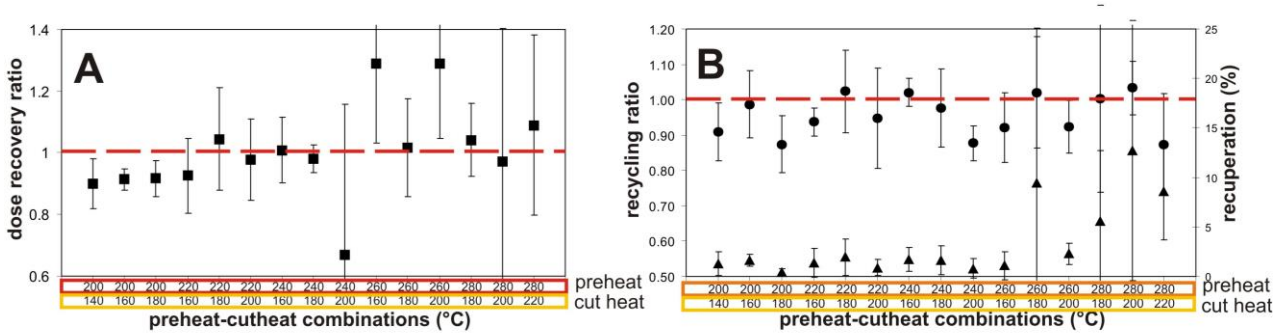

Fig. 3 Results of a combined preheat-cutheat and dose recovery test of a coarse grain quartz sample (OSZ245). A) dose recovery ratio; B) recycling ratio and recuperation

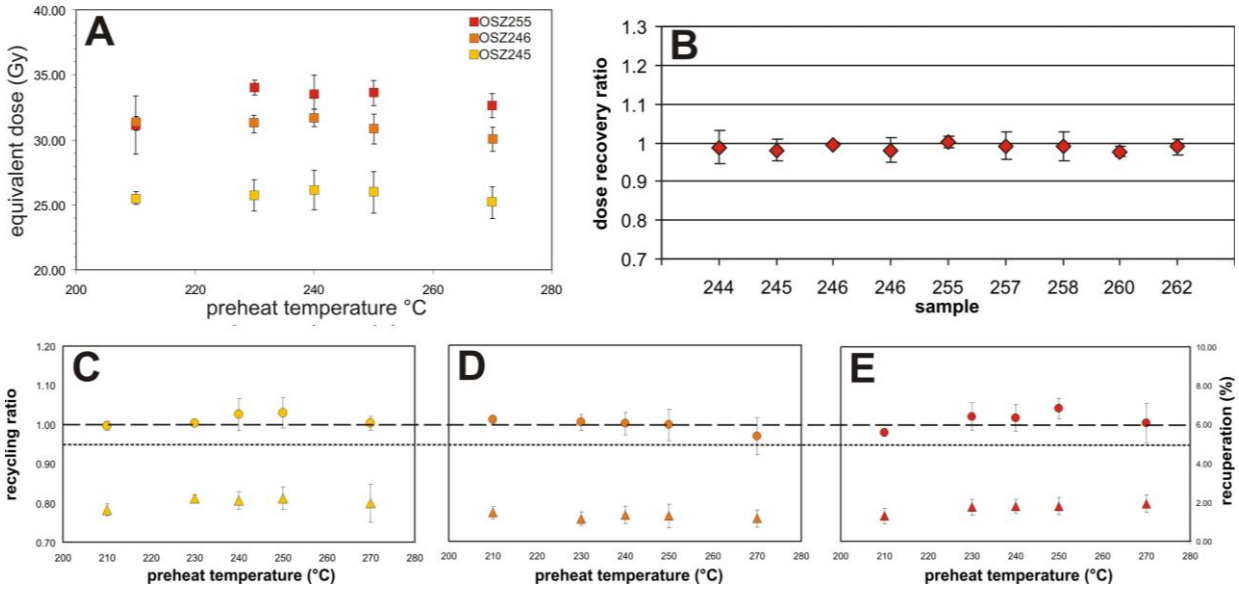

Fig. 4 Preheat and dose recovery test of polymineral fine grain samples. A) D_e at various preheat temperatures, B) The dose recovery ratio values of several fine grain samples, C, D, E) Recycling ratio and recuperation of samples indicated on Fig. 4A, colours are identical

RESULTS AND DISCUSSION

Looking at the thermal tests in general, as it was expected, coarse grain samples showed a much higher scatter in terms of SAR internal check parameters and also in terms of dose recovery ratios than fine grain samples (Fig. 3 and Fig. 4). Concerning recuperation coarse grain samples performed fairly well up till a preheat temperature of 260-280°C (Fig. 3), thus this parameter has not seemed to be problematic in terms of final measurements. However, recycling ratios were rather poor at almost each preheat-cutheat combinations. Acceptable results were received at either the 240°C/160°C (Fig. 3) and the 220°C/160°C combinations. At these temperature settings dose recovery was also within thresholds (Fig. 3).

Meanwhile, in case of fine grain samples a high stability of equivalent doses was observed at various preheat temperatures, and the recovery of artificial doses was also very precise (Fig. 4). Recycling ratios remained close to unity and recuperation was also insignificant (Fig. 4).

As a consequence of the above during the final SAR measurements, aiming at determining D_e, 40-50 % of aliquots had to be rejected in terms of coarse grain quartz samples during the age analysis. However, by applying even stricter rejection criteria for fine grain samples 95 % of results were still applicable.

Following age calculation fine grain results were relatively close to coarse grain result (Table 1, Fig. 5). Significant overestimation was experienced in three cases, on the other hand three other fine grain ages were practically identical to their coarse grain equivalent (Fig. 5). The mean overestimation related to fine grain ages was 1.5 ka, meaning that general trends might be inferred from fine grain fluvial data in the region, and major channel generations can be separated, but the date of shifts and changes can hardly be determined without the use of coarse grain data.

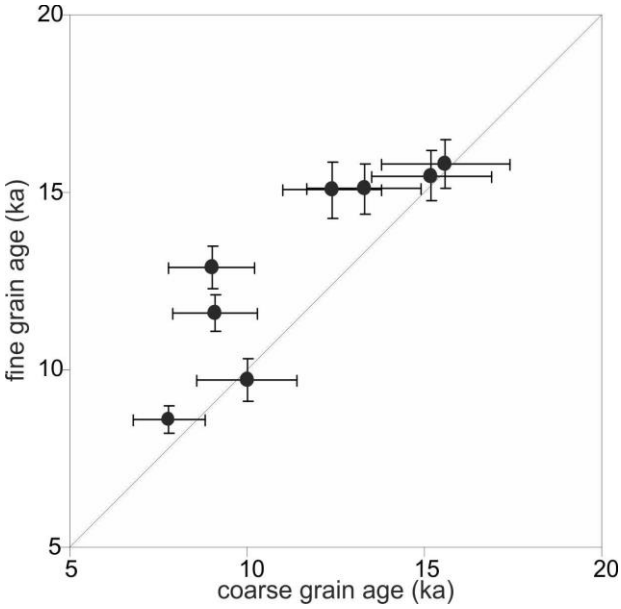

Fig. 5 Coarse grain and fine grain ages plotted against each other in case of samples where both were determined

Based on coarse grain derived ages, the point bars related to the upper floodplain meander (Site 1) started to develop 14-16 ka ago, and were probably formed up till 13-15 ka. Going closer to the palaeochannel, a less elevated bar (drilling C) yielded a coarse grain age of 12.4±1.4 ka at a 2.6 m depth, which is in good correspondence with the topmost sample of drilling B with an age 13.3±1.6 ka (Fig. 6). Consequently, a second phase of channel formation is suggested at this time, which was also accompanied by a slight incision, as the point bar sequence can be separated into two levels (Fig. 6). At a 1.4 m depth however, an age of 7.8±1.0 was received, which is very young compared to previous results and might indicate either post formational aggradation, or a next phase of channel development. Nevertheless, this can only be confirmed if further drillings are made closer to the channel.

Table 1 Dose rate, equivalent dose and age data of the investigated samples

Sample	depth (m)	U (ppm)	Th (ppm)	K (%)	$D^*_{(90\text{-}150\ \mu m)}$ (Gy/ka)	$D^*_{(4\text{-}11\ \mu m)}$ (Gy/ka)	$D_{e\ (90\text{-}150\ \mu m)}$ (Gy)	$D_{e\ (4\text{-}11\ \mu m)}$ (Gy)	Age $_{(90\text{-}150\ \mu m)}$ (ka)	Age $_{(4\text{-}11\ \mu m)}$ (ka)
Site 1										
OSZ255	1.4	2.53±0.24	9.28±1.04	1.73±0.17	2.72±0.14	3.21±0.14	21.14±2.53	27.73±0.30	7.8±1.0	8.6±0.4
OSZ257	2.6	2.60±0.21	9.42±1.05	1.85±0.09	2.64±0.10	3.11±0.13	32.70±3.37	46.9±0.78	12.4±1.4	15.1±0.7
OSZ258	1.1	2.43±0.20	8.85±1.00	1.62±0.08	2.68±0.11	3.18±0.14	39.03±4.39	41.99±0.69	14.5±1.8	13.2±0.6
OSZ260	2.6	2.27±0.15	8.20±0.82	1.54±0.07	2.37±0.09	2.80±0.12	36.96±4.09	44.25±0.57	15.6±1.8	15.8±0.7
OSZ262	2.1	2.82±0.23	10.65±1.17	1.90±0.09	2.93±0.11	3.48±0.14	44.59±4.64	53.74±0.79	15.2±1.7	15.5±0.7
Site 2										
OSZ242	1.4	2.55±0.20	9.44±1.04	1.59±0.08	-	3.43±0.16	-	37.91±0.67	-	11.1±0.5
OSZ244	1.6	2.47±0.17	8.33±0.86	1.42±0.07	-	3.12±0.15	-	42.14±0.62	-	13.5±0.7
OSZ245	1.0	1.74±0.15	6.28±0.74	1.11±0.06	1.99±0.10	2.35±0.13	19.8±2.56	22.74±0.57	10.0±1.4	9.7±0.6
OSZ246	1.3	1.74±0.15	6.28±0.74	1.11±0.06	2.00±0.10	2.37±0.13	18.23±2.34	27.46±0.23	9.1±1.3	11.6±0.5
OSZ247	2.0	2.15±0.17	7.86±0.86	1.35±0.06	-	2.74±0.13	-	33.98±1.1	-	12.4±0.7
OSZ248	1.5	2.64±0.21	8.38±0.96	1.48±0.07	-	3.17±0.15	-	32.99±0.43	-	10.4±0.5
OSZ254	2.2	2.43±0.19	8.34±0.94	1.37±0.07	2.34±0.10	2.80±0.13	20.98±2.59	36.15±0.60	9.0±1.2	12.9±0.6

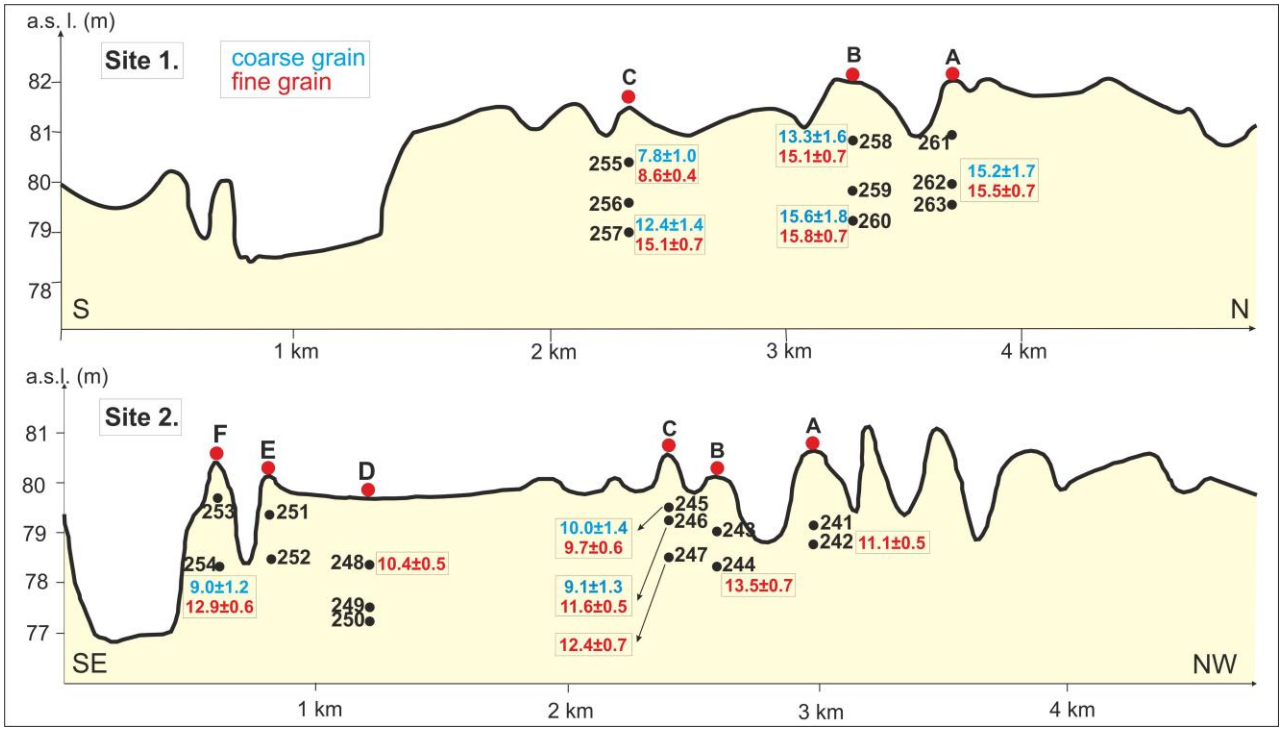

Fig. 6 Coarse and fine grain OSL ages at Site 1 (Hódmezővásárhely) and Site 2 (Deszk)

Concerning Site 2 both coarse grain and fine grain data indicate that the point bar sequence developed relatively intensively between 11 ka and 9 ka, thus one continuous phase of development can be identified. Consequently, lateral development was much faster than in case of the meander on the upper floodplain. Age data indicate that the intermediate floodplain level developed right after the second development stage (at 12-13 ka) of the upper floodplain meander, thus a continuous incision process can be hypothesised during the Pleistoene-Holocene transition.

The difference in the dynamics of meander evolution can partly be explained by changing palaeoenvironment and discharge values. The first phase of evolution on the upper floodplain can be related to a high discharge period during the Bølling-Allerød interstadial as observed at other sites by Gábris and Nádor (2007) and Kiss et al. (2015). Nevertheless, a relatively low intensity of development is inferred, which may refer to the significance of vegetation control under a warm and humid climate. The second phase and the start of the incision process can be related to the Younger Dryas, which obviously brought much lower discharges and although vegetation control was limited also, meander development was slow. This might also be caused by the fact that the major tributary of the Tisza (River Maros) shifted its course frequently in the region at this time (Sümeghy et al., 2013, Kiss et al., 2015). The slight Younger Dryas incision, however, underlies the importance of tectonic forcing over climatic control in the development of floodplain levels along the river.

On the other hand, during the development of the intermediate floodplain level, fluvial processes accelerated suddenly in the Preboreal, as it is resembled by the data of site 2. In this case large discharges as a matter of glacier melting and fairly low vegetation control can explain intense meander formation.

CONCLUSIONS

Based on the tests, both coarse grain and fine grain samples have adequate properties for the application of luminescence dating on fluvial sediments in the Lower Tisza region. Nevertheless, coarse grain samples have poorer characteristics, and therefore extensive measurements are required to have sufficient number of aliquots passing the rejection criteria.

According to the comparative analyses, the resetting of fine grain sediments in the Tisza system is obviously less efficient than that of coarse grains, however overestimation is not general if parallel dated samples of the present study are considered. Therefore, in the given time range, fine grain ages can still provide valuable data for identifying trends, but on their own they are not suitable for drawing sound conclusions. Thus when it is possible some samples has to be subjected to fine grain and coarse grain measurements at the same time to determine the possible degree of overestimation, and this needs to be incorporated to the error term of fine grain results.

Concerning the morphological evolution of the floodplain levels along the river, results support the Late Pleistocene – Early Holocne development of the intermediate floodplain, meaning that the lower floodplain developed in the Holocene, in accordance with previous results (Hernesz, 2015). Incision is suggested to be controlled by tectonics, and therefore it might be possible later to differentiate more stages of the process by the means of further OSL results.

Climate and palaeo-environment on the other hand can have a key role in the dynamics of lateral fluvial development and the rate of point bar formation in case of meanders. Nevertheless, further details can be recovered if detailed measurements are initiated on other mega-meanders of the region.

Acknowledgements

The research was supported by the following projects: HURO/1101/126/2.2.1, NKFIH K-119309 and NKFIH K-119193.

References

Adamiec, G., Aitken, M. 1998. Dose-rate conversion factors: update. *Ancient TL* 16 (2), 37–50.

Aitken, M. J. 1998. An Introduction to Optical Dating. Oxford University Press. London.

Alexanderson, H. 2007. Residual OSL signals from modern Greenlandic river sediments. *Geochronometria* 26, 1–9. DOI: 10.2478/v10003-007-0001-6

Borsy, Z. 1989. Az Alföld hordalékkúpjának negyedidőszaki fejlődéstörténete (The Quaternary development of the Great Hungarain Plain). *Földrajzi Értesítő* 38, 211–224. (in Hungarian)

Bøtter-Jensen, L., McKeever, S. W. S., Wintle, A. G. 2003. Optically Stimulated Luminescence Dosimetry. Elsevier.

Somogyi, S. 1967. Ősföldrajzi és morfológiai kérdések az Alföldről (Palaeo-geographical and geomorphological questions on the Great Hungarian Plain). *Földrajzi Értesítő* 16, 319–337. (in Hungarian)

Sümeghy, B., Kiss, T., Sipos, Gy., Tóth, O. 2013. A Maros hordalékkúp felső-pleisztocén–holocén fluviális képződményei. (Fluvial forms on the Maros alluvial fan from the Upper Pleistocene-Holozene) *Földtani Közlöny* 143 (3), 265–278. (in Hungarian)

Gábris, Gy. 1986. Alföldi folyóink holocén vízhozamai (Holocene discharge of rivers on the Great Hungarian Plain). *Alföldi Tanulmányok 10*, 35–48. (in Hungarian)

Gábris, Gy., Nádor, A. 2007. Long-term fluvial archives in Hungary: response of the Danube and Tisza rivers to tectonic movements and climatic changes during the Quaternary: a review and new synthesis. *Quaternary Science Reviews* 26, 2758–2782. DOI: 10.1016/j.quascirev.2007.06.030

Galbraith, R. F., Roberts, R. G., Laslett, G. M., Yoshida, H., Olley, J. M. 1999. Optical dating of single and multiple grains of quartz from Jinmium rock shelter, northern Australia. Part I: Experimental design and statistical models. *Archeometry* 41, 339–364. DOI: 10.1111/j.1475-4754.1999.tb00987.x

Hernesz, P. 2015. Késő-pleisztocén és holocén ártérfejlődés az Alsó-Tisza mentén. (Late Pleistocene and Holocene floodplain development along the Lower Tisza River). PhD dissertation, 118 p. (in Hungarian)

Hu, G., Zhang, J.F., Qui, W.L., Zhou, L.P. 2010. Residual OSL signals in modern fluvial sediments from Yellow River (HuabgHe) and the implications for dating young sediments. *Quaternary Geochronology* 5, 187–193. DOI: 10.1016/j.quageo.2009.05.003

Kiss, T., Hernesz, P. 2011. Az Alsó-Tisza-vidék árterének geomorfológiai jellegzetességei és kora. (Geomorphological features of the Lower Tisza floodplain and their dating) *Földrajzi Közlemények,* 135 (3), 261–275. (in Hungarian)

Kiss, T., Hernesz, P., Sipos, Gy. 2012. Meander cores on the floodplain – an early Holocene development of the low floodplain along the lower Tisza region, Hungary. *Journal of Environmental Geography* 5, 1–10.

Kiss, T., Sümeghy, B., Hernesz, P., Sipos, Gy., Mezősi, G. 2013. Az Alsó-Tisza menti ártér és a Maros hordalékkúp késő-pleisztocén és holocén fejlődéstörténete. (Late Pleistocene and Holocene development of the Lower Tisza floodplain and the alluvial fan of the River Maros) *Földrajzi Közlemények* 137 (3), 269–278. (in Hungarian)

Kiss, T., Hernesz, P., Sümeghy, B., Györgyövics, K., Sipos, Gy. 2015. The evolution of the Great Hungarian Plain fluvial system, Fluvial processes in a subsiding area from the beginning of the Weichselian. *Quaternary International* 388, 142–155. DOI: 10.1016/j.quaint.2014.05.050

Mauz, B., Bode, T., Mainz, E., Blanchard, H., Hilger, W., Dikau, R., Zöller, L. 2002. The luminescence dating laboratory at the University of Bonn: Equipment and procedures. *Ancient TL* 20, 53–61.

Nádor, A., Thamó-Bozsó, E., Magyari, Á., Babinszki, E. 2007. Fluvial responses to tectonics and climate change during the Late Weichselian in the eastern part of the Pannonian Basin (Hungary). *Sedimentary Geology* 202, 174–192. DOI: 10.1016/j.sedgeo.2007.03.001

Prescott, J. R., Hutton, J. T. 1994. Cosmic ray contributions to dose rates for luminescence and ESR dating: large depths and long-term time variations. *Radiation Measurements* 23, 497–500. DOI: 10.1016/1350-4487(94)90086-8

Rittenour, T. M. 2008. Luminescence dating of fluvial deposits: applications to geomorphic palaeosemic and archeological research. *Boreas* 37, 613–635. DOI: 10.1111/j.1502-3885.2008.00056.x

Roberts, H., Wintle, A. G. 2001. Equvalent dose determination for polymineralic fine-grains using the SAR protocol: application to a Holocene sequence of the Chinese Loess Plateau. *Quaternary Science Reviews* 20, 859–863. DOI: 10.1016/s0277-3791(00)00051-2

Vandenberghe, D., Derese, C., Houbrechts, G. 2007. Residual doses in recent alluvial sediments from Ardenne (S Belgium). *Geochronometria* 28, 1–8. DOI: 10.2478/v10003-007-0024-z

Vandenberghe, D. 2004. Investigation of the Optically Stimulated Luminescence dating method for application to young geological sediments. PhD dissertation, Universitiet Gent

Wintle, A. G., Murray, A. S. 2006. A review of quartz optically stimulated luminescence characteristic and their relevance in single-aliquot regeneration dating protocols. *Radiation Measurement* 41, 369–391. DOI: 10.1016/j.radmeas.2005.11.001